2006-11-16

Quantitative Analysis of Hedgehog Gradient Formation Using an Inducible Expression System: a Dissertation

Vivian F. Su
University of Massachusetts Medical School

Let us know how access to this document benefits you.

QUANTITATIVE ANALYSIS OF HEDGEHOG GRADIENT

FORMATION USING AN INDUCIBLE EXPRESSION SYSTEM

A Dissertation Presented

By

Vivian F. Su

Submitted to the Faculty of the
University of Massachusetts Graduate School of Biomedical Sciences, Worcester
in partial fulfillment of the requirements for the degree of

DOCTOR OF PHILOSOPHY

November 16, 2006

Gene Function and Expression

**QUANTITATIVE ANALYSIS OF HEDGEHOG GRADIENT
FORMATION USING AN INDUCIBLE EXPRESSION SYSTEM**

A Dissertation Presented By

Vivian F. Su

The signatures of the Dissertation Defense Committee signifies
completion and approval as to style and content of the Dissertation.

_____
Inge The PhD., Thesis Advisor

_____
Silvia Corvera PhD., Member of Committee

_____
Tony Ip PhD, Member of Committee

_____
William Theurkauf PhD., Member of Committee

_____
Laurel Raftery, PhD., Member of Committee

The signature of the Chair of the Committee signifies that the written dissertation meets
the requirements of the Dissertation Committee

_____
Heidi Tissenbaum

The signature of the Dean of the Graduate School of Biomedical Sciences signifies that
the student has met all graduate requirements of the school.

_____
Anthony Carruthers PhD,
Dean of the Graduate School of Biomedical Sciences

Interdisciplinary Graduate Program

November 16, 2006

ACKNOWLEDGEMENTS

ABSTRACT

The Hedgehog (Hh) family of proteins are secreted growth factors that play an essential role in the embryonic development of all organisms and the main components in the pathway are conserved from insects to humans. These proteins affect patterning and morphogenesis of multiple tissues. Therefore, mutations in the Hh pathway can result in a wide range of developmental defects and oncogenic diseases. Because the main components in the pathway are conserved from insects to humans, *Drosophila* has been shown to provide a genetically tractable system to gain insight into the processes that Hh is involved in.

In this study, the roles of Hh cholesterol modification and endocytosis during gradient formation are explored in the *Drosophila* larval wing imaginal disc. To exclude the possibility of looking at a redistribution of preexisting Hh instead of Hh movement, a spatially and temporally regulated system has been developed to induce Hh expression. Functional Hh-GFP with and without the cholesterol-modification was expressed in a wild-type or shi^{ts1} endocytosis mutant background. The Gal80 system was used to temporally express (pulse) the Hh-GFP transgenes to look at the rate of Hh gradient formation over time and determine whether this process was affected by cholesterol modification and/or endocytosis.

Hh with and without cholesterol were both largely detected in punctate structures and the spreading of the different forms of Hh was quantified by measuring distances of

these particles from the expressing cells. Hh without cholesterol showed a greater range of distribution, but a lower percentage of particles near the source. Loss of endocytosis blocked formation of intracellular Hh particles, but did not dramatically alter its movement to target cells. Staining for Hh, its receptor Ptc and cortical actin revealed that these punctate structures could be classified into four types of Hh containing particles: cytoplasmic with and without Ptc, and cell surface with and without Ptc. Cholesterol is specifically required for the formation of cytoplasmic particles lacking Ptc. While previous studies have shown discrepancies in the localization of Hh following a block in endocytosis, Hh with and without cholesterol is detected at both apical and basolateral surfaces, but not at basal surfaces. In the absence of cholesterol and endocytosis, Hh particles can be observed in the extracellular space.

Through three-dimensional reconstruction and quantitative analysis, this study concludes that the cholesterol modification is required to restrict Hh movement. In addition, the cholesterol modification promotes Ptc-independent internalization. This study also observes that Dynamin-dependent endocytosis is necessary for internalization but does not play an essential role in Hh distribution. The data in this thesis supports the model in which Hh movement occurs via planar diffusion.

TABLE OF CONTENTS

ix

LIST OF FIGURES

Figure 1.1 - Morphogens..1

Figure 1.2 - Ventral cuticular pattern of *Drosophila melanogaster* embryos from wild-type and homozygous *hh* mutant flies...6

Figure 1.3 - The Hh signaling pathway...10

Figure 1.4 - Schematic representation of the *Drosophila* wing imaginal disc and expression systems..12

Figure 1.5 - Models for morphogen distribution...21

Figure 2.1 - HhNp-GFP is functional...47

Figure 2.2 - HhNp-GFP localizes at the membrane, in endocytic compartments, and extracellularly..52

Figure 2.3 – Extracellular Hh localizes apically in particles and basolaterally in particles along the membrane..54

Figure 2.4 - Schematic diagram of Gal4-Gal80 inducible expression system..............58

Figure 2.5 - Cholesterol restricts HhNp-GFP distribution but endocytosis is not required for distribution...59

Figure 2.6 - Hh gradient forms by 24hr of induction..61

Figure 2.7 - Quantitative analysis of Hh-GFP distribution: Cholesterol is required to restrict distribution but endocytosis is not required for distribution............62

Figure 2.8 - Full distribution profiles of Hh-GFP...64

Figure 2.9 - Individual histograms of raw data with median, 90% maximum, and % within 8µm values..66

LIST OF TABLES

LIST OF ABBREVIATIONS

A/P boundary - anterior/posterior boundary

Botv - Brother of tout velu

Ci - Cubitus interruptus

DCAD - D-cadherin

Disp - Dispatched

Dlp - Dally-like

Dpp - Decapentaplegic

En - Engrailed

Hh - Hedgehog

HhC - C-terminal Hedgehog

HhF - Full length Hedgehog

HhN – non-cholesterol modified N-terminal Hedgehog

HhNp - cholesterol modified and cleaved N-terminal Hedgehog

HPE - holoprosencephaly

HSPG - heparan sulfate proteoglycan

Ptc - Patched

Shf - Shifted

Shh - Sonic Hedgehog

ShhN – non-cholesterol modified N-terminal Sonic Hedgehog

ShhNp – cholesterol modified and cleaved N-terminal Sonic Hedgehog

Shi - Shibire

Smo - Smoothened

Sotv - Sister of tout velu

SSD – sterol-sensing domain

Ttv - Tout velu

Wg - Wingless

Statement of Contribution

In Chapter II, Kelly Jones, a technician in the The Lab, performed the Western blot and embryo *in situ* experiments. The ANOVA statistical calculations were done by Stephen Baker MSCPH, from the University of Massachusetts Medical School. I am solely responsible for all other experiments presented in this thesis.

CHAPTER I

Introduction

During development, groups of cells that are originially homogeneous differentiate into cells with different cell fates resulting in patterns or structures. Morphogens, or "form producing" substances, were believed to be the factors that could account for morphogenesis (Turing, 1952). Morphogens are defined by the ability to travel many cells away from the source, and to directly signal to cells in a concentration dependent manner, resulting in different cell fates depending on local concentrations (Figure 1.1; Tabata and Takei, 2004). Several secreted proteins, such as the Wnt, Transforming Growth Factor β, and Hedgehog family members have been proposed to be morphogens. Thus as a morphogen, Hedgehog (Hh) would elicit a concentration dependent response in the target cells leading to different cells fates.
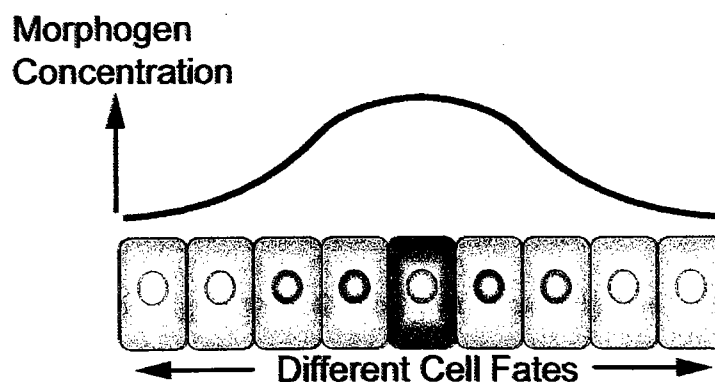
Figure 1.1 - Morphogens

Morphogens are molecules that signal directly to target cells, inducing cells to differentiate with different fates in a concentration dependent manner.

Hh and human disease

One reason for the intense study of Hh is due to its role in human disease. Hh pathway disruption has been associated with several human developmental disorders and cancers (Murone et al., 1999). One specific developmental disease is holoprosencephaly (HPE- "smooth brain"). *Sonic Hedgehog (SHH)* loss of function or *Patched (PTC*; the SHH receptor) gain of function (loss of SHH signaling) has been found in HPE patients. In HPE, the embryonic forebrain does not develop normally in the two hemispheres. This developmental disease can cause severe brain malformations usually leading to death before birth, and less severe malformations such as mild facial defects. One severe facial defect is cyclopia, the development of a single eye. Interestingly, a link was discovered between sheep born with cyclopia and their mothers ingesting a compound, cyclopamine, that was later found to inhibit Shh signaling (Rodenburg and Van der Horst, 2005).

Hh pathway mutations have also been linked to many types of cancers. *PTC* loss of heterozygosity is the primary cause of Gorlin's syndrome, or nevoid basal cell carcinoma. Patients with Gorlin's syndrome have a predisposition particularly to basal cell carcinomas and medullablastomas. Sporadic basal cell carcinomas have an upregulation of HH signaling as well, that is most frequently due to inactivation of *PTC* but also attributable to SMO (a positive regulator of the HH pathway) activation. Medullablastomas are the most common malignant pediatric brain tumor, and can most commonly be found with *PTC* loss of heterozygosity that results in inappropriate HH activity. Interestingly, tumors with activated HH signaling also have increased levels of

genes involved in cell proliferation, including *N-myc*, *C-myc*, *CyclinD1*, and *CyclinD2* (Dellovade et al., 2006).

The activation of the HH signaling pathways in several cancers have led to the search for molecules with therapeutic effects (Dellovade et al., 2006). In particular, several small molecules have been identified that are able to reduce the size of HH-based tumors. Using xenografts of medullablastomas or mouse models that have these tumors, the natural molecules cyclopamine and jervine as well as the synthetic HhAntag-691 are able to reduce and occasionally eliminate these tumor cells. Subsequent studies later found that these small molecules interfere with HH signaling at the SMO level, causing inactivation of SMO and preventing constitutive HH signaling (Dellovade et al., 2006). Because these small molecules do not appear to affect other pathways, they have potential as therapeutic agents for HH-based diseases.

Drosophila embryonic development

Drosophila embryos consist of segments that have alternating regions of naked cuticle and denticle (hairs) belts. Patterning of the embryo into these segments is the result of a series of activities of various classes of genes throughout oogenesis and embryogenesis (Akam, 1987; Gilbert, 2000). The initial activities in the embryo are due to maternal effect genes. This maternally produced RNA is deposited into the oocyte by the mother and translation into proteins occurs after the oocyte is fertilized. These maternal effect gene products act as transcription factors, post-transcriptional regulators, and/or signaling molecules during oogenesis and the early stages of embryogenesis.

They then activate or repress the gap genes, which are transcription factors that function during the syncytial blastoderm and cellularization stages of embryo development, dividing the embryo into broad regions. Gap gene products subsequently activate the pair-rule genes, which encode transcription factors that are active from the blastoderm cellularization stage through gastrulation. Finally, the pair-rule genes regulate the expression of the segment polarity genes. Segment polarity genes consist of transcription factors and signaling molecules that act later in embryonic development starting during gastrulation up until the larval stages. This activity completes the patterning of the embryonic segments (Akam, 1987; Gilbert, 2000).

Drosophila hedgehog

Drosophila hh was first discovered in 1980, in a large screen for genes affecting the development and segmental patterning of the Drosophila embryo. This screen, conducted by Christiane Nusslein-Volhard and Eric Wieschaus, identified 15 genes involved in patterning segments in Drosophila embryos. These genes were classified into three groups based on their mutant segment patterning phenotypes: gap genes, pair-rule genes, and segment polarity genes. hh was classified as a segment polarity gene since every segment in the embryo was affected in the mutant (Nusslein-Volhard and Wieschaus, 1980).

The hh gene was further characterized with the identification and analysis of different hh mutant alleles. Mutant hh embryos had only 40% the length of a wild-type embryo, resulting from the loss of the naked cuticle sections of each segment and

producing a "lawn of denticles" phenotype (Figure 1.2). Mosaic analysis of the adult cuticle found that *hh* mutant clones in anterior compartments had little effect. However, posterior *hh* mutant clones had a nonautonomous effect, disrupting proper specification of anterior compartment cells that were not mutant for *hh*. These posterior *hh* mutant clones were adjacent to wild-type cells with cuticle defects, consistent with "domineering" nonautonomy, meaning that mutant clones first result in inappropriate behavior within the clone (i.e. a gene is mutated), and subsequently affects neighboring cells (i.e. consequences from the mutated gene). This implied that there was either a failed cascade of processes that began within the mutant clone, or the defective clone normally produced a diffusible molecule that was necessary for proper signaling in the adjacent tissue, such as a morphogen (Mohler, 1988).
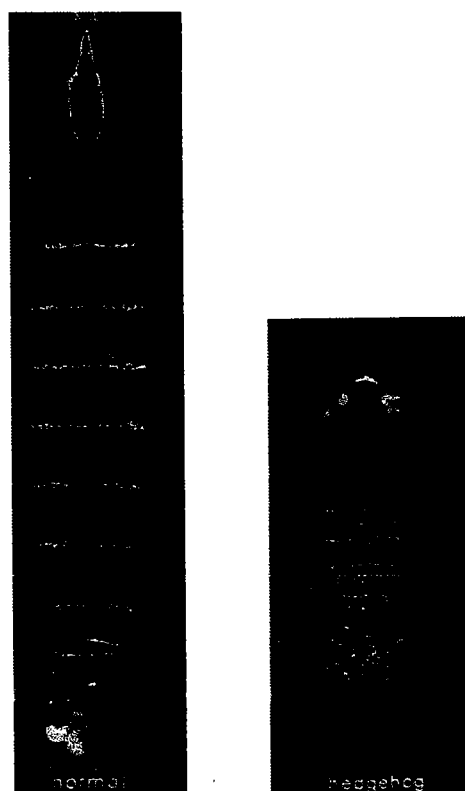
Figure 1.2 - Ventral cuticular pattern of *Drosophila melanogaster* embryos from wild-type and homozygous *hh* mutant flies.

Wild-type embryo cuticles are patterned into alternating bands of naked cuticle and denticles (hairs). *hh* mutant embryos have only 40% the length of wild-type and are deleted for the naked cuticle portion of the segment pattern, and have only denticle, resulting in the "lawn of denticles" phenotype. This "lawn of denticles" phenotype resembled the hedgehog animal, resulting in the gene being named *hh* (Nusslein-Volhard and Weischaus, 1980).

The *hh* gene

The location of the *hh* gene was mapped based on *hh* mutants that were associated with rearrangement breakpoints, such as inversions and deletions (Mohler and Vani, 1992) and also based on the location of an enhancer trap insertion thought to be *hh* (Tabata et al., 1992). Subsequently, embryonic cDNA libraries were screened and the *hh* cDNA was isolated. Sequence analysis found hydrophobic sequences at the amino terminus (amino acids 63-81) flanked by basic hydrophilic sequences, which is typical of transmembrane domains (Mohler and Vani, 1992; Tabata et al., 1992).

Vertebrate homologues were subsequently identified in zebrafish, chick, and mouse. Unlike *Drosophila*, several *hh* genes were found in vertebrates/mammals: *Sonic Hedgehog (Shh), Indian Hedgehog (Ihh),* and *Desert Hedgehog (Dhh)*. Additional *hh* genes were found in zebrafish, including *Tiggy-winkle Hedgehog (Twhh;* Ingham and McMahon, 2001). With the identification of the *hh* gene, the Hh signaling pathway could be elucidated.

The Hh signaling pathway

Identification of the *hh* gene allowed *in situ* analyses in embryos that localized the Hh transcript to the posterior compartment (Mohler and Vani, 1992; Tabata et al., 1992). Observations that the localization of Hh correlated to that of the transcription factor Engrailed (En) led to the discovery that En activates *hh* gene expression, initiating the Hh pathway in the posterior compartment (Figure 1.3; Tabata et al., 1992). As with Hh itself, identification of other Hh pathway components stemmed from analysis of mutant

embryonic phenotypes. The *hh* mutant was first documented with an embryonic segment polarity phenotype and almost all mutants of Hh pathway components exhibit the same embryonic loss of naked cuticle and "lawn of denticles" phenotype (Ingham and McMahon, 2001).

After translation, Hh undergoes a series of cleavage and lipid modifications (discussed in a later section; Lee et al., 1994; Porter et al., 1996b). Mature Hh is secreted from the expressing cells, aided by Dispatched (Disp; Burke et al., 1999). Disp is a twelve transmembrane domain protein thought to aid Hh secretion by either shuttling Hh to the membrane (Gallet et al., 2003) or targeting Hh to specific domains for secretion (Burke et al., 1999). After being secreted, Hh is distributed to target cells in the anterior compartment. The mechanism of this distribution is unclear but it involves the heparan sulfate proteoglycans (HSPGs) Dally and Dally-like (Dlp; Desbordes and Sanson, 2003; Han et al., 2004b; Lum et al., 2003a; Takeo et al., 2005) and the secreted protein Shifted (Shf; Glise et al., 2005; Gorfinkiel et al., 2005). HSPGs are cell surface glycoproteins that are modified by the Ext family of HSPG modifying enzymes Tout velu (Ttv), Sister of Tout velu (Sotv), and Brother of Tout velu (Botv; Bellaiche et al., 1998; Bornemann et al., 2004; Han et al., 2004a; Takei et al., 2004; The et al., 1999). Shf is a secreted factor that has been shown to be required for proper Hh distribution (Glise et al., 2005; Gorfinkiel et al., 2005). After reaching target cells, Hh binds to its receptor Patched (Ptc; Chen and Struhl, 1996; Ingham et al., 1991), which relieves the Ptc-dependent inhibition of Smoothened (Smo; Alcedo et al., 1996; Chen and Struhl, 1996; Denef et al., 2000; van den Heuvel and Ingham, 1996). Smo is a seven transmembrane domain protein and

belongs to the G-protein-coupled receptor family, although it does not have a known role as a receptor in Hh signaling. Ptc normally inhibits Smo from activating the pathway, possibly by regulating Smo subcellular localization (Zhu et al., 2003). Once Smo inhibition is released, the kinesin-like protein Costal-2 (Cos2) binds to the cytoplasmic C-terminal tail of Smo, and recruits the complex containing Cos2, Fused, Suppressor of Fused, and Cubitus interruptus (Ci; Hooper, 2003; Jia et al., 2003; Lum et al., 2003b; Monnier et al., 1998; Robbins et al., 1997; Ruel et al., 2003; Sisson et al., 1997). The recruitment of this complex to Smo results in the release of the activated form of the Ci transcription factor (Hooper, 2003; Jia et al., 2003; Ruel et al., 2003). Ci is a zinc finger protein that is cleaved in the absence of Hh signaling to a repressor form (Aza-Blanc et al., 1997) through Protein Kinase A phosphorylation (Chen et al., 1998; Wang et al., 1999). Interestingly, this cleaved form of Ci represses Hh target genes. Hh signaling activates full-length Ci, which then translocates into the nucleus to activate Hh target genes, which includes *ptc*, *decapentaplegic* (*dpp*), and *wingless* (*wg*; Alexandre et al., 1996; Forbes et al., 1993; Hepker et al., 1997; Von Ohlen et al., 1997; Wang et al., 2000; Wang and Holmgren, 2000).

Target Cell (Anterior)   **Producing Cell (Posterior)**
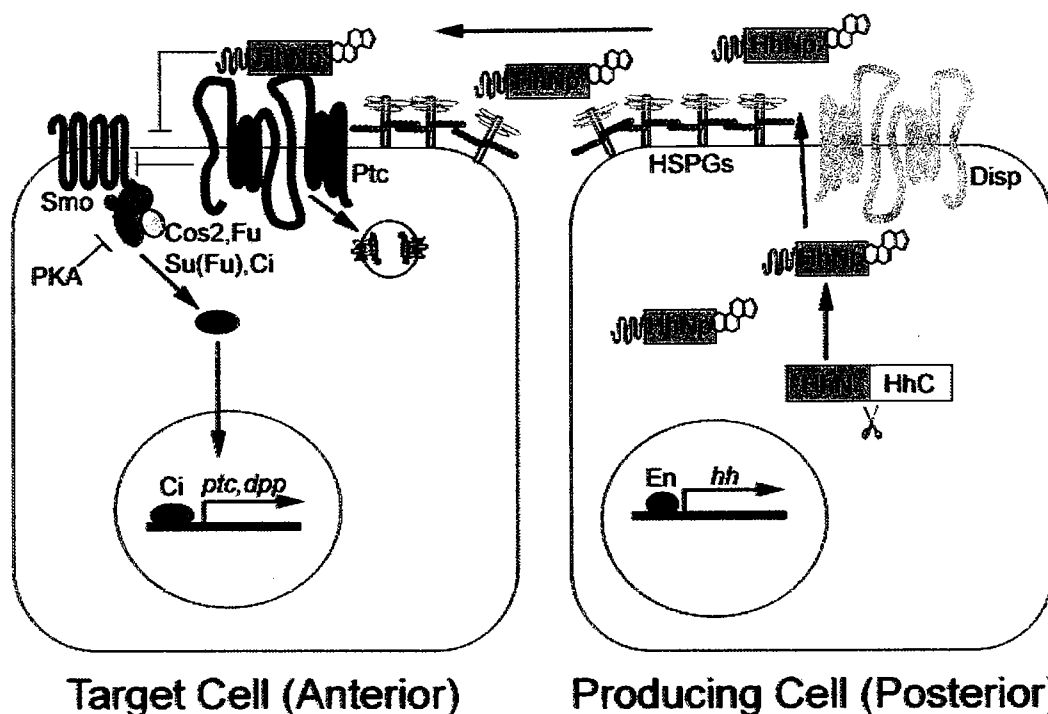
Figure 1.3 - The Hh signaling pathway.

The En transcription factor activates *hh* gene expression. After translation, the full length

Hh protein undergoes an autoproteolytic cleavage catalyzed by the C-terminus, during

which a cholesterol moiety is covalently attached to the C-terminus of the N-terminal

fragment. In addition, an acyltransferase attaches a palmitoyl moiety to the N-terminus

of this fragment. The signaling molecule HhNp is then secreted from the producing cell

with the help of Disp. HhNp travels from producing cells in the posterior compartment to

target cells in the anterior compartment; this movement is facilitated by HSPGs. Once at

the target cell, HhNp binds to its receptor Ptc and is internalized. This binding releases

the Ptc-dependent inhibition of Smo, to initiate a cascade of events resulting in the

stabilization of the active full length Ci and its translocation into the nucleus. The

transcription factor Ci then activates Hh target genes, including *ptc* and *dpp*.

Hh as a morphogen

An early study implied that Hh had morphogenetic properties and the proper regulation of Hh levels are important for patterning and cell specification during development (Mohler, 1988). During the same period, two other secreted proteins important in development, Dpp of the TGF-β family and Wg of the Wnt/Wg family were also thought to be potential morphogens. Interestingly, Dpp and Wg were Hh targets, and the relationship between the three proteins and their morphogenetic properties was unclear then.

Morphogen distribution has been extensively studied in *Drosophila* which has been a useful genetic tool for dissecting the pathway of morphogen gradient formation. Many studies have used the embryo and the larval wing imaginal disc to analyze morphogen gradients. Embryos are segmented, and each segment consists of an anterior and a posterior compartment which have different cellular properties. In a similar fashion, the wing disc is also separated into anterior/posterior (A/P) compartments (Figure 1.4). The wing imaginal disc is a thin sac-like structure comprised of two single layers of epithelial cells, separated by the lumen. The peripodial membrane consists of large squamous cells. The columnar epithelium (the disc proper) consists of polarized epithelial cells with the apical surface oriented towards the inside, facing the peripodial membrane. While compartment boundaries were known, it was thought that interaction between compartments might lead to synthesis or direction of signaling molecules to lead to the appropriate cell behavior (Crick and Lawrence, 1975).

Figure 1.4 - Schematic representation of the *Drosophila* wing imaginal disc and expression systems.

A

Anterior
Compartment

Posterior
Compartment

B

Peripodial
Membrane
Cells

Lumen

Columnar
Epithelial
Disc
Cells

C

Promoter Gal4   UAS gene x

D

flpase

a   b

b

E

flpase
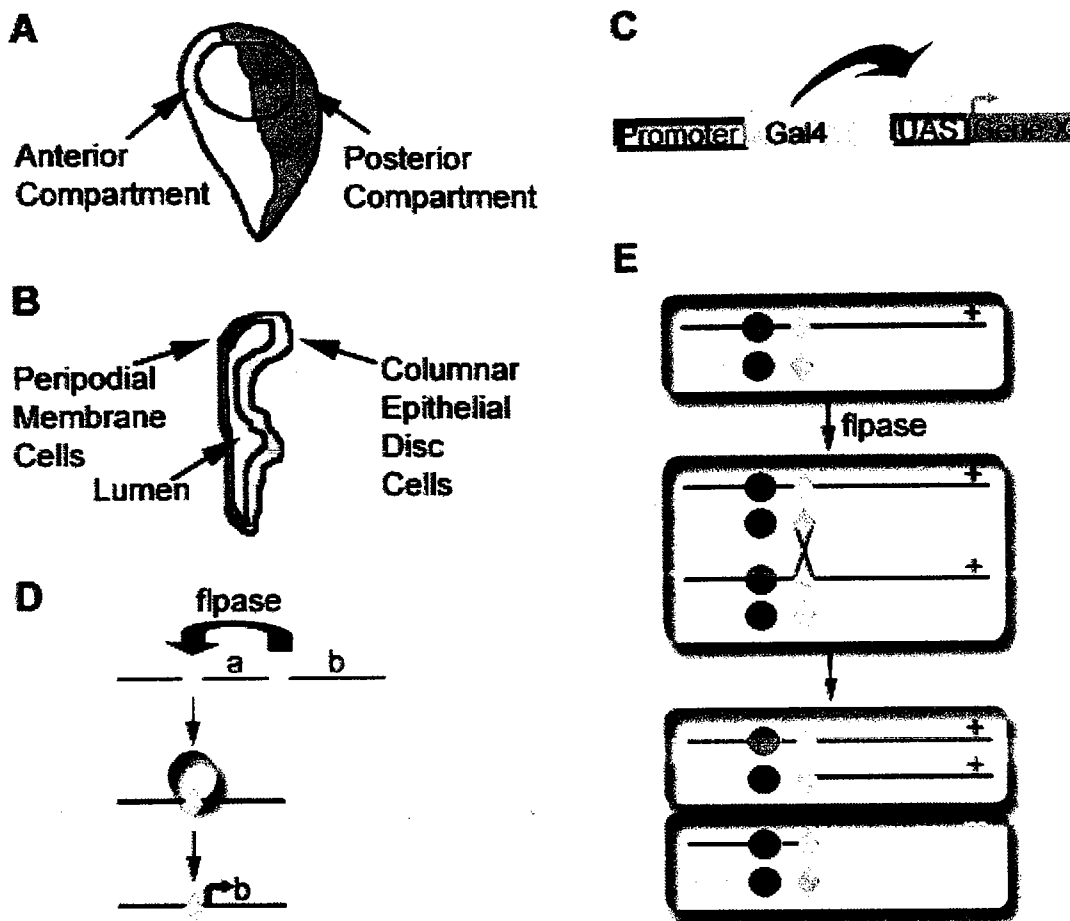
Figure 1.4 - Schematic representation of the *Drosophila* wing imaginal disc and expression systems.

(A) Front view of the larval wing imaginal disc that gives rise to the adult wing. The wing disc is segmented into the anterior and posterior (green) compartments. Posterior compartment cells express Hh that is secreted to reach target cells in the anterior.

(B) Transverse view of the wing disc. The wing disc is comprised of two epithelial layers. The peripodial membrane (red) consists of squamous epithelial cells and the columnar epithelial disc cells (yellow) are a single layer of pseudostratified cells. The two layers are separated by the lumen.

(C) Gal4-UAS system. The Gal4 protein (gray) binds to UAS sites to induce Gene-X in a tissue specific manner. The expression pattern of Gene-X depends on the promoter used to express Gal4.

(D) Ectopic expression using Flp-out clones. In the uninduced state, the target Gene-X is downstream of a stuffer gene or a stop codon (a). When the flpase enzyme is expressed, recombination between FRT sites (blue diamonds) is catalyzed, removing the stuffer region. This allows the target Gene-X to be expressed.

(E) Clonal analysis using FRT-Flp. During mitosis, the flpase enzyme catalyzes recombination between FRT sites (blue diamonds) located near the centromere (red circles). Chromosome arms are exchanged, resulting in one cell that has two copies of the wild-type gene (+) adjacent to the other cell that is homozygous for the mutated gene (m), at the end of mitosis. The cells will proliferate and form clones of homozygous wild-type and homozygous mutant cells in heterozygous tissue.

The question of whether Hh is a morphogen or not has been extensively debated. The experiments leading to both of these assumptions are discussed below.

Hh is not a morphogen

Experiments where Hh was ectopically expressed in the wing showed that Hh indirectly controls limb patterning through activation of expression of the secreted molecules Dpp and Wg (Basler and Struhl, 1994). While Hh did act at long range to cells in a stripe several cells wide and did directly act on these cells, Hh was not considered to be a morphogen. Hh was shown to induce expression of Dpp or Wg in cells adjacent to Hh expressing clones, which would in turn act as morphogens to induce proper wing and leg patterning. Therefore, Hh was proposed to be the initiator of a cascade of events, activating other long-range signaling molecules (Basler and Struhl, 1994).

The Gal4-UAS system was employed as well to induce ectopic Hh expression (Figure 1.4; Brand and Perrimon, 1993). Ectopic expression of En in anterior cells resulted in ectopic activation of *hh* within the En clone and activation of *dpp* in cells surrounding the clone. These anterior cells acquired a posterior identity due to En expression and thus, were unable to respond to Hh signaling. Direct ectopic expression of Hh, using UAS-*hh* induced in the anterior, circumvented an acquisition of posterior identity and resulted in Dpp expression both in and around the clone. Dpp is normally expressed in a stripe of cells at the A/P boundary. Ectopic expression of Dpp with UAS-*dpp* had a long range effect on neighboring tissue by reorganizing both anterior and posterior wing patterns. This was particularly evident in Dpp-expressing clones that were

further from the A/P boundary, where ectopic Dpp resulted in extra wing material in the form of winglets. It appeared that Hh induced wing patterning by short range signaling that activated Dpp, and that Dpp had long range concentration dependent signaling activities (Zecca et al., 1995). These results led to the conclusion that Hh itself was not a morphogen, but instead that Dpp was the morphogen induced by Hh signaling.

Hh is a morphogen

One of the earliest studies that provided evidence for Hh acting as a morphogen came from studies in the embryo (Heemskerk and DiNardo, 1994). These embryonic studies investigated the Hh-dose dependent response and made use of the fact that Hh signaling is responsible for specifying different cell fates in the embryonic cuticle. Using multiple copies of a heat-shock wild-type *hh* transgene, different levels of Hh were expressed in the embryo based on the number of transgene copies and length of heat-shock treatment. This resulted in the shifting of cuticle cell fates depending on the amount of Hh expressed, suggesting that Hh directly specified cell fates in a concentration dependent manner (Heemskerk and DiNardo, 1994).

Subsequent analysis examined wing patterning by Hh and the Hh target, Dpp, by ectopically expressing Hh and Dpp (Ingham and Fietz, 1995). Expression of Hh in the wing margin in both posterior and anterior compartments resulted in an enlarged anterior compartment, as well as ectopic Dpp expression in areas of low Hh activity. Similar to the previous embryo study, varying levels of ectopic Hh expression also caused graded

effects, observed in wing patterning, consistent with Hh acting as a long range morphogen (Ingham and Fietz, 1995).

These studies demonstrated that Hh had long range effects but did not conclusively rule out the possibility of a secondary signal that would be expressed differently in response to varying levels of Hh and act directly on the target cells instead of Hh. Studies by Struhl et al. in the *Drosophila* abdomen found that ectopic expression of Hh gave a range of results of cell fate specification based on the distance of the clone in the anterior compartment from the A/P boundary (Struhl et al., 1997a; Struhl et al., 1997b). This indicated that Hh organized cell patterning and cell polarity within the anterior compartment (Struhl et al., 1997a). Subsequent experiments constitutively activated or blocked Hh signaling cell autonomously to determine whether Hh or a secondary signal was responsible for activating target cells. Activating Hh signaling with a *PKA* mutant and blocking Hh signaling with a *smo* mutant resulted in altered cell fates in a cell autonomous manner. These observations inferred that Hh was directly acting on cells in the anterior to specify different cell types. Thus, Hh functioned as a gradient morphogen (Struhl et al., 1997b).

Furthermore, evidence for Hh as a morphogen came from wing studies (Strigini and Cohen, 1997). A concentration dependent effect of Hh for activating target genes was observed, using a temperature sensitive *hh* mutant allele. *en* was a target gene in the anterior compartment that was activated by high levels of Hh signaling. Activation of *en* was affected by partial loss of Hh at a lower *hh^{ts}* restrictive temperature; however, *dpp* (a low level target) was only affected when there was even less Hh expressed at the higher

restrictive temperature. Thus, the local concentration of Hh determined what target genes were activated. Additionally, the same study found that tethering Hh to the cell membrane by fusion to the transmembrane domain of human CD2 resulted in the activation of target genes only in immediately adjacent cells. It became clear that Hh itself had to be able to travel to target cells to activate targets like *dpp* (normally activated in a row 8-10 cells wide), and not a secondary signal. These results demonstrated that Hh had the behavior and characteristics of a morphogen - Hh directly signals to target cells at a distance and elicits dose-dependent responses. This was the most convincing evidence that Hh indeed acted as a morphogen in the wing (Strigini and Cohen, 1997).

Models for Hh morphogen gradient formation and distribution

While much has been elucidated about Hh signaling and target gene activation, the mechanism of how the Hh concentration gradient is formed and regulated is unclear. Proposed models for morphogen distribution and the formation of the morphogen gradient include free diffusion and planar movement (Figure 1.5). In the free diffusion model, morphogens are secreted from the producing cells into the extracellular space, and then diffuse in three-dimensions out to the target cells. Evidence for free diffusion has been described for *Xenopus* Activin, a member of the TGF-β family (McDowell and Gurdon, 1999). *Xenopus* embryo caps were incubated with activin-coated beads before being placed with untreated caps. Activin was able to diffuse through the untreated tissue and even through unreceptive tissue containing a mutant activin receptor, to active target genes (McDowell and Gurdon, 1999). Subsequent studies demonstrated that endocytosis

defective tissue did not alter Activin target gene activation (Jullien and Gurdon, 2005; Kinoshita et al., 2006). This suggested that Activin was able to freely diffuse to reach its target cells.

Another model for morphogen distribution is planar movement. This can further be subdivided into two types: restricted extracellular planar diffusion along cell surfaces and planar transcytosis. Studies involving the extracellular cell surface proteins HSPGs provide the strongest evidence for restricted extracellular planar diffusion. Clones of mutations affecting proper production of HSPGs restrict Hh, Wg, and Dpp distribution and signaling to cells at the edge closest to the expressing cells (Bellaiche et al., 1998; Bornemann et al., 2004; Callejo et al., 2006; Han et al., 2004b; Takei et al., 2004; The et al., 1999). These morphogens accumulate in front of the HSPG mutant clones (Belenkaya et al., 2004; Han et al., 2005; Takei et al., 2004) while mutant cells in the clone and competent wild-type cells on the other side of the clone do not have target gene activation (Belenkaya et al., 2004; Bellaiche et al., 1998; Han et al., 2005). However, the morphogens can be detected along the sides of the clone, suggesting that morphogens are forced to travel around the mutant clones. Furthermore, extracellular localization of the Wg and Dpp morphogens in HSPG-defective clones is dramatically reduced (Belenkaya et al., 2004; Han et al., 2005), suggesting that these morphogens are normally retained at the extracellular cell surface by HSPGs.

In the planar transcytosis model, the morphogen undergoes successive rounds of endocytosis and exocytosis to travel from the producing cells, through cells, to the target cells. This model has been studied by blocking endocytosis, and the results are

inconsistent. For example, Wg has been detected in intracellular vesicles named argosomes (Greco et al., 2001), which would support transcytosis. However, Wg movement was unaffected when the endocytic pathway is blocked with *shibire* (*shi*) or *rab5* mutants (Marois et al., 2006; Strigini and Cohen, 2000). Shi is the *Drosophila* homolog of vertebrate Dynamin, a GTPase required for endocytosis and Rab5 is another small GTPase required for endocytosis. Since Wg movement is unaffected by blocking Shi-mediated endocytosis (Strigini and Cohen, 2000), this would suggest that Wg distribution occurs through diffusion. In addition, blocking endocytosis using a dominant negative Rab5 mutant resulted in the extracellular accumulation of Wg on either the apical or basal surfaces, indicating that blocking endocytosis did not prevent extracellular Wg movement. Additionally, disrupting conventional recycling pathways did not affect Wg distribution (Marois et al., 2006). These results suggested that transcytosis was not the mechanism for Wg distribution.

There have also been conflicting results on whether endocytosis affects Dpp movement. Initial studies blocking Shi-mediated endocytosis found a reduced range of Dpp signaling and a shadow on the far side of the mutant clone, reflecting the absence of Dpp. This was interpreted as Dpp movement occurring around the endocytosis-defective tissue (Entchev et al., 2000). Subsequent studies using the same endocytosis mutant, however, had the opposite result where Dpp distribution was not impeded. In this case, Dpp was found on the other side of the clone (Belenkaya et al., 2004). Because of conflicting reports, sometimes even with the same mutants, it is not clear what role endocytosis plays in shaping the morphogen gradient.

In addition to the main three models, long cellular processes called cytonemes have been implicated in morphogen distribution. Cytonemes were initially found to be attracted to another protein important in development, fibroblast growth factor (FGF), and projected themselves towards the FGF source (Ramirez-Weber and Kornberg, 1999). Recently, cytonemes have been observed to be influenced by Dpp and Dpp signaling (Hsiung et al., 2005). In addition, Dpp transmission along cellular processes from the peripodial membrane through the wing disc lumen has also been described (Gibson et al., 2002). While cytonemes have been difficult to detect, their role as a vehicle for morphogen distribution is still a viable possibility.
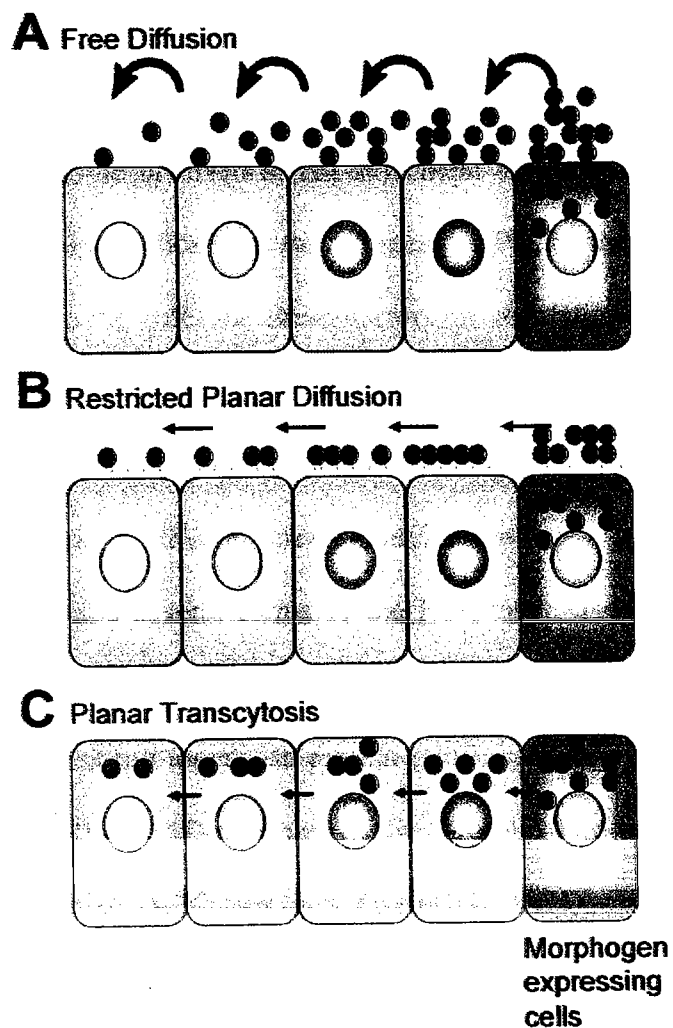
Figure 1.5 - Models for morphogen distribution.

(A) The free diffusion model. Morphogens are secreted from the producing cells into the extracellular space, where they diffuse in three-dimensions out to the target cells.

(B) The restricted planar diffusion model. Morphogens travel in the extracellular space in two-dimensions on cell surfaces, movement that may be facilitated by heparan sulfate proteoglycans (HSPGs) acting as co-receptors or membrane tethers.

(C) The transcytosis model. Morphogens undergo successive rounds of endocytosis and exocytosis to travel through cells, moving from the producing to the target cells.

Components involved in shaping the Hh gradient

Many studies have sought to explain how the Hh gradient forms. Several factors have been demonstrated to be involved in Hh movement and shaping the Hh gradient. These include the Hh lipid modifications, the Hh receptor Ptc, endocytosis, and HSPGs. The current evidence for the roles of these factors in regulating Hh distribution is discussed below.

Identification and the role of the Hh cholesterol modification

Early studies detected several forms of the Hh protein and at that time it was unclear how these different forms were produced or what their role was in Hh signaling. Initial studies found a 46kD full length Hh protein (HhF), a 39kD Hh consistent with a signal sequence cleaved off, a 19kD fragment of the N-terminal portion from full length Hh, and a 25kD fragment of the C-terminus (Lee et al., 1994). Interestingly, the C-terminus of Hh had some similarity to sequences found in serine proteases, specifically amino acids 323-329. Mammalian serine proteases typically have a catalytic histidine (Alberts et al., 1994). Thus, of particular interest in the Hh protein was the histidine found at position 329, which is conserved from *Drosophila* to vertebrates, and when mutated to an alanine, prevented the appearance of the 19kD and 25kD Hh fragments. This histidine is required for the autoproteolysis, as full length Hh is cleaved into the 19kD and 25kD fragments through an intramolecular proteolysis mechanism (Lee et al., 1994). The same study demonstrated that this cleavage was necessary for Hh signaling since uncleaved Hh was unable to activate Wg signaling in embryos, and Dpp signaling

in discs. The N-terminal fragment was further studied and found to be primarily cell-associated, and had a punctate staining pattern, while the C-terminal fragment was found to be secreted and had a more diffuse staining pattern. This led to an early model where the N-terminal fragment might be responsible for short range signaling, while the C-terminal fragment might be responsible for long range signaling (Lee et al., 1994). When constructs designed to replicate these fragments were generated and expressed in wings, the C-terminal fragment was found to have no effect beyond cleavage, while the N-terminus was able to activate Hh targets. Thus, the N-terminal fragment was identified as the active signaling molecule (Fietz et al., 1995).

Similar studies on the Hh fragments were also done with mammalian Shh that found Shh was similarly cleaved and with cleavage requiring the C-terminus (Bumcrot et al., 1995). Interestingly, sequence comparisons found that the N-terminus was the most conserved region of the protein between species. There was 69% sequence identity between the *Drosophila* and mouse Hh, and 99% identity between mouse and chick. This dropped to 30% and 71%, respectively, when further sequences were compared (Bumcrot et al., 1995). This is consistent with all of the actual signaling activity residing within the N-terminus.

Further analysis found differences in an N-terminal Hh generated after full length Hh cleavage (HhNp- for processed), and an N-terminal Hh truncated at the cleavage site (HhN). HhNp was found in cell membranes of *Drosophila* S2 tissue culture cells (derived from embryos; (Porter et al., 1996b), and in "large punctate structures" that localized basolaterally in embryos (Gallet et al., 2003). However, truncated HhN was not

found in S2 or embryo cell membranes, or in these large punctate structures in embryos (Gallet et al., 2003; Porter et al., 1996a). Instead, HhN was localized apically and distributed further away in embryos from the expressing cells. Biochemical experiments found that HhNp had a higher mobility than HhN, and was more hydrophobic, containing an additional 430 daltons than HhN. Subsequently, HhNp was discovered to have an unidentified moiety covalently attached to the carboxyl terminus (Porter et al., 1996a). Additional studies identified cholesterol as this attachment based on its size and other biochemical characteristics (Porter et al., 1996b).

Further studies on the role of cholesterol produced contradictory observations. Studies in both embryos and the wing disc suggested that cholesterol was necessary for the long-range signaling abilities of HhNp (Gallet et al., 2003; Gallet et al., 2006). However, other studies found that HhN was in fact, able to signal to cells further away than HhNp, indicating that the cholesterol moiety may actually restrict HhNp distribution (Burke et al., 1999; Callejo et al., 2006; Dawber et al., 2005; Porter et al., 1996b). Furthermore, peripodial membrane specific expression found that only HhN is able to traverse the lumen to activate genes in the other membrane of the disc (Callejo et al., 2006; Gallet et al., 2006). This suggests that the cholesterol is responsible for restricting HhNp to prevent free diffusion through the lumen. HhN distribution is unaffected in Disp and HSPG mutants (Callejo et al., 2006; Dawber et al., 2005; Gallet et al., 2003), implicating the cholesterol attachment as the cause of the HhNp restricted distribution. In addition, mainly low level target genes are activated by HhN signaling (Callejo et al.,

2006; Torroja et al., 2004), suggesting that cholesterol somehow enhances HhNp activity, possibly by enabling HhNp accumulation.

Mammalian studies of the role of the cholesterol modification also reported conflicting observations (Gofflot et al., 2003; Lewis et al., 2001; Li et al., 2006). Initial studies in mouse systems concluded that the cholesterol was necessary for long-range signaling (Lewis et al., 2001). However, subsequent studies with conditional expression of ShhN without cholesterol found that ShhN was able to activate target genes further away. In addition, the shape of the concentration gradient of ShhN was altered, with less signaling in the cells closer to the expressing cells and more signaling further away. ShhN protein was also observed to be localized to areas further away from the expressing cells than the cholesterol-modified form (Li et al., 2006). Difference between the studies were believed to be the result of technical differences between expression systems where the initial study may have had lower levels of ShhN expressed (Li et al., 2006).

Identification and the role of the Hh palmitate modification

After the discovery of the cholesterol modification, biochemical analysis determined that there was another moiety unaccounted for, which was determined to be a palmitoyl group covalently attached to the amino group on a cysteine at the N-terminus (Pepinsky et al., 1998). Central Missing/Skinny Hedgehog/Sightless/Rasp was discovered to be the acyltransferase responsible for the palmitate addition to Hh (Amanai and Jiang, 2001; Chamoun et al., 2001; Lee and Treisman, 2001; Micchelli et al., 2002). This was the first known instance of an N-linked palmitoylation, since palmitates are

normally thiol-linked. Although the non-palmitoylated Hh could still be secreted and reach target cells, the dually lipidated Hh was 30 times more potent than HhN, indicating that this was the active signaling molecule (Chamoun et al., 2001; Micchelli et al., 2002). Thus, it appears that the primary role of the palmitoylation involves signaling instead of distribution.

To summarize Hh processing, Hh is synthesized as a 45kDa full length precursor protein that undergoes a series of posttranslational modifications as it goes through the secretory pathway. Full length Hh is targeted to the secretory pathway by a signal sequence that is cleaved off. Hh then undergoes an autoproteolytic cleavage between amino acids 257 (Gly) and 258 (Cys), that is catalyzed by the C-terminus of the full length protein. When this cleavage occurs, a cholesterol moiety is covalently attached to the C-terminal end of the N-terminal signaling molecule (Lee et al., 1994; Porter et al., 1996a; Porter et al., 1996b). An additional palmitoyl group is attached to the N-terminus of the signaling molecule through the activity of an acyltransferase (Amanai and Jiang, 2001; Chamoun et al., 2001; Lee and Treisman, 2001; Micchelli et al., 2002; Pepinsky et al., 1998) to produce the 19kDa active Hh signaling molecule, HhNp.

"Large punctate structures"

The cholesterol modification is thought to produce an association with membranes (Peters et al., 2004); therefore, it is unclear how a membrane-associated protein is able to travel away from the producing cells to reach the target cells and initiate signaling. The cholesterol modification could have a role in facilitating movement, for

example by enabling Hh association into more hydrophilic micelle-like larger structures consisting of multiple Hh molecules or other multimeric forms as has been proposed by several groups (Callejo et al., 2006; Chen et al., 2004; Feng et al., 2004; Gallet et al., 2006; Zeng et al., 2001).

One observation made in early studies of Hh protein localization was that Hh was present in "dots" outside of the En expression domain (Forbes et al., 1993) or in "large punctate structures" in *Drosophila* S2 cells (Porter et al., 1996a). Further studies showed that the "large punctate structures" required Disp to form (Gallet et al., 2003; Gallet et al., 2006) and required Ttv for movement (Callejo et al., 2006; Gallet et al., 2003). Most of these particles localized to endosomes (Callejo et al., 2006; Gallet and Therond, 2005; Torroja et al., 2004), and all particles, including ones that did not co-localize with endosomal markers, appeared intracellularly in wing discs (Callejo et al., 2006). Interestingly, in embryos, a class of pre-endocytic particles were identified that were most likely extracellular (Gallet and Therond, 2005). Whether these structures are the vehicle for Hh movement, or whether Hh accumulates in these particles once at the target cells is unclear.

Gel filtration assays identified HhNp multimers of 160kDa from *Drosophila* salivary glands, Clone 8 cells (derived from wing disc cells), and S2 cells (Callejo et al., 2006; Gallet et al., 2006). Interestingly, HhNp multimers required both lipid modifications and could not be detected with the cholesterol or palmitate mutant Hh forms (Callejo et al., 2006; Chen et al., 2004; Gallet et al., 2006). Cell culture experiments using a Ci-luciferase system as a read-out of Hh signaling also suggested

that the multimeric form of Hh had stronger signaling abilities than the monomeric form (Gallet et al., 2006).

In mammalian tissue culture cells, vertebrate ShhNp was also biochemically detected in large multimers that required both lipids (Chen et al., 2004; Feng et al., 2004; Goetz et al., 2006; Zeng et al., 2001), similar to *Drosophila*. These were established to be ShhNp multimers in co-immunoprecipitation assays which demonstrated that ShhNp could bind to other ShhNp proteins (Zeng et al., 2001), possibly in an effort to bury its hydrophobic moieties. These multimers appeared to be relatively stable and resistant to high salt or high detergent conditions (Goetz et al., 2006). Without any lipid modification, Shh could only be found in monomers that had a significantly weaker ability to signal (Chen et al., 2004; Feng et al., 2004; Goetz et al., 2006). Furthermore, biologically active ShhNp multimers could also be isolated from chick limb bud tissue (Zeng et al., 2001), indicating that these multimers were also present *in vivo*. Thus, multimeric ShhNp could be the primary active biological Shh (Goetz et al., 2006; Zeng et al., 2001). It is thought that these multimers may increase ShhNp activity and keep ShhNp in a form that is capable of moving through the extracellular environment (Goetz et al., 2006).

The role of Ptc

Initial genetic studies implicated Ptc as the Hh receptor (Schuske et al., 1994). Further experiments with *ptc* mutants found that Ptc could bind and restrict Hh movement, and this resulted in the activation of Hh target genes, one of them being *ptc*

itself (Chen and Struhl, 1996). Ptc had two distinct functions: the first was to activate Hh signaling, and the other was to bind and sequester Hh. Ptc contained a sterol sensing domain (SSD) that was implicated in being involved in signaling activation. Evidence for this comes from experiments where Ptc-SSD mutants are able to bind and sequester Hh, but have autonomous activation of only low level targets regardless of Hh levels (Martin et al., 2001; Strutt et al., 2001). Additionally, a gain of function *ptc* allele that has relatively low binding affinity for Hh is constitutively active (Mullor and Guerrero, 2000). Thus, the ability of Ptc to bind to Hh is separable from its capacity to activate signaling. The role of Ptc in activating Hh signaling is evident. The question remains as to whether Ptc has an active role in Hh transport through cells.

Under normal conditions, Ptc binds Hh and the complex is endocytosed in a Shi-dependent manner (Capdevila et al., 1994; Incardona et al., 2000). Hh endocytosis also appeared to be dependent on Ptc in mammalian systems (Incardona et al., 2002; Incardona et al., 2000). Endocytosis of Ptc results in removal of Hh from the extracellular space, as well as Smo relocalization to the cell surface and C-terminus modification (Denef et al., 2000; Hooper, 2003; Incardona et al., 2002; Ingham et al., 2000; Jia et al., 2003; Ruel et al., 2003; Zhu et al., 2003). After the Hh-Ptc complex is endocytosed, the complex is targeted to lysosomes for degradation (Callejo et al., 2006; Gallet and Therond, 2005; Torroja et al., 2004). It appears that Ptc-dependent endocytosis leads to the eventual degradation of Hh; however, Hh dissociation from Ptc and recycling after Ptc-dependent endocytosis cannot definitively be ruled out. In *ptc* mutant embryos, there is an apical accumulation of Hh particles at target cells (Gallet and

Therond, 2005), suggesting that Ptc was not necessary for Hh movement. Additionally, *ptc* mutant clones in the wing disc do not block Hh distribution; in fact, Hh is able to travel further, past the clone (Chen and Struhl, 1996). It appears that while Ptc does not have a role in Hh movement, it is a critical player in shaping the Hh gradient by sequestering Hh and removing Hh from the system. Interestingly, Ptc-independent endocytosis has been observed but the identity of these vesicles is unknown (this study; (Callejo et al., 2006; Gallet and Therond, 2005; Torroja et al., 2004).

Endocytosis and morphogen distribution

If transcytosis had a significant role in Hh gradient formation, blocking endocytosis should have a dramatic effect on Hh distribution. In the receiving cells, Ptc binds Hh and the complex is endocytosed. As previously stated, Hh that is endocytosed by Ptc is targeted for degradation (Callejo et al., 2006; Gallet and Therond, 2005; Torroja et al., 2004). No evidence has been found to suggest that Hh endocytosed by Ptc is recycled and released from the cell (Gallet et al., 2006). Loss of Ptc results in Hh relocalization but does not prevent Hh movement (Chen and Struhl, 1996; Gallet and Therond, 2005).

To better examine whether endocytosis affects morphogen distribution, endocytosis mutants have been utilized in *Drosophila*. Using a dominant negative mutant in embryos to block endocytosis does not appear to affect Hh movement (Gallet and Therond, 2005). In wing discs, blocking endocytosis affects Hh localization leading to the accumulation of HhNp at the cell membranes basolaterally (Han et al., 2004b;

Torroja et al., 2004) while HhN accumulates apically (Callejo et al., 2006). Interestingly, signaling and movement of Hh is unaffected within the mutant clone (Callejo et al., 2006; Han et al., 2004b; Torroja et al., 2004). Since temperature sensitive endocytic mutants were used in most of these studies, endocytosis was only blocked for a short five hour period of the Hh distribution process while Hh expression occurred throughout development. Thus, this accumulation may be the result of a redistribution of Hh that was already present at those cells instead of an ability of Hh to travel despite the endocytosis block. Wing disc studies where endocytosis is blocked during gradient formation instead of at the gradient steady-state will be necessary to distinguish between redistribution and movement, and determine whether endocytosis really affects Hh distribution.

HSPGs aiding Hh distribution

HSPGs in the extracellular matrix have been implicated in affecting HhNp distribution. Initial studies found that HhNp could bind to heparin beads and may interact with heparin-modified proteins in the extracellular matrix (Lee et al., 1994). In addition, while HhNp was barely detectable in tissue culture media, it could be displaced by heparin treatment, leading to the same idea that Hh may interact with proteins in the extracellular matrix or cell membranes (Bumcrot et al., 1995). Disruption of HSPG biosynthesis using the Ext family of proteins (Ttv, Sotv, and Botv) has been shown to affect all three morphogen pathways (Bellaiche et al., 1998; Bornemann et al., 2004; Han et al., 2004a; Takei et al., 2004; The et al., 1999). The Exts are glycosyl transferases,

enzymes essential for the proper production of HSPGs. Mutations in *ttv* and *sotv* have been shown to result in decreased heparan sulfate glycosaminoglycan chain synthesis (Bornemann et al., 2004). Therefore, the *Ext* genes affect Hh distribution through proper HSPG production. The *Ext* mutants caused a decrease in Hh signaling levels, as well as decreased levels of Hh protein in the mutant wing disc tissue (Bornemann et al., 2004; Han et al., 2004a; Takei et al., 2004). Ttv is required for the long range distribution of HhNp (Gallet et al., 2003; The et al., 1999). In both *ttv* mutant embryos and in *ttv* mutant clones in the wing disc, the activation of Hh signaling, as well as movement of Hh is only detected in the first row of cells closest to the Hh producing cells (Bellaiche et al., 1998; The et al., 1999). Hh accumulates in the wild-type tissue in front of the mutant clone and no Hh signaling is observed behind the clones (Bellaiche et al., 1998; Takei et al., 2004). In addition, clonal analysis indicates that the absence of functional HSPGs forces HhNp movement around the clone. These observations suggest that properly modified HSPGs are required for the planar movement of HhNp.

The HSPG core proteins themselves, specifically the GPI-linked glypicans Dally and Dally-like (Dlp), have been shown to affect HhNp distribution as well (Han et al., 2004b). In embryos, Dlp was shown to be required for Hh signaling and epistasis experiments placed Dlp upstream of Ptc (Desbordes and Sanson, 2003), indicating that Dlp action occurs during distribution. In *dally/dlp* double mutant wing disc clones, there is reduced Hh signaling and HhNp distribution to only the first row of the mutant clone (Han et al., 2004b), similar to *Ext* mutant clones. Since Ttv is responsible for proper biosynthesis of the heparan sulfate chains for Dally and Dlp (Han et al., 2004b), this

suggests that the effects of the *Ext* and glypican mutants arise from the same defect, that is loss of HSPGs. Furthermore, HhNp co-localized with Dlp (Han et al., 2004b) and RNAi experiments in *Drosophila* Clone 8 cells identified Dlp as a possible co-receptor (Lum et al., 2003a). Similar to the *Ext* experiments, these observations point to HSPG-mediated planar movement of HhNp.

The secreted protein Shifted (Shf) is a HSPG-interacting protein that also affects Hh distribution. Mutant clones of *shf* demonstrate reduced Hh signaling, reduced range of HhNp distribution, and reduced amounts of basolateral HhNp (Glise et al., 2005; Gorfinkiel et al., 2005). Double mutant clones of *shf* and *ttv* in Hh-expressing cells in the posterior compartment show reduced levels of HhNp protein, the same phenotype as the *ttv* single mutant (Gorfinkiel et al., 2005). This indicates that Shf acts upstream of HSPGs during Hh distribution, and also is suggestive of a role for HSPG in HhNp distribution.

Interestingly, HSPGs (Callejo et al., 2006; Gallet et al., 2003), and Shf (Glise et al., 2005; Gorfinkiel et al., 2005) have no effect on the non-cholesterol modified HhN. The GPI-linked glypicans could localize to lipid microdomains (lipid rafts) and thus, interact with cholesterol modified Hh in these compartments. Therefore, the cholesterol modification would confer the ability for HhNp to interact with HSPGs.

HSPGs clearly have an important role in Hh distribution and gradient formation. However, their exact role is undefined. While previous studies strongly support HSPG involvement in the extracellular planar diffusion of Hh, HSPG involvement in a transcytosis mechanism cannot be conclusively ruled out. Current results do not make a

clear distinction between whether HSPGs are simply co-receptors that aid in signaling, or whether they have a more active role in Hh distribution. Further study is necessary to be able to elucidate the precise role of HSPGs.

Theoretical Modeling of morphogen gradient formation

Theoretical modeling has attempted to establish mathematical models to explain which mechanisms must be the cause of qualitative observations. However, even theoretical studies have shown conflicting results on whether morphogen gradients arise solely through diffusion or through a combination of short-range diffusion and long range transcytosis. Lander et al. generated a model for the mechanism of morphogen transport where they take into account diffusion, receptor binding, internalization, and degradation (Lander et al., 2002). Their analysis stemmed from observations made in earlier Dpp distribution studies (Entchev et al., 2000; Teleman and Cohen, 2000). According to their theoretical analysis, the diffusion model can explain previous results of internalized Dpp, the blockage of endocytosis resulting in a "shadow" behind mutant clones, as well as a reduced range of signaling. The conclusion from the initial study by Entchev et al. was that Dpp requires endocytosis for distribution (Entchev et al., 2000). However, in the diffusion model, the endocytosis block would result in an increased number of receptors on the cell surface that would bind Dpp, and thus a steeper Dpp gradient through the clone which may be steep enough to produce the shadow effect by sequestering Dpp (Lander et al., 2002). This would explain the reduced range in signaling as well. The previous data showed this shadow was present at a 5 hour time point after blocking

endocytosis and eventually gets filled by 24 hours (Entchev et al., 2000), which is also supported by the diffusion modeling (Lander et al., 2002). Additionally, previous data analyzing the rates of gradient formation found it took 7 hours for the Dpp gradient to form and the rate of transcytosis from EGF studies in cultured cells estimated at 0.6-4 hours per cell. Furthermore, the bucket brigade mechanism was determined to be a minimum of 771 seconds per cell. These rates are far too slow to account for the rapid rate of gradient formation calculated to be 54-148 seconds per cell (Lander et al., 2002).

A separate theoretical modeling of morphogen transport also based their analysis on the same Dpp distribution studies but took additional factors into account (Kruse et al., 2004), including a comparison of theoretical expected results and actual experimental results. Kruse et al. analyzed transport with a two-dimensional description, while Lander et al. simplified the process to one-dimension. Also, Kruse et al. slightly altered one of the parameters in the diffusion modeling while looking at the block in endocytosis results so that there was not an instantaneous increase in receptor levels in mutant tissue. In doing so, Kruse et al. demonstrated that the original theoretical diffusion model would have resulted in a steady increase in receptor and ligand in the mutant tissue, which would have produced a more pronounced shadow through time, instead of a transient shadow. This result from the model does not agree with the experimental data: there was no significant increase in receptor or ligand (extracellular Dpp) and the shadow is only transient (Entchev et al., 2000). The conclusion is that the theoretical diffusion model is unable to explain Dpp distribution results, implying a role for other factors such as receptor trafficking and other mechanisms in morphogen distribution (Kruse et al., 2004).

There is agreement about the time of gradient formation appearing to be rather rapid compared to current data about transcytosis and turnover time, although the actual rate of various processes, including extracellular diffusion, endocytosis, and recycling, has yet to be determined for morphogens in the wing (Kruse et al., 2004; Lander et al., 2002).

Much more quantitative analysis of morphogen distribution and movement is needed, particularly during gradient formation as opposed to gradient steady state, to provide data enabling the generation of accurate mathematical models of morphogen gradient formation.

Summary

The morphogen Hh has been identified as one of the factors responsible for determining cell fates and producing patterns in tissues during development of many organisms. Disruption of Hh distribution and signaling can have serious consequences during development as demonstrated by human birth defects and disease. Since Hh was first discovered in *Drosophila*, this organism has proven to be a useful model system to study the Hh gradient and signaling pathway.

Previous studies have provided much information about Hh distribution; however, these studies also had limitations. I have attempted to address these limitations to clarify previous conflicting data. One limitation of previous studies was that overexpressed Hh and/or preexisting pools of Hh were examined, instead of newly produced protein. Therefore, the observed accumulation of Hh may be the result of a redistribution of protein that was already present instead of an ability of Hh to move despite a block in

endocytosis. This issue has been addressed by using an inducible system, allowing the study of newly synthesized protein. Another limitation to the previous work is the analysis of Hh distribution at the gradient steady state and not during gradient formation, which may provide more information of how Hh moves. This too can be addressed with an inducible system. Finally, observations made about Hh distribution were qualitative, while quantitative data came primarily from target gene activation instead of Hh itself. This has been addressed by quantifying Hh particle distances with image analysis software.

Thus, questions remain over the role of cholesterol modification in regulating Hh distribution, and whether endocytosis is required for Hh gradient formation. By addressing limitations of previous studies, these questions can be answered. This thesis presents data to support the hypothesis that Hh movement is restricted by the cholesterol modification and that endocytosis is not required for Hh movement, which occurs through a planar diffusion mechanism.

CHAPTER II

QUANTITATIVE ANALYSIS OF HEDGEHOG GRADIENT FORMATION USING AN INDUCIBLE EXPRESSION SYSTEM

Background

Members of the Hh family have an evolutionarily conserved role in regulating growth and differentiation during development of many organisms (Ingham and McMahon, 2001). Hh directly induces different cell fates in a concentration dependent manner, and thus is classified as a morphogen. This concentration gradient is tightly regulated and any disruption can cause abnormal cell specification (Heemskerk and DiNardo, 1994; Strigini and Cohen, 1997). Mutations in Hh pathway components have also been shown to lead to human disorders and disease (Hooper and Scott, 2005).

In *Drosophila*, the Hh morphogen is produced and secreted from posterior compartment cells in embryos and imaginal wing discs. Hh travels to anterior target cells and forms a concentration gradient from its source (Ingham and McMahon, 2001; Tabata and Takei, 2004). Models that have been proposed for morphogen distribution and gradient formation include free diffusion and planar movement. In the free diffusion model, the morphogen is secreted from the producing cells into the extracellular space and diffuses in three-dimensions out to the target cells. In the planar movement model, the morphogen moves directly from cell to cell, always remaining in the two-dimensional epithelial cell layer. Two mechanisms for planar movement have been proposed:

restricted extracellular planar diffusion along the cell surface and transcytosis, where successive rounds of endocytosis and exocytosis move Hh through cells (Hooper and Scott, 2005; Tabata and Takei, 2004).

Hh proteins in all organisms are dually lipid modified as part of their intracellular processing to produce HhNp (p for processed) and these modifications are likely to affect movement of the morphogen. In *Drosophila*, Hh is synthesized as a 45 kDa full length precursor protein that undergoes an autoproteolytic cleavage (Lee et al., 1994; Porter et al., 1996a). Cholesterol is covalently attached to the C-terminus of the N-terminal signaling molecule as part of this process (Porter et al., 1996b). A palmitoyl group is attached at the N-terminus by a membrane bound O-acyltransferase to produce a dually lipidated 19 kDa HhNp molecule (Amanai and Jiang, 2001; Chamoun et al., 2001; Lee and Treisman, 2001; Micchelli et al., 2002; Pepinsky et al., 1998). Because the protein is lipid modified, Hh movement must include a mechanism that prevents this modification from restricting Hh to the membranes of the producing cells. One mechanism to mobilize lipid modified Hh may be to form micelle-like structures; in gel filtration assays, Hh and Shh multimers, which require both lipid modifications, can be detected (Callejo et al., 2006; Chen et al., 2004). This high molecular weight Hh fraction will associate with cell membranes in tissue culture cells while the monomeric forms do not (Feng et al., 2004; Gallet et al., 2003). The hydrophobic moieties could be hidden inside multimeric micelle-like structures to make the HhNp complexes more soluble in order to diffuse (Chen et al., 2004; Zeng et al., 2001). Therefore, the cholesterol modification could be required for multimerization that enables long range movement and proper

gradient formation. The requirement for cholesterol modification in signaling is not clear due to conflicting reports from both *Drosophila* and mammalian studies. In some studies, using *Drosophila* wing discs and mouse limb buds, the unmodified Hh (HhN) has long range activity (Burke et al., 1999; Callejo et al., 2006; Dawber et al., 2005; Li et al., 2006; Porter et al., 1996b). However, other *Drosophila* and mammalian studies suggest that cholesterol is required for long range activity (Gallet et al., 2003; Gallet et al., 2006; Gofflot et al., 2003; Lewis et al., 2001).

In *Drosophila* and vertebrates, the extracellular matrix components heparan sulfate proteoglycans (HSPGs) are involved in Hh movement. Loss of HSPGs block Hh movement, and signaling in adjacent wild-type cells is impaired (Bellaiche et al., 1998; Bornemann et al., 2004; Desbordes and Sanson, 2003; Han et al., 2004b; Lum et al., 2003a; Takei et al., 2004; The et al., 1999). Interestingly, HSPG regulation of Hh movement depends on cholesterol, as unmodified HhN is unaffected by the loss of HSPGs (Callejo et al., 2006). The cholesterol may mediate Hh and HSPG association, as cholesterol-modified Hh and Shh are able to bind heparin (Bumcrot et al., 1995; Lee et al., 1994). One interpretation of these results is that HSPGs are required to mediate planar movement of cholesterol-modified Hh across or through target cells, but that unmodified Hh is able to move via free diffusion. In support of this model, unmodified Hh expressed in the peripodial cell layer of the developing *Drosophila* wing can move through the extracellular space of the wing lumen while cholesterol-modified Hh is restricted to the layer of cells in which it is expressed (Callejo et al., 2006; Gallet et al., 2006).

Receptor-mediated endocytosis has also been proposed to regulate the spreading of Hh. In addition to transducing the Hh signal, Patched (Ptc), the receptor for Hh, has been shown to sequester and limit the range of distribution by binding and internalizing Hh (Chen and Struhl, 1996; Torroja et al., 2004). Hh is thought to be primarily endocytosed together with Ptc and then targeted for degradation (Callejo et al., 2006), although Ptc-independent cytoplasmic Hh particles have been detected as well (Gallet and Therond, 2005; Torroja et al., 2004). A role for endocytosis in Hh gradient formation has been proposed, either as part of transcytosis or by removing Hh to limit the distribution range. Blocking endocytosis in embryos and wing discs with a *dynamin* mutant (*shibire* in *Drosophila* or *shi*) does not appear to affect Hh target gene expression or spreading (Callejo et al., 2006; Gallet et al., 2003; Han et al., 2004b; Torroja et al., 2004). These observations suggest that Shi-mediated endocytosis may be required for Hh degradation but not Hh distribution. However, in these experiments, *shi* is inactivated in tissues with a preexisting gradient of Hh. It is unclear whether the Hh distribution observed reflects this preexisting pool or newly synthesized Hh produced following *shi* inactivation.

While previous studies provided much information about Hh distribution, these studies also have some limitations that may contribute to conflicting conclusions. One limitation that had been suggested was that overexpressed Hh and/or preexisting pools of Hh, instead of newly produced protein, were examined (Wendler et al., 2006). Therefore, the observed distribution of Hh may reflect redistribution of preexisting protein instead of the ability of Hh to move despite the endocytosis block. This issue can be addressed by

using an inducible system where the movement of newly synthesized protein is studied. Another limitation is that Hh distribution was examined after the Hh gradient had reached a steady state; analysis during gradient formation may provide more information about Hh movement. This too can be addressed with an inducible system. Finally, observations made about Hh distribution were largely qualitative, while quantitative data came primarily from target gene activation instead of determination of Hh protein levels.

This study has attempted to resolve these issues by quantitatively investigating the distribution of GFP-tagged forms of Hh using an inducible expression system. To determine whether the cholesterol modification and/or endocytosis have any effect on the process of gradient formation, functional Hh-GFP with and without the cholesterol-modification is expressed in a wild-type or shi^{ts1} mutant background. Specifically, the Gal80-Gal4 system was used to temporally express (pulse) Hh-GFP transgenes in their normal expression domain (the posterior compartment of the developing wing); this method allows the rate of Hh gradient formation over time to be observed. This study demonstrates that both HhNp-GFP and HhN-GFP are present in punctate structures (particles). A system has also been developed for quantitative measurement of Hh distribution and found that HhN-GFP migrates further than HhNp-GFP while less is retained near the expressing cells. This study demonstrates that when endocytosis is blocked, newly synthesized HhNp-GFP is still detected in particles and can still move anteriorly, arguing against an essential role of transcytosis. Lumenal HhN-GFP particles were observed, indicating cholesterol is responsible for retaining Hh on cell surfaces. I propose that HhNp and HhN spread through both apical and basolateral regions by planar

diffusion and that the cholesterol modification serves to retain Hh on the cell surface and

promotes formation of a steep gradient.

Results

Generation of Hh-GFP fusion constructs and functional characterizations.

To study movement and distribution of newly synthesized Hh, Hh-GFP fusion proteins were generated that are suitable for both live and fixed tissue experiments. The HhF-GFP fusion construct (Figure 2.1A) contains GFP coding sequences placed between Hh amino acids 254 (H) and 255 (V). The same location was used previously to generate functionally tagged HhNp (Burke et al., 1999; Callejo et al., 2006), which is expected to be processed into a HhNp-GFP and an untagged Hh-C. To express unprocessed HhN-GFP, an expression construct was made that encodes the N-terminus of Hh fused to GFP.

Several experiments were performed to determine whether HhNp-GFP is functional. First, HhNp-GFP was constitutively expressed with the Gal4-UAS system (Brand and Perrimon, 1993) using Hh-Gal4, which would express the transgene using the endogenous *hh* promoter. DsRed protein was co-expressed with the Hh fusion protein to identify expressing cells and mark the anterior/posterior (A/P) boundary in this and subsequent experiments. HhNp-GFP was secreted from the dsRed-expressing cells similar to untagged wild-type HhNp (Figure 2.1B-D). Second, anti-Hh and anti-GFP antibodies were used to detect HhNp-GFP and both co-localized with HhNp-GFP (Figure 2.1E-J). Third, HhNp-GFP and HhN-GFP were expressed in salivary glands using the ubiquitous 71B-Gal4 driver and the glands were extracted to identify the Hh fusion proteins on a Western blot (Figure 2.1K). For HhN-GFP, an approximately 46 kDa protein band was detected corresponding to the predicted size of the N-terminus fused to

GFP (lane 3). For HhNp, an approximately 70 kDa band representing the uncleaved full length HhF-GFP protein (U) and a 46 kDa band representing the cleaved HhNp-GFP signaling molecule (P, lane 4) were observed. These results indicate that both Hh-GFP fusion proteins are expressed and properly processed. Fourth, the ability of HhNp-GFP to rescue the embryonic lethality of homozygous hh^{GS1} mutants was tested. Expressing HhNp-GFP in the posterior compartment using the En-Gal4 driver, hh^{GS1} mutants were fully rescued to adulthood. These animals appeared to develop normally, as demonstrated by a normal though slightly smaller wing (Figure 2.1M). The wings of flies ectopically expressing functional untagged HhNp (Porter et al., 1996a) and wings expressing HhNp-GFP had similar phenotypes of merged wing veins L2 and L3 (Figure 2.1N and 2.1O). Finally, the ability of HhNp-GFP to rescue hh^{GS1} mutant embryonic phenotypes was tested. Cuticle preparations demonstrated that HhNp-GFP expressed in the posterior compartment with the En-Gal4 driver in the hh^{GS1} mutant was able to rescue the mutant "lawn of denticles" phenotype in the expected Mendelian ratios (Figure 2.1P-R and Table 1). Additionally, *in situ* hybridization showed that posterior HhNp-GFP expression restores activation of *rhomboid* (*rho*), an embryonic Hh target gene, in hh^{GS1} mutant embryos. These results demonstrate that the Hh-GFP fusion proteins are properly synthesized, and that HhNp-GFP has the same properties as previously described for wild-type HhNp (Ingham, 1998).
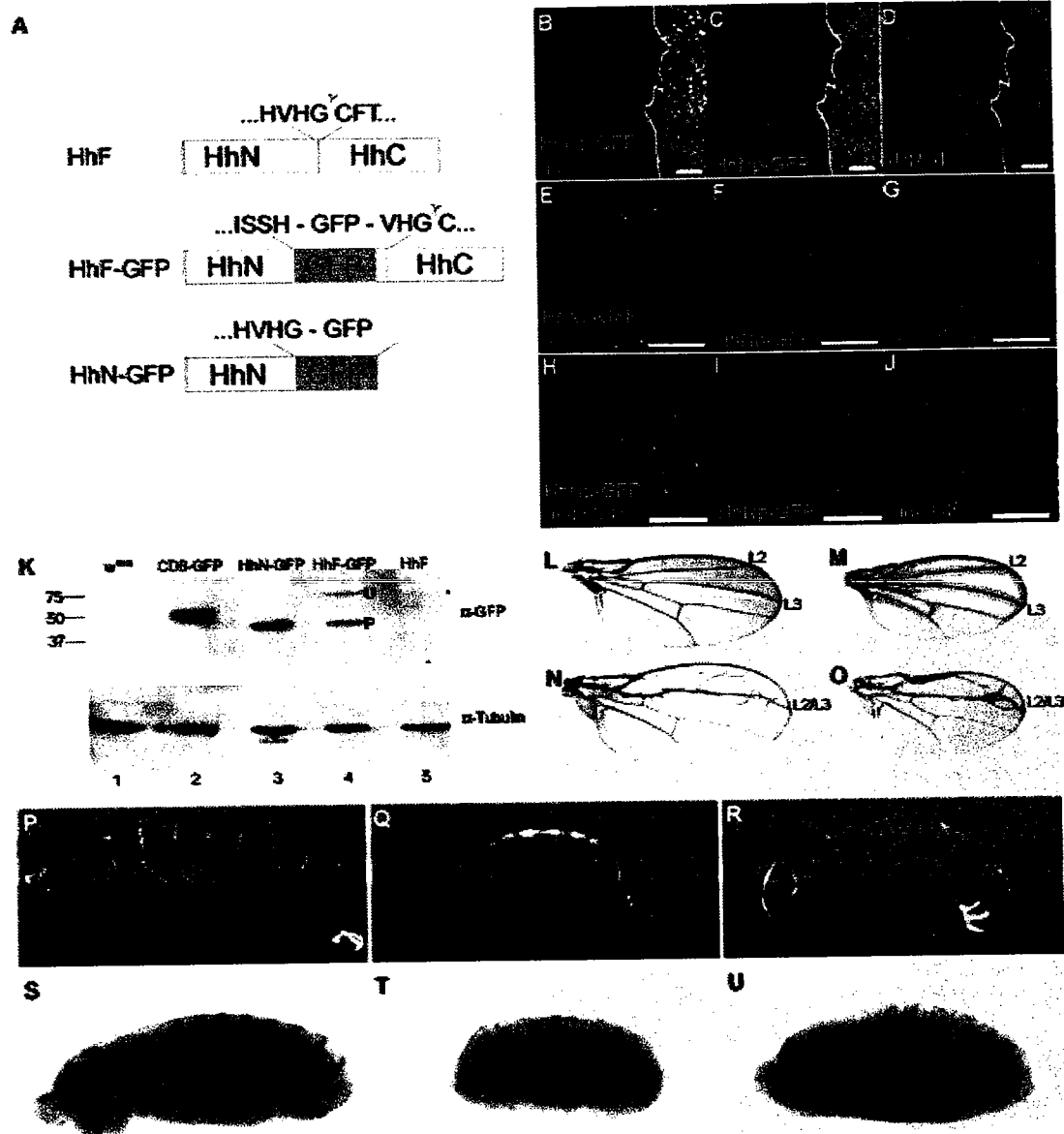
Figure 2.1 - HhNp-GFP is functional.

(A) Scheme of HhF-GFP (middle) and HhN-GFP (bottom) fusion constructs and predicted processing as compared to wild-type HhF (top). HhF-GFP is predicted to be processed into HhNp-GFP.

(B-D) HhNp-GFP (green, C) is expressed in posterior cells labeled by fluorescent protein dsRed (red, D) and is secreted (B), similar to wild-type HhNp (A/P boundary marked by a solid white line). Scale bar: 5μm

(E-J) HhNp-GFP (E,H) can be detected using the anti-Hh antibody (F,G) and anti-GFP antibody (I,J). Scale bar: 8μm

(K) Western blot of salivary gland protein extracts labeled with anti-GFP (upper panel) or tubulin (lower panel). Upper panel: as negative controls, extracts of wild-type w^{1118} larvae (lane 1) and larvae expressing an untagged HhF (lane 5) were used, CD8-GFP was used as a positive control (lane2). A single 46 kDa band is seen in the lane with HhN-GFP expressing larvae (lane 3) and in the lane loaded with extract of HhF-GFP expressing larvae, two bands of 70 kDa and 46 kDa are seen (lane 4; U: unprocessed full-length HhF-GFP, P: processed HhNp-GFP). Lower panel: the same blot was reprobed with anti-tubulin for loading control.

(L-O) HhF expression in adult wings. (L) Wild-type wing. (M) Wing from HhF-GFP rescue of hh^{GSI} mutant has a similar phenotype to wild-type. (N) As a positive control, untagged HhF is expressed with 71B-Gal4 resulting in merged veins L2 and L3. (O) Ectopic expression of HhF-GFP has a similar phenotype to untagged HhF.

(P-R) HhF-GFP expression rescues hh^{GSI} mutant cuticle phenotype. (P) Wild-type embryonic cuticle. (Q) hh^{GSI} mutant embryonic cuticle is characterized by a 40% length of wild-type, loss of naked cuticle, and the "lawn of denticles" phenotype. (R) HhF-GFP expression under the En-Gal4 promoter can rescue the hh^{GSI} mutant phenotype, restoring some of the naked cuticle in the segments.

(S-U) HhF-GFP expression restores *rho* expression in hh^{GS1} mutant. (S) *In situ* hybridization of *rho* in a wild-type embryo. (T) *rho* expression in the hh^{GS1} mutant is dramatically reduced, (U) HhF-GFP expression under the En-Gal4 promoter restores expression of *rho* in the hh^{GS1} mutant.

Table 1. HhF-GFP Rescue cuticles

Genotype	Normal	Intermediate	Mutant
En-Gal4; hh^{GS1}/TM3	89.5% (325)	2% (7)	8.5% (31)
En-Gal4 HhF-GFP; hh^{GS1}/TM3	74% (218)	25% (71)	1% (4)

Percentages were calculated, total numbers are indicated in parenthesis.

Analysis of HhNp-GFP localization in living tissue.

The *Drosophila* larval wing imaginal disc consists of two layers of epithelial cells, separated by the peripodial lumen. On the apical side, a squamous epithelial layer forms the peripodial membrane, while on the basal side, the disc epithelium is found that will give rise to the wing and notum. Most previous studies exploring HhNp localization in the disc epithelium have been performed with fixed discs. In these studies and my own experiments with fixed discs, most HhNp in the anterior compartment is found in punctate structures, as detected by immunostaining. To rule out the possibility of fixation-induced alterations in Hh localization, I took advantage of the GFP tag to examine the localization of HhNp-GFP in live tissues. Hh-Gal4 was used to express HhNp-GFP in the endogenous Hh expression domain in the posterior compartment of the wing imaginal disc (Tanimoto et al., 2000). In live discs, HhNp-GFP co-localized with the membrane marker FM4-64 in the posterior compartment and was also found in particles in both the posterior and anterior compartments (Figure 2.2A). These particles were found in both apical and basolateral regions (Figure 2.2B). HhNp has previously been observed in endosomes (Callejo et al., 2006; Gallet et al., 2003; Gallet and Therond, 2005; Torroja et al., 2004). Endocytosed dextran was used to determine whether the particles containing HhNp-GFP in live discs included endosomes. In both the anterior and posterior compartments, many, but not all, of the HhNp-GFP particles co-localized with dextran (Figure 2.2C-D), confirming that at least some HhNp particles correspond to endosomes. The non-co-localizing HhNp-GFP vesicles could represent endosomes

formed before or after dextran incubation, non-endocytic vesicles, or extracellular particles.

The extracellular distribution of HhNp-GFP was investigated, using an *"in vivo"* extracellular labeling method as described by Strigini and Cohen (Strigini and Cohen, 2000). In this procedure, live discs are incubated with anti-GFP antibody and then washed prior to fixation and detergent treatment. In control experiments using this method, a protein with an extracellular GFP tag (GFP-Dally-like) was detected while an intracellular YFP tag (Ptc-YFP) was not detected, demonstrating that the staining procedure reliably distinguished between extracellular and intracellular localization (Figure 2.3A-B). When similar experiments were performed for HhNp-GFP, strong extracellular staining was observed in the apical and basal regions in the posterior compartment of the disc where Hh is produced (Figure 2.2E and Figure 2.3C-D). In the anterior compartment, extracellular HhNp-GFP was detected in apical particles (Figure 2.2E and Figure 2.3C-D, arrows), basolateral particles (Figure 2.2E and Figure 2.3C-D, arrowheads) and on the basolateral membrane (Figure 2.2E and Figure 2.3C-D, bracket). These localization results are consistent with previously published data for both untagged and tagged HhNp (Callejo et al., 2006; Gallet et al., 2006; Torroja et al., 2004). In conclusion, the largely punctate localization of tagged and native Hh observed in the anterior compartment of the developing wing after fixation accurately reflects the localization of Hh in living tissues.

Figure 2.2 - HhNp-GFP localizes at the membrane, in endocytic compartments, and extracellularly.
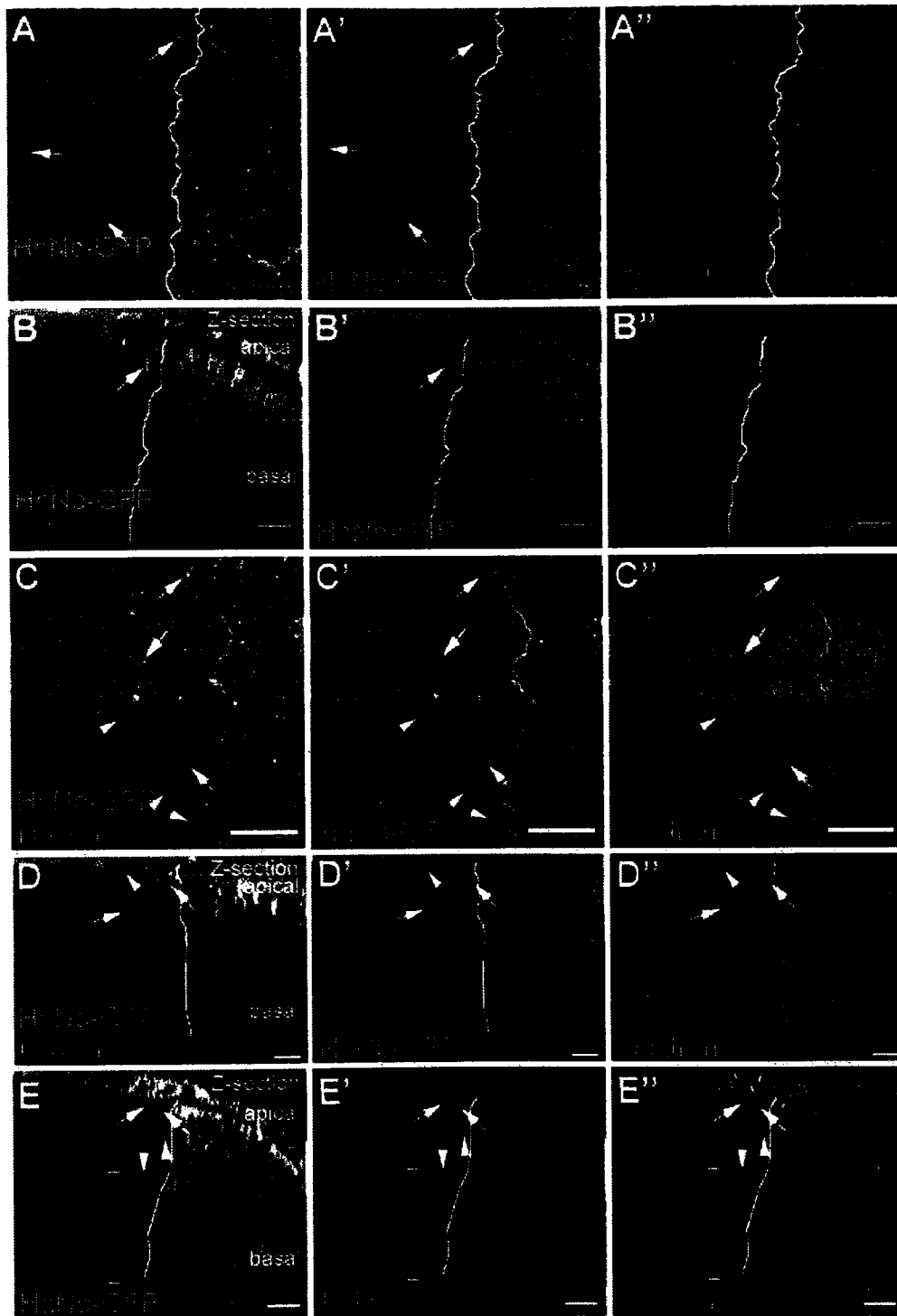
Figure 2.2 - HhNp-GFP localizes at the membrane, in endocytic compartments, and extracellularly.

(A-E) Localization of HhNp-GFP (green), expressed with Hh-Gal4, with FM4-64 (red, A-B), dextran (red, C-D), as well as extracellular labeling with the anti-GFP antibody and DCAD to mark the apical region (red and blue, E). (B,D,E) Z-sections. HhNp-GFP (A') co-localizes with FM4-64 (A") at the membrane in the posterior (A/P boundary marked by the solid white line) as seen in the merge (A). Anterior HhNp-GFP appears in particles (arrows). Most of the particles localize apically (B). Many of the anterior HhNp-GFP particles co-localize (arrows in C-D) with dextran but some can be found without dextran (arrowheads in C-D). Incubation of anti-GFP in cold medium detects extracellular HhNp-GFP in the anterior apically in particles (arrows in E), and basolaterally both in particles (arrowheads in E) and with a membrane association (bracket in E). Scale bar: 8μm

Figure 2.3 – **Extracellular Hh localizes apically in particles and basolaterally in particles and along the membrane.**
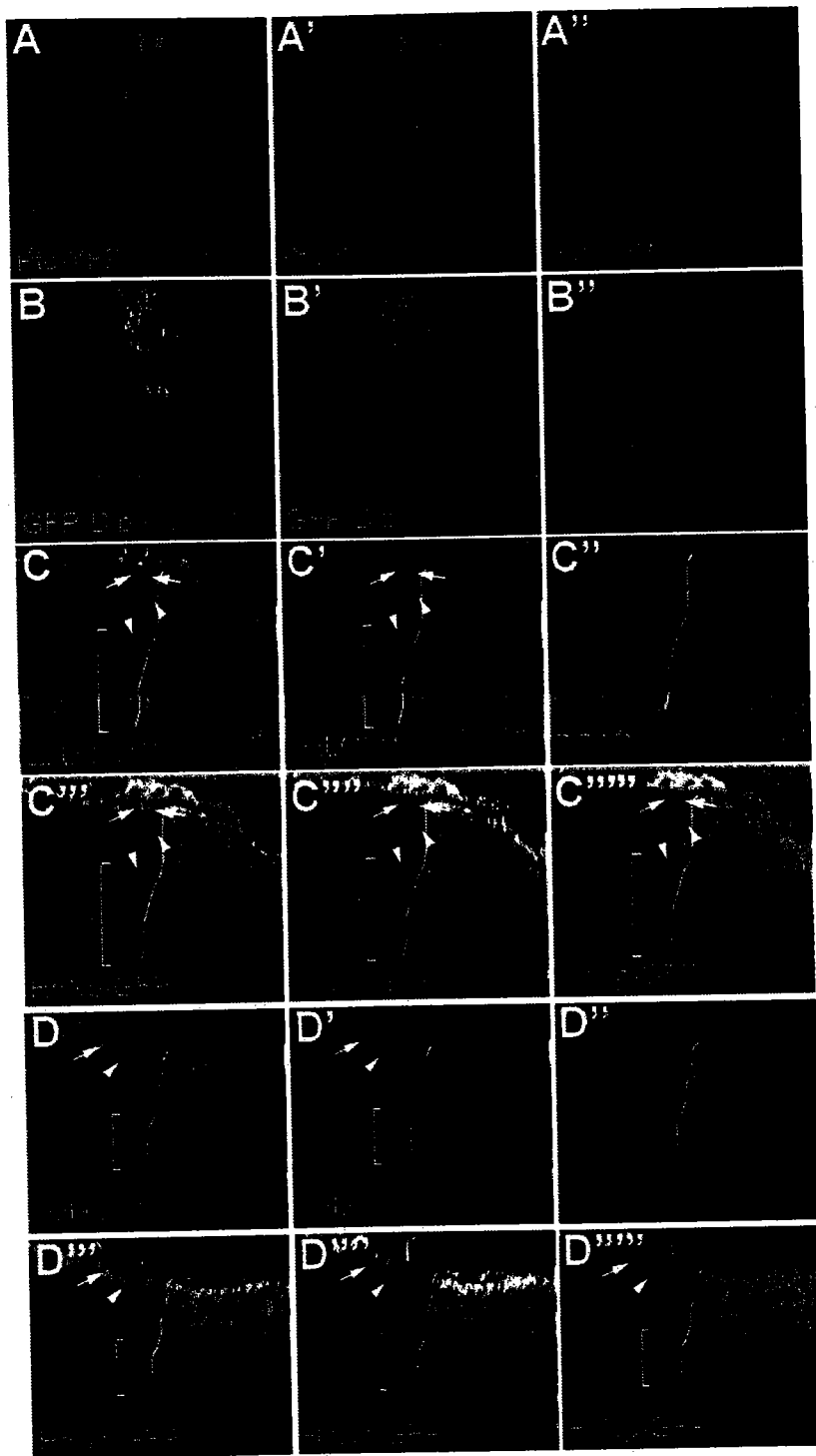
Figure 2.3 – Extracellular Hh localizes apically in particles and basolaterally in particles and along the membrane.

(A-B) Ptc-YFP (green, A) and GFP-Dlp (green, B), and extracellular labeling (red). As controls for the extracellular labeling protocol with the anti-GFP antibody, Ptc-YFP was used as a negative control since YFP is attached to the cytoplasmic region of Ptc and GFP-Dlp was used as a positive control since GFP is attached to the extracellular region of Dlp.

(C-D) HhNp-GFP (green), extracellular labeling with the anti-GFP antibody (red), and DCAD to mark the apical region (blue- C,C'',D,D''; purple-C''',D'''). Two separate examples of extracellular HhNp-GFP, extracellular HhNp-GFP is detected in the anterior apically in particles (arrows in C and D), and basolaterally both in particles (arrowheads in C and D) and with a membrane association (bracket in C and D).

Induction and quantitative analysis of a Hh gradient.

In the experiments described above and by other groups, Hh distribution in the developing wing is characterized following expression over a period of several days. To examine the movement and distribution of newly synthesized Hh, the Gal80-Gal4 temperature-sensitive inducible system was employed (McGuire et al., 2003). At low temperature, Gal80 inhibits Gal4 activity (Figure 2.4A). Following a shift to higher temperature, Gal80 is inactivated and Hh-Gal4 activates expression of Hh-GFP in posterior wing disc cells. With this system, Hh distribution was analyzed at different time points following induction (Figure 2.5). At 8 hours following induction, Hh-GFP exists as particles in the anterior compartment, primarily near the A/P boundary. At 24 and 72 hours following induction, increased numbers of particles are observed, both near the A/P boundary and further from the expressing cells (Figures 2.5, 2.6, and 2.7).

To examine how different factors alter the distribution of newly synthesized Hh, an assay was developed to quantify the distance of individual particles of Hh-GFP from the A/P boundary. First, a series of optical sections were transformed into a three-dimensional reconstruction of Hh-GFP and dsRed localization in a region of the wing disc near the A/P boundary (Figure 2.7A). Next, the dsRed expressing cells were converted into a single surface and the distance of Hh-GFP particles from this surface was determined (see Methods and Figure 2.4A-C, individual data sets are shown in Figure 2.9). Because the number of particles induced was variable, the percentages of Hh-GFP particles at different distances from the A/P boundary were used to normalize

distributions profiles within and between different experimental conditions (Figures 2.7 and 2.8).

To establish how long the Hh gradient takes to form (Figures 2.5 and 2.7), we analyzed the change in HhNp-GFP distribution at 8, 24, and 72 hours following induction (Figure 2.7D-F, Table 2). At each time point, the majority of HhNp-GFP was detected within 8μm (approximately 3-4 cells wide) of the A/P boundary. This distance represents the average width of the region expressing high levels of the Hh target gene *ptc* (unpublished results). The percentage of HhNp-GFP particles in this region significantly decreased from 8 to 24 hours, but not from 24 to 72 hours (Table 3). Similarly, both the median and the 90th percentile distance values for the HhNp-GFP distributions significantly increased from 8 to 24 hours, but not from 24 to 72 hours. From this analysis, I conclude that the HhNp-GFP gradient is still forming at 8 hours and is approaching its final shape by 24 hours.
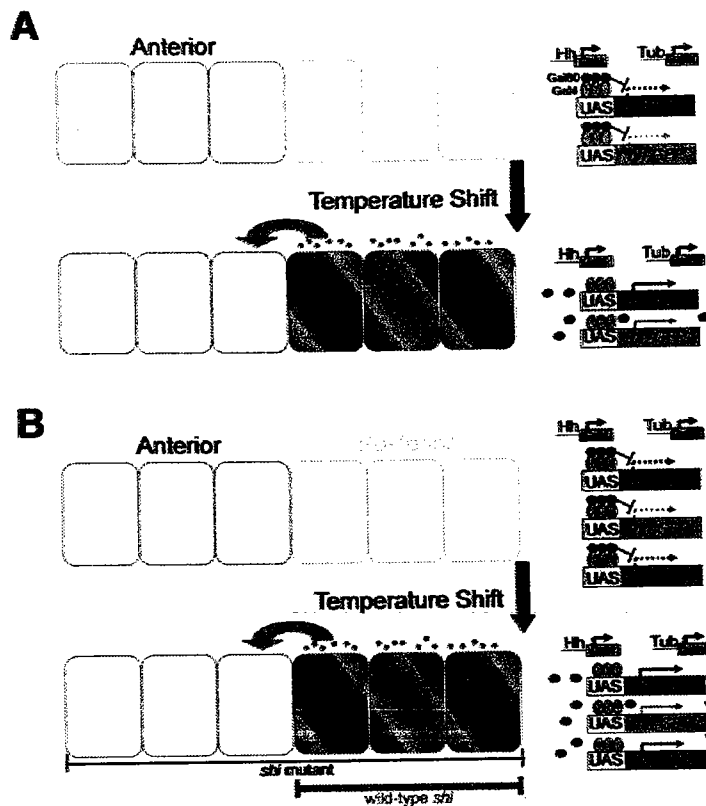
Figure 2.4 - Schematic diagram of Gal4-Gal80 inducible expression system.

(A) Inducing Hh-GFP expression. Vials are kept at 18°C, the Gal80 permissive temperature where tubulin-Gal80 blocks Gal4-mediated transcription. Upon a shift to 32°C, Gal80 repression is relieved and Gal4 transcription proceeds. Hh-GFP is expressed in the posterior cells with Hh-Gal4, and UAS-dsRed marks the expressing cells.

(B) Inducing Hh-GFP expression in shi^{ts1} mutant background. Vials are kept at 18°C, the Gal80 permissive temperature and shi^{ts1} mutant restrictive temperature. Upon a shift to 32°C, Gal4 transcription proceeds while endocytosis is blocked. Wild-type Shi is expressed in the posterior to restore endocytosis in the expressing cells. The resulting Hh-GFP movement into the anterior would be due solely to shi independent mechanisms. Hh-Gal4 is used again to drive transgene expression.

Figure 2.5 - Cholesterol restricts HhNp-GFP distribution but endocytosis is not required for distribution.
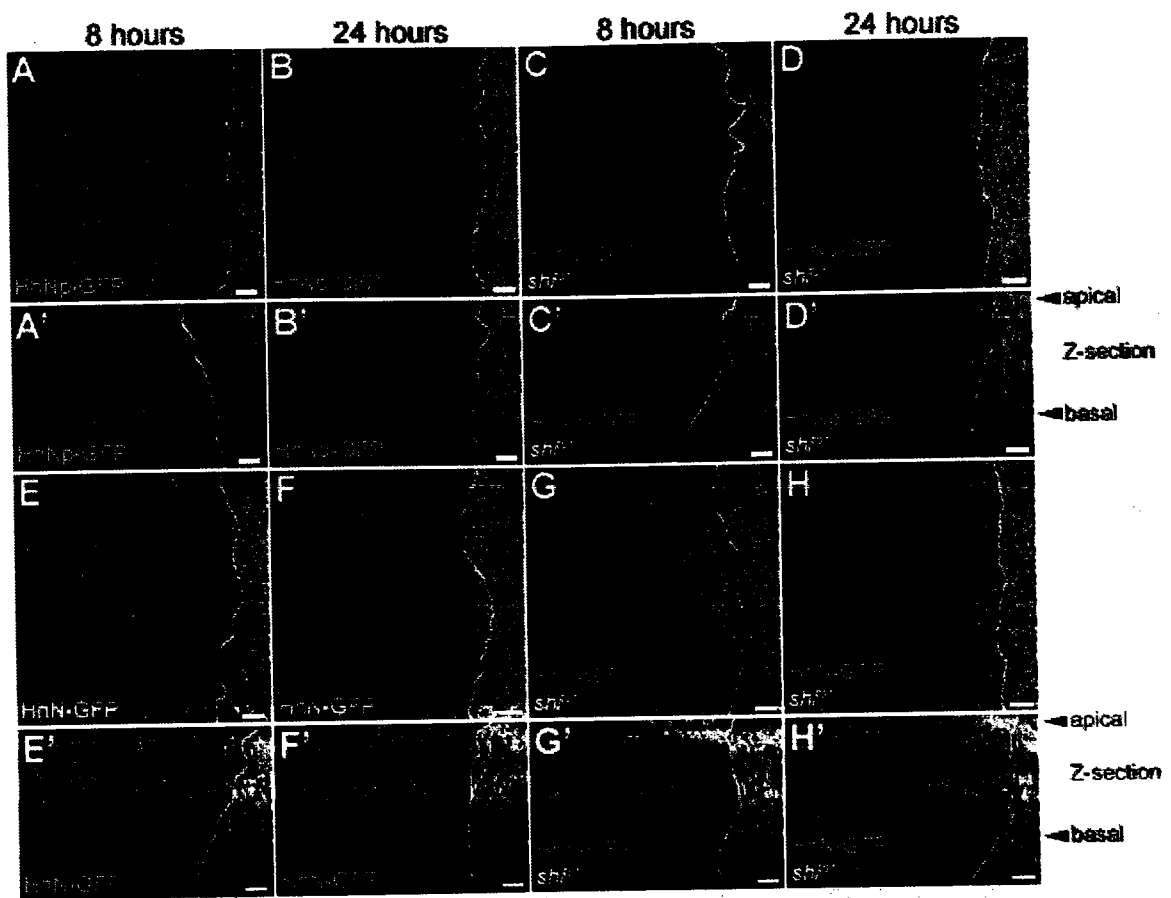
Figure 2.5 - Cholesterol restricts HhNp-GFP distribution but endocytosis is not required for distribution.

(A-H) Induced expression of HhNp-GFP in wild-type (A-B) and *shi^{ts1}* background (C-D) and HhN-GFP in wild-type (E-F) and *shi^{ts1}* background (G-H). (A-H) 25μm projections; (A'-H') 20μm Z-section projections. At 8hr, HhNp-GFP particles are found near the A/P boundary, marked by the solid white line (A,A'). After 24hr, more particles can be found further away (B,B'). HhN-GFP particles are detected further from the A/P boundary than HhNp-GFP at both time points (E-F). When endocytosis is blocked, HhNp-GFP particles are still detected in anterior cells (C-D). In wild-type and *shi^{ts1}* backgrounds, HhNp-GFP particles appear closer to the apical side (A'-D') as well as HhN-GFP in wild-type. When endocytosis is blocked, HhN-GFP moves into the anterior but there is reduced punctate staining and more membrane accumulation (G-H), primarily on the apical side of cells (G'-H'). Scale bar: 5μm
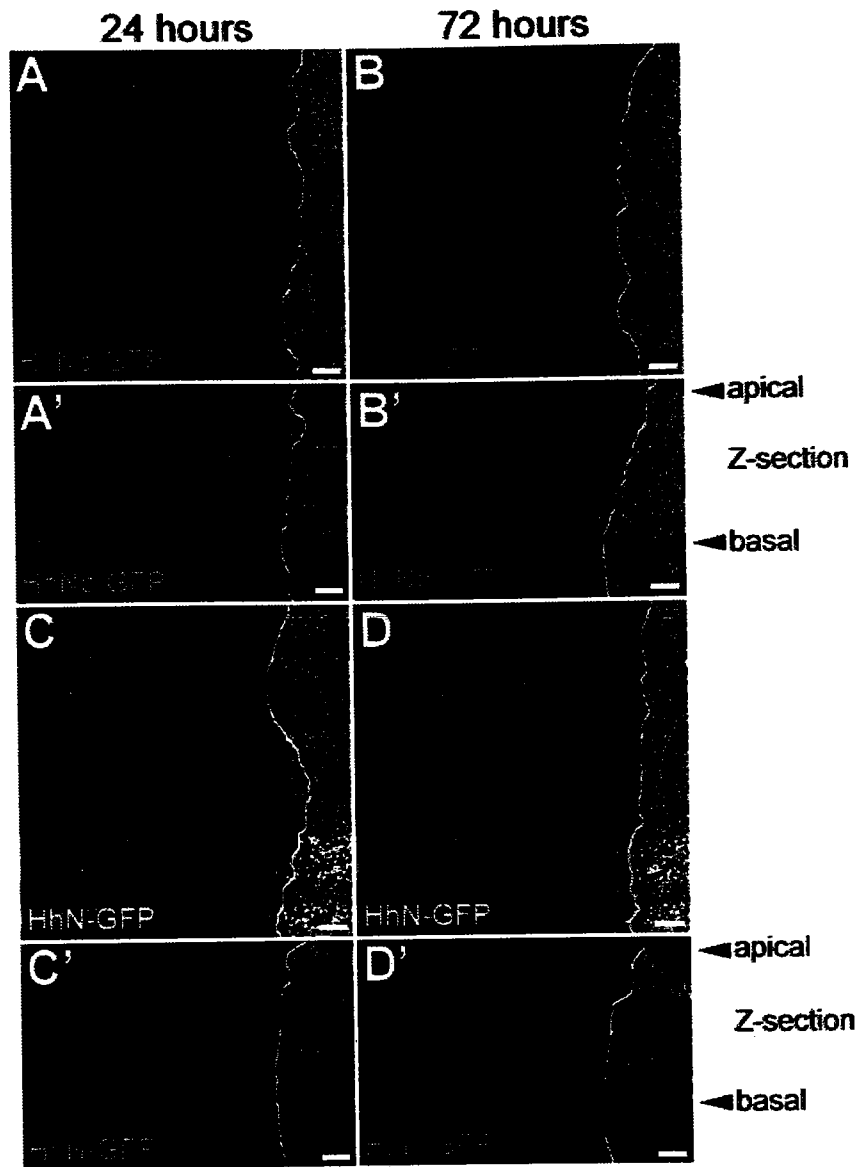
Figure 2.6 - Hh gradient forms by 24hr of induction.

(A-D) Induced expression of HhNp-GFP (A-B) and HhN-GFP (C-D) in wild-type

background. (A-D) 25μm projections; (A'-D') 20μm Z-section projections. 24 and 72hr

distribution of HhNp-GFP appears similar, also seen for HhN-GFP. Scale bar: 5μm

Figure 2.7 - Quantitative analysis of Hh-GFP distribution: Cholesterol is required to restrict distribution but endocytosis is not required for distribution.
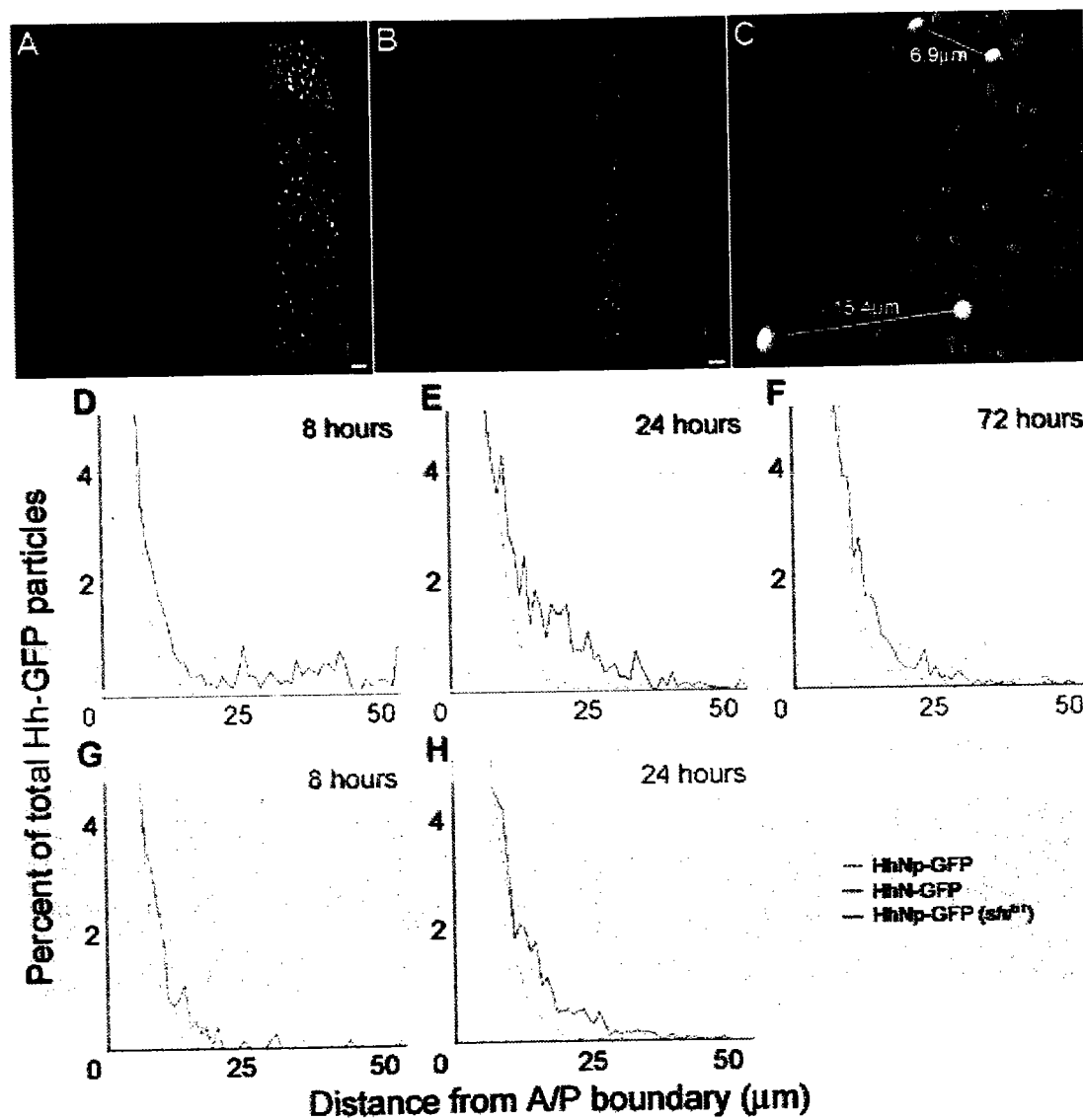
Figure 2.7 - Quantitative analysis of Hh-GFP distribution: Cholesterol is required to restrict distribution but endocytosis is not required for distribution.

(A-C) Schematic illustration of quantitative analysis. (A) Three-dimensional reconstruction of a confocal z-stack with Hh-GFP (green) and dsRed (red) marking the expressing cells. (B) Generation of isosurfaces. DsRed isosurfacing was used to generate a distance map used to measure distances of Hh-GFP particles. Hh-GFP particles were isosurfaced to identify particles using an intensity threshold and size criteria. (C) Depiction of particle distance measurements. Particles were measured for the shortest distance to the expressing cells (lines depict manual measurements but all measurements were calculated in an automated fashion). Scale bar: 5μm

(D-F) Mean of normalized HhNp-GFP (green) versus HhN-GFP (red) distribution profiles in a wild-type background. All samples were normalized to generate percentages of particles at the distances. Normalized data was then averaged to generate distribution profiles. Enlargement of the distribution near the x-axis shows more HhN-GFP is detected further from the A/P boundary (0 on the x-axis) at 8 (D; HhNp-GFP n=5, HhN-GFP n=4) and 24hr (E; HhNp-GFP n=16, HhN-GFP n=7). The same is seen at 72hr (F; HhNp-GFP n=5, HhN-GFP n=6).

(G-H) Mean of normalized HhNp-GFP distribution profiles in wild-type background (green) versus shi^{ts1} mutant background (blue). At 8 (G; shi^{ts1} n=4) and 24hr (H; shi^{ts1} n=7), HhNp-GFP in the mutant background is less restricted and found further away from the A/P boundary than in the wild-type background. The same HhNp-GFP distribution profiles in the wild-type background from D and E are used for G and H, respectively.
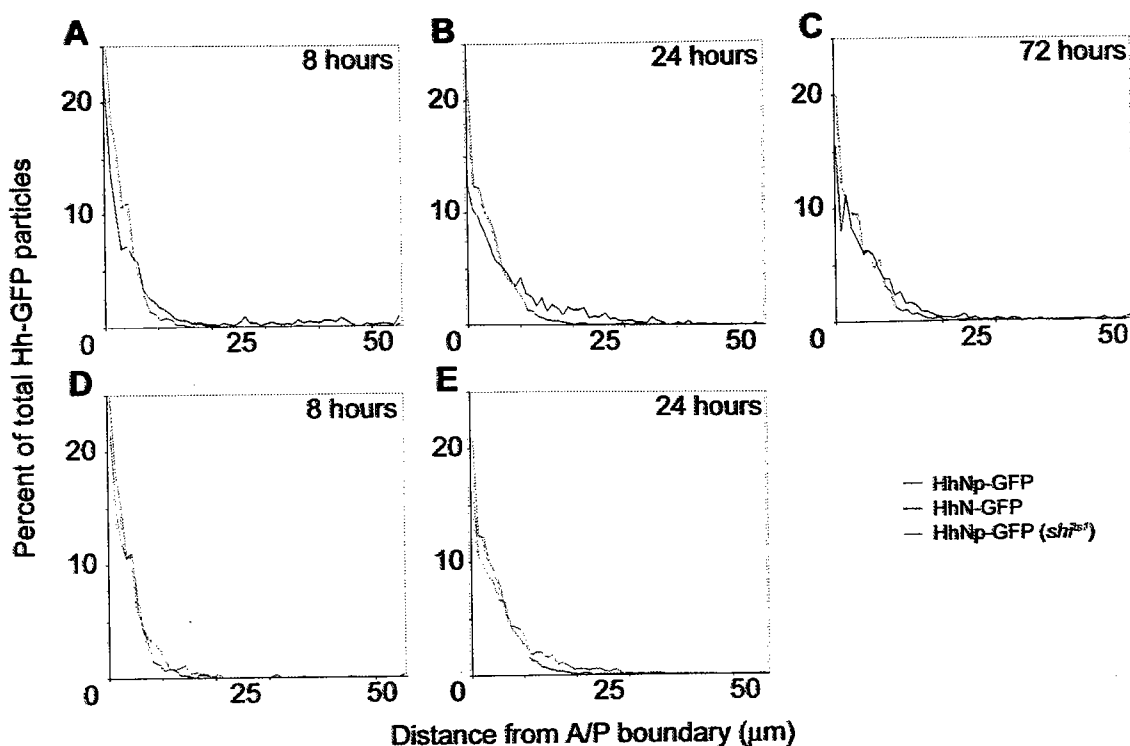
Figure 2.8 - Full distribution profiles of Hh-GFP.

(A-C) Mean of normalized HhNp-GFP (green) versus HhN-GFP (red) distribution profiles in a wild-type background at 8 (A), 24 (B), and 72hr (C) time points. More HhNp-GFP is found closer to the A/P boundary (0 on the x-axis) than HhN-GFP at 8hr (A), 24hr (B), and 72hr (C) time points.

(D-E) Mean of normalized HhNp-GFP distribution profiles in wild-type background (green) versus shi^{ts1} mutant background (blue). More HhNp-GFP is also found closer to the A/P boundary (0 on the x-axis) in the wild-type background than in the shi^{ts1} mutant background at 8 (D) and 24hr (E). The same HhNp-GFP distribution profiles in the wild-type background from A and B are used for D and E, respectively.

Table 2. Analysis of Hh-GFP particle distribution in wing discs

Time point	Sample	Median	90th percentile distance	% within 8μm
8hr	HhNp-GFP	2.5μm ± 0.6μm	8μm ± 1.4μm	93 ± 3.2
	HhN-GFP	4.4μm ± 3.0μm	27μm ± 15.8μm	75 ± 18.4
	HhNp-GFP(shi^{ts1})	2.7μm ± 0.4μm	10μm ± 1.8μm	85 ± 6.4
24hr	HhNp-GFP	3.5μm ± 0.9μm	11μm ± 2.4μm	82 ± 7.7
	HhN-GFP	6.1μm ± 1.9μm	25μm ± 7.0μm	64 ± 10.7
	HhNp-GFP(shi^{ts1})	4.8μm ± 1.2μm	16μm ± 4.8μm	70 ± 8.8
72hr	HhNp-GFP	3.8μm ± 0.6μm	12μm ± 2.1μm	79 ± 8.4
	HhN-GFP	5.1μm ± 1.2μm	31μm ± 3.7μm	70 ± 11.5

Between 4-16 discs were counted for each genotype and time point. Standard deviation was calculated for each measurement.

Table 3. ANOVA calculated P-values for significance

	Median	90th percentile distance	% within 8μm
HhNp vs. HhN	<0.0001	<0.0001	<0.0001
HhNp vs. HhNp(shi^{ts1})	0.1887	0.0131	0.0417
8hr vs. 24hr	0.0009	0.0011	0.0131
24hr vs. 72hr	0.8641	0.1341	0.7693

There was no significant interaction between the time factor and the genotype factor. Therefore, the significance of the main effects (time irrespective of genotype or genotype irrespective of time) are reported. P-values less than are 0.05 are considered significant.

Figure 2.9 - Individual histograms of raw data with median, 90th percentile distance, and % within 8μm values.
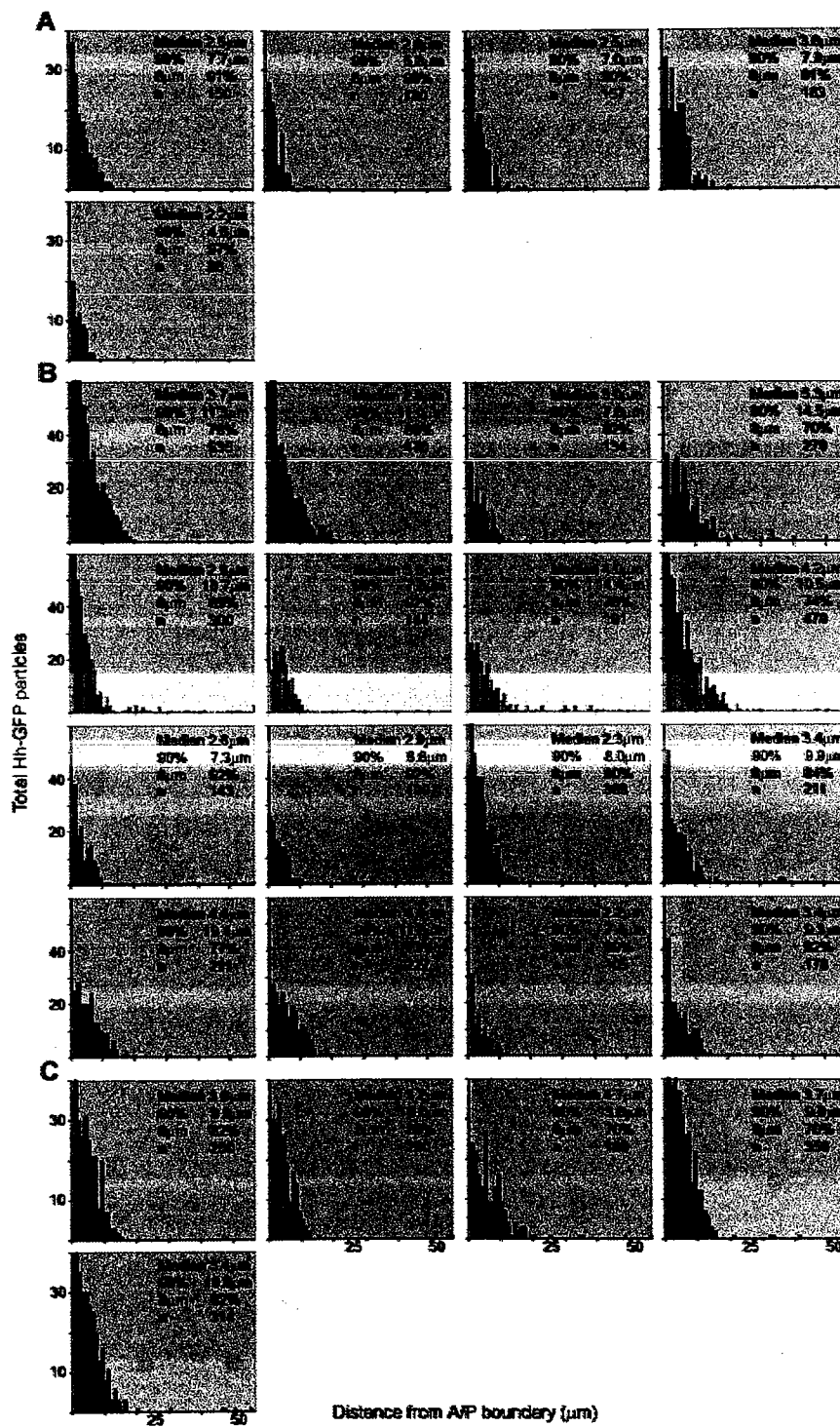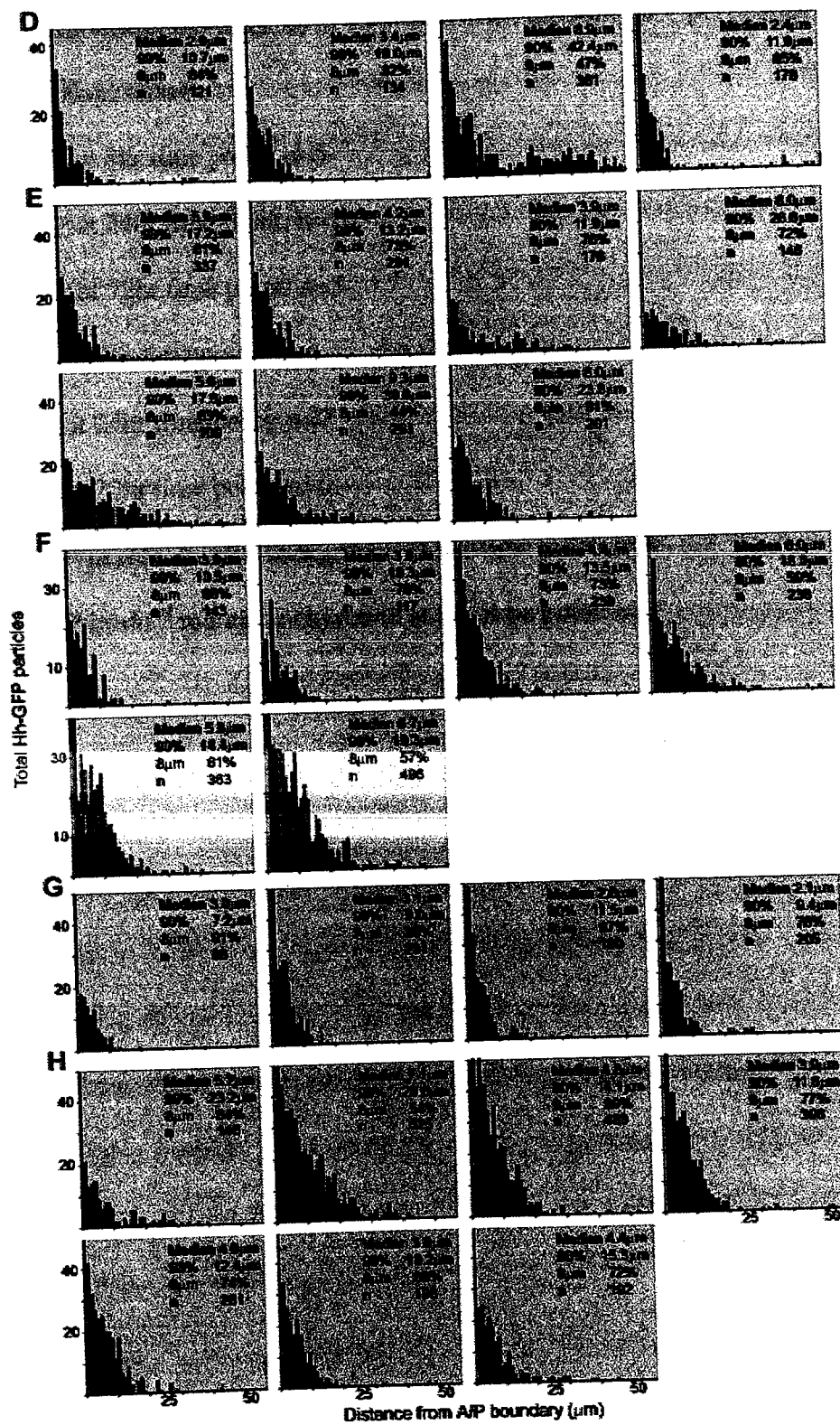
Figure 2.9 - Individual histograms of raw data with median, 90th percentile distance, and % within 8µm values.

(A) HhNp-GFP at 8hr time point: n=5

(B) HhNp-GFP at 24hr time point: n=16

(C) HhNp-GFP at 72hr time point: n=5

(D) HhN-GFP at 8hr time point: n=4

(E) HhN-GFP at 24hr time point: n=7

(F) HhN-GFP at 72hr time point: n=6

(G) HhNp-GFP in shi^{ts1} mutant background at 8hr time point: n=4

(H) HhNp-GFP in shi^{ts1} mutant background at 8hr time point: n=7

Cholesterol modification is required for proper Hh distribution.

Having identified time points when newly synthesized HhNp is forming a gradient (8 and 24 hours) or has reached a steady state (72 hours), the distribution of HhN-GFP, which lacks the cholesterol modification, was examined at these same time points. Similar to HhNp-GFP, the majority of HhN-GFP was detected within the first 8μm from the A/P boundary (Table 2) and the median value, 90th percentile distance, and percent of particles at 8μm changed significantly from 8 to 24 hours, but not from 24 to 72 hours (Table 3 and Methods). However, the shape of the gradient is different for HhN than HhNp. Comparisons of composite distribution profiles reveal that the distribution of HhN-GFP is shifted further from the A/P boundary at all time points (Figure 2.7E-F). The median and 90th percentile distance values are significantly greater for HhN-GFP than for HhNp-GFP (Tables 2 and 3) indicating that HhN is able to move further from the producing cells. In addition, the percentage of HhN-GFP within 8μm was significantly lower (Tables 2 and 3). This quantitative analysis extends previous studies indicating that HhN is able to move further into the anterior compartment than HhNp (Burke et al., 1999; Callejo et al., 2006; Dawber et al., 2005). This difference is not simply a result of greater amounts of HhN being secreted from producing cells. Rather, the cholesterol modification of Hh contributes to the shape of the gradient. Specifically, cholesterol is required to create a steeper Hh gradient with a higher percentage near the A/P boundary and a decreased maximum distance traveled.

Movement of newly synthesized HhNp-GFP particles does not require Shi.

Several studies have shown that Hh is internalized with Ptc and localizes in endocytic compartments through a mechanism that requires the *Drosophila* Dynamin homolog Shi (Callejo et al., 2006; Han et al., 2004b; Torroja et al., 2004); transient inhibition of Shi-dependent endocytosis blocks Hh internalization, but does not affect Hh-dependent gene expression. These experiments may indicate that endocytosis is not required for movement of Hh into its target cells. However, because Hh is synthesized prior to Shi inhibition, it is not clear whether Hh observed in target cells is newly synthesized or was present prior to *shi* inactivation.

To address this question, the inducible Hh-GFP system was used to simultaneously initiate a pulse of Hh-GFP expression in the posterior compartment and inhibit Shi function in the anterior compartment. Initially, HhNp-GFP was expressed throughout development (i.e. without Gal80) and then endocytosis was blocked for 8 hours with the temperature sensitive mutation shi^{ts1}; under these conditions, HhNp-GFP accumulated at the basal membranes of the anterior cells similar to previously published results (Callejo et al., 2006; Han et al., 2004b; Torroja et al., 2004) and in more apical punctate structures (Figure 2.10). Next, the effects of simultaneously inducing Hh-GFP expression while transiently blocking endocytosis were examined. In these experiments using the Gal80-Gal4 system, the same temperature shift induces Hh-GFP and dsRed expression and inactivates shi^{ts1}. In addition, wild-type Shi was also expressed in the posterior compartment, rescuing the endocytosis defect in the expressing cells (Figure 2.4B). Thus, Hh-GFP was induced in the posterior cells concurrently with a block in Shi-

dependent endocytosis. Newly synthesized HhNp-GFP was observed in the anterior compartment even when *shi* function was simultaneously inactivated (Figure 2.5C'and D'). The absence of cytoplasmic particles of Hh-GFP confirms that endocytosis is blocked in these experiments (Figure 2.13, discussed below). These results directly demonstrate that Hh does not require Shi function to move into and across target cells in the anterior compartment. Based on these observations, I conclude that Shi-dependent transcytosis is not essential for movement of HhNp-GFP.

In contrast to the results with constitutively expressed HhNp-GFP which accumulated on the basolateral membranes of the anterior compartment in the absence of Shi, induced HhNp-GFP was predominantly found in particles and no basal membrane accumulation was observed (Figure 2.5). These particles could be detected at both 8 and 24 hours when Shi-dependent endocytosis is blocked (Figure 2.5C-D) and could be found in both apical and basolateral positions.

The distribution of HhNp-GFP particles in the absence of Shi function was quantified as described above. Overall, the distribution profiles are similar for HhNp-GFP in the wild-type and shi^{ts1} mutant backgrounds (Figures 2.7 and 2.8) with the majority of HhNp-GFP found within 8μm of the A/P boundary (Table 2). The median values were not significantly different in the shi^{ts1} mutant than in a wild-type background, although the percentage of particles within 8μm was significantly different in the shi^{ts1} mutant (Table 3). These results suggest that while HhNp-GFP movement through the anterior compartment is not drastically altered when Shi-mediated endocytosis is blocked, Shi function does contribute to the shape of the Hh gradient; following

inhibition of Shi, the HhNp-GFP gradient is less steep with a lower percentage of particles retained near the A/P boundary.

The distribution of newly synthesized HhN-GFP following *shi* inactivation was also examined. Under these conditions, HhN-GFP predominantly accumulated at the apical surface of the cells (Figure 2.5G-H), although some basolateral punctate structures were still detected. HhN-GFP could also be observed in the lumenal space between the peripodial and disc proper cell layers, consistent with previous reports where HhN has been shown to traverse the lumen (Callejo et al., 2006; Gallet et al., 2006); interestingly, at least some of the lumenal HhN-GFP was present as punctate structures (Figure 2.11). Quantitative analysis of total HhN-GFP particle distribution in these experiments was not possible since the extracellular accumulation in the shi^{ts1} mutant prevented reliable identification of individual particles. Nonetheless, visual inspection of the HhN-GFP distribution clearly indicates that Shi-dependent endocytosis is not essential for movement of HhN-GFP across the anterior compartment and that much higher levels of apical HhN-GFP accumulate in the absence of Shi function (Figure 2.5G-H). These results suggest that most HhN-GFP is apically secreted and then degraded via Shi-dependent endocytosis. However, the presence of some basolateral HhN-GFP in these experiments indicates that not all HhN-GFP is apically secreted.
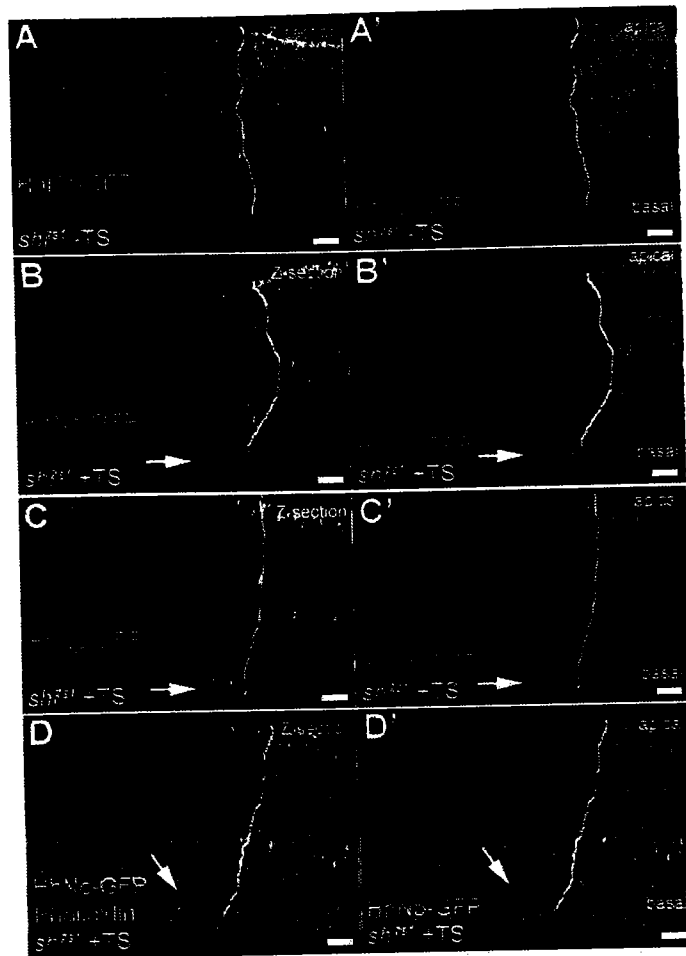
Figure 2.10 - Constitutively expressed HhNp-GFP accumulates at basal membranes after blocking endocytosis.

(A-D) HhNp-GFP (green) localization prior to (A) and after an 8hr (B-D) endocytosis block in the shi^{ts1} mutant background with Phalloidin (red) as a cell surface marker; 3μm Z-section projections. HhNp-GFP does not normally accumulate at cell surfaces in the anterior compartment (A/P boundary is marked by a solid white line). At the shi^{ts1} permissive temperature, HhNp-GFP accumulates primarily at the basal cell surfaces in the anterior to varying degrees (B-high, C-intermediate, D-low). Scale bar: 5μm
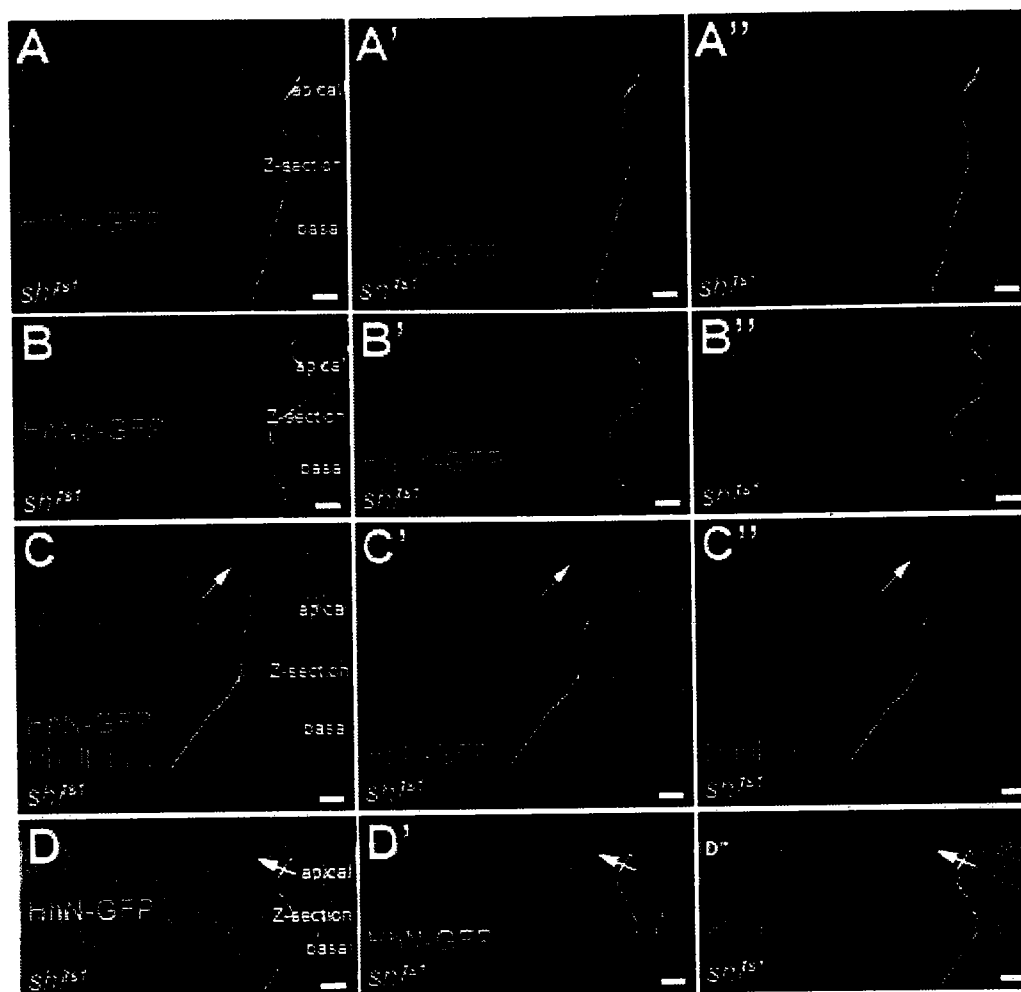
Figure 2.11 - HhN-GFP is detected in the lumen.

(A-D) Z-sections of HhNp-GFP (green, A-B) and HhN-GFP (green, C-D) localization

after an 8hr induction and 8hr endocytosis block in the shi^{ts1} mutant background with

Phalloidin (red) as a cell surface marker (A/P boundary marked by the solid white line).

In two examples for each, HhN-GFP is detected in the lumen (arrow), the area between

the top peripodial epithelial layer and bottom disc proper epithelial layer, while HhNp-

GFP is not found in the lumenal space. Scale bar: 5μm

Ptc-independent punctate structures require cholesterol and endocytosis.

In all of the experiments using inducible Hh-GFP, punctate staining patterns were observed. These particles were classified into four groups using Phalloidin, which labels cortical actin near the cell surface marking cell outlines, and an antibody specific for the Hh receptor Ptc (Figures 2.12, 2.13, and 2.14). Approximately 60 percent of induced HhNp-GFP or HhN-GFP particles in the anterior compartment of wild type discs were at or near the cell surface and classified as "surface-associated" (Table 4); a substantial fraction of these particles were associated with Ptc. Within the 40 percent of HhNp-GFP that was cytoplasmic, there was an even distribution of HhNp-GFP cytoplasmic vesicles with and without Ptc, suggesting that HhNp can be endocytosed without binding to Ptc (Table 5). In contrast, nearly all cytoplasmic HhN-GFP was associated with Ptc, suggesting that the cholesterol modification mediates Ptc-independent endocytosis (Table 5). In shi^{ts1} animals, very few cytoplasmic HhNp-GFP particles could be detected (6 percent of total, Table 4) and none of them appeared to co-localize with Ptc (Table 5). This result confirms that inhibition of Shi blocks most endocytosis of Hh, including all Ptc-dependent endocytosis. The majority of Ptc-independent endocytosis is also blocked. It cannot be definitively concluded whether the classification of remaining Ptc-negative Hh-GFP particles as cytoplasmic are due to incomplete cell surface labeling with Phalloidin or represent cytoplasmic particles formed by a Ptc- and Shi-independent mechanism.

Table 4. Hh-GFP co-localization with Ptc in wing discs

	Cytoplasmic			Membrane-associated		
	%Total	%Ptc	%no Ptc	%Total	%Ptc	%no Ptc
HhNp-GFP	40 ± 7	22 ± 7	18 ± 2	60 ± 8	16 ± 6	44 ± 7
HhN-GFP	40 ± 12	37 ± 11	3 ± 2	60 ± 12	22 ± 8	38 ± 11
HhNp-GFP(shi^{ts1})	6 ± 2	0	6 ± 2	94 ± 2	27 ± 1	67 ± 1

3 samples were counted for each genotype. Phalloidin co-localization was counted as membrane-associated.

Table 5. Non-membrane-associated Hh-GFP co-localization with Ptc in wing discs

	% Co-localized with Ptc	% Not co-localized with Ptc
HhNp-GFP	55 ± 7	45 ± 7
HhN-GFP	92 ± 3	8 ± 3
HhNp-GFP(shi^{ts1})	0	100

Since inhibition of Shi blocks most or all cytoplasmic particles (Table 4), but leads to greater movement through the anterior compartment (Table 2), these results indicate that transcytosis does not play a major role in spreading HhNp-GFP. In addition, a Ptc-independent mechanism for HhNp-GFP uptake is observed that is dependent on both the cholesterol modification and endocytosis.
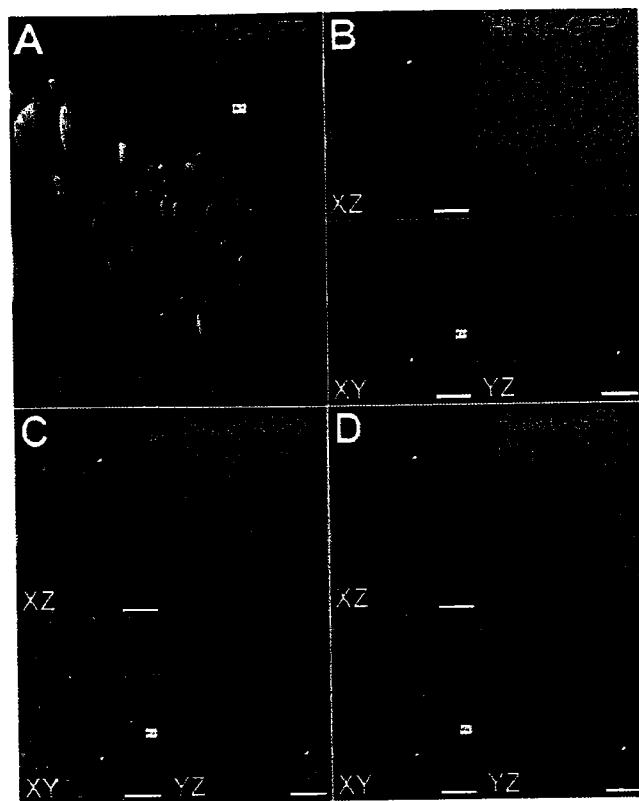
Figure 2.12 - Quantification scheme of Hh-GFP membrane localization and co-localization with Ptc.

(A) Hh-GFP surfaces were generated to identify particles based on the same criteria used in particle distance measurements. Each particle was individually located for particle classification (white arrow connected to box).

(B-D) Classification of particles. After particle identification, Hh-GFP particles (green) were located in XY, XZ, and YZ views (B). Co-localization was determined with Phalloidin (purple, C) and Ptc (red, D) in these views through the z-stack (white arrows identify the same particle in XZ and YZ views that was originally identified in the XY view). Scale bar: 5μm

Figure 2.13 - Non-Ptc containing Hh-GFP particles require cholesterol but not endocytosis.
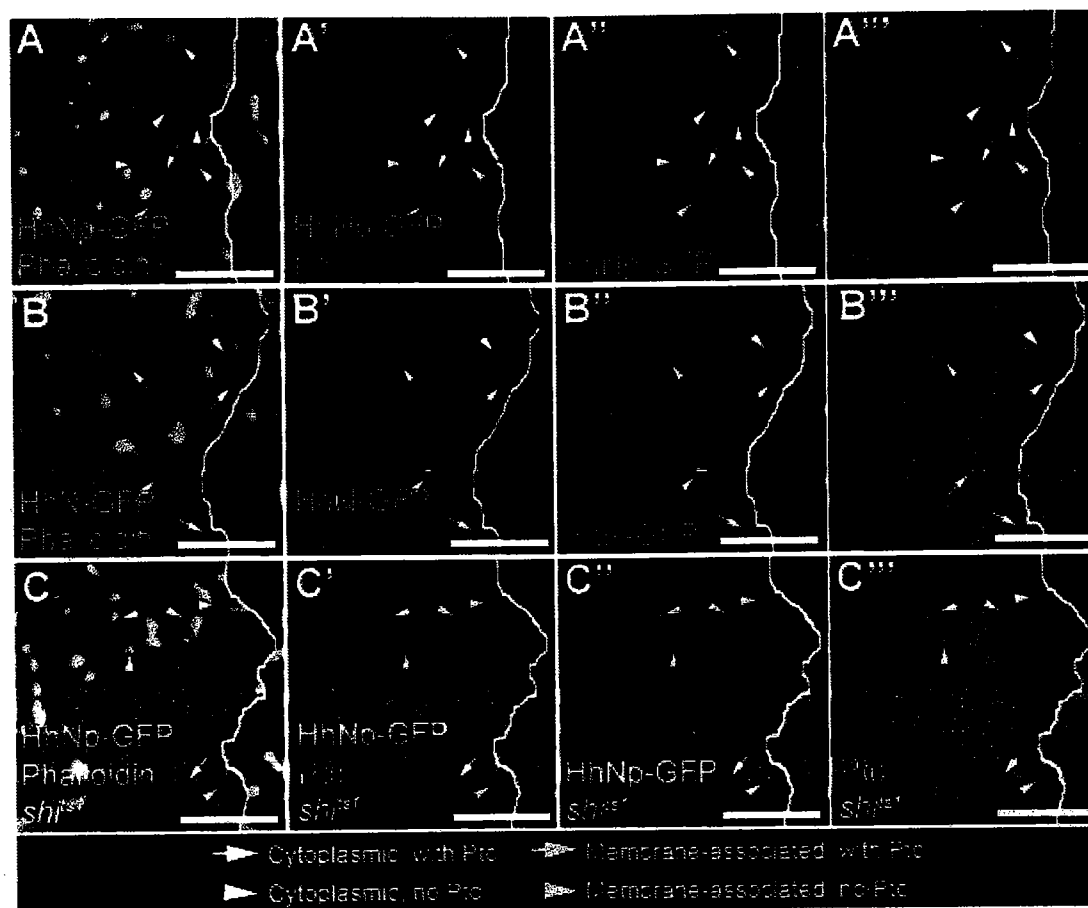
Figure 2.13 - Non-Ptc containing Hh-GFP particles require cholesterol but not endocytosis.

(A-C) Ptc co-localization with HhNp-GFP (A), HhN-GFP (B), and HhNp-GFP in the shi^{ts1} background (C) after expression induced for 8hr. (A-C) Hh-GFP (green) labeled with Phalloidin (purple). (A'-C') Hh-GFP (green) labeled with Ptc (red). (A"-C") Hh-GFP only. (A'''-C''') Ptc only. 4 classes of Hh-GFP particles are seen: non-Phalloidin associated (cytoplasmic) with Ptc (white arrow), non-Phalloidin associated (cytoplasmic) without Ptc (white arrowhead), Phalloidin (membrane) associated with Ptc (yellow arrow), Phalloidin (membrane) associated without Ptc (yellow arrowhead). Most HhNp-GFP particles are membrane-associated and do not contain Ptc, but cytoplasmic particles have a relatively even distribution with and without Ptc. More HhN-GFP also localizes with Phalloidin, and almost all cytoplasmic HhN-GFP particles contain Ptc. HhNp-GFP particles in shi^{ts1} mutant background are Phalloidin-associated and many do not contain Ptc. The A/P boundary is marked by a solid white line. Scale bar: 5μm

Figure 2.14 - Non-Ptc containing Hh-GFP particles require cholesterol but not endocytosis (Z-sections).
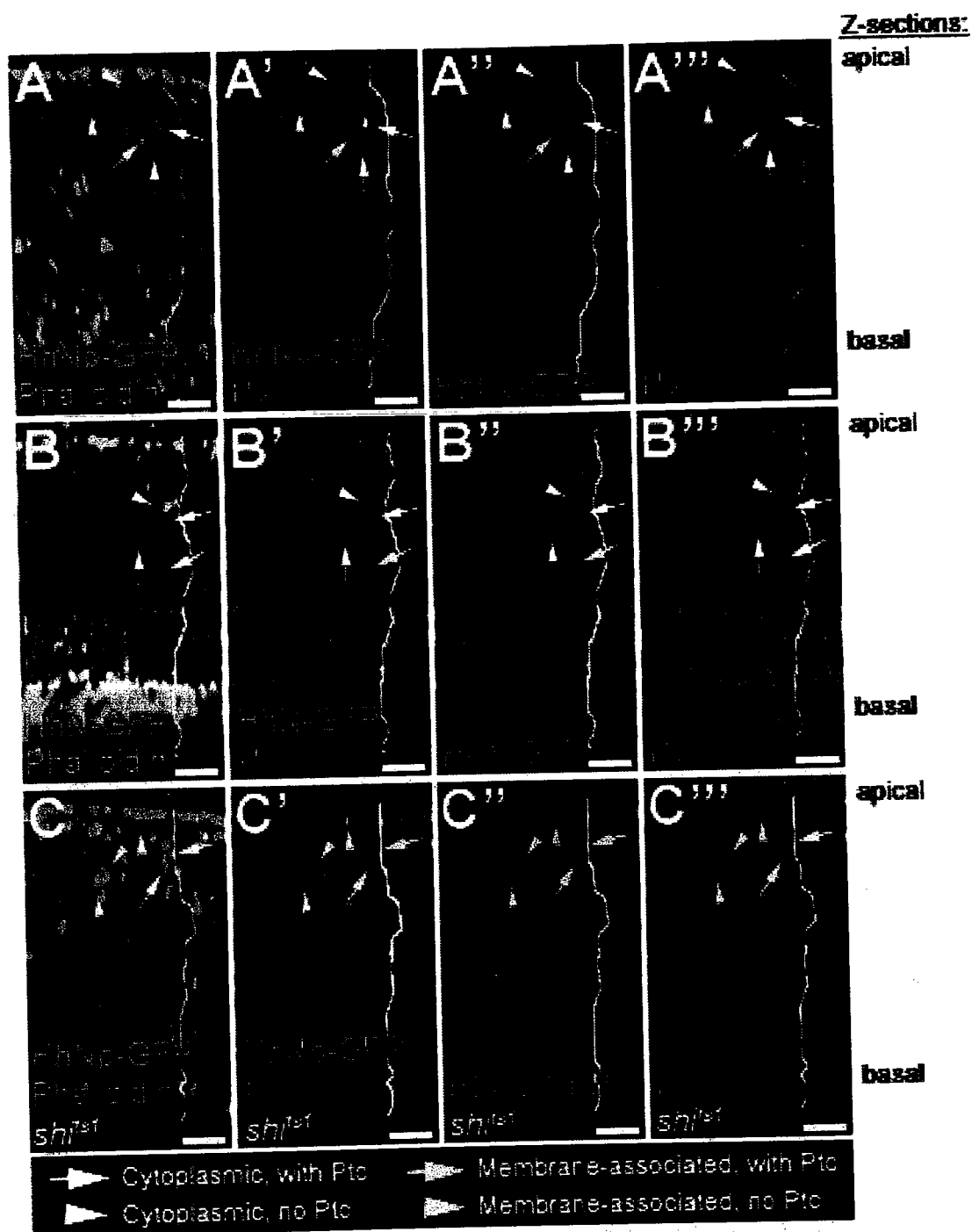
Figure 2.14 - Non-Ptc containing Hh-GFP particles require cholesterol but not endocytosis (Z-sections).

(A-C) Z-section of Ptc co-localization with HhNp-GFP (A), HhN-GFP (B), and HhNp-GFP in the shi^{ts1} background (C) after expression induced for 8hr. (A-C) Hh-GFP (green) labeled with Phalloidin (purple). (A'-C') Hh-GFP (green) labeled with Ptc (red). (A''-C'') Hh-GFP only. (A'''-C''') Ptc only. 4 classes of Hh-GFP particles are seen: non-Phalloidin associated (cytoplasmic) with Ptc (white arrow), non-Phalloidin associated (cytoplasmic) without Ptc (white arrowhead), Phalloidin (membrane) associated with Ptc (yellow arrow), Phalloidin (membrane) associated without Ptc (yellow arrowhead). Most HhNp-GFP particles are Phalloidin-associated and do not contain Ptc, but cytoplasmic particles have a relatively even distribution with and without Ptc. More HhN-GFP also localizes with Phalloidin, and almost all of the cytoplasmic HhN-GFP particles contain Ptc. HhNp-GFP particles in shi^{ts1} mutant background are Phalloidin-associated and many do not contain Ptc. The A/P boundary is marked by a solid white line. Scale bar: 5 µm

Discussion

Hh-GFP distribution and gradient formation

Inducible and functional GFP-tagged versions of full length and N-terminal Hh have been generated, which allows the study of newly synthesized Hh movement and distribution in live samples, as well as fixed tissues. The initial analysis of HhNp-GFP localization in living tissue demonstrated similar localization to endogenous HhNp, in particles that were mostly endosomes in the anterior. Upon close examination of HhNp-GFP and HhN-GFP distribution, both were found in punctate structures that localized more apically in the anterior compartment, although basolateral structures were also observed. It was also seen that the Hh gradient appears to require a minimum of 24 hours to fully form. The minimum HhNp rate of movement is approximated to be at least 1μm/hour (8μm distance of the 90th percentile over the first 8 hours) and the 90th percentile distance at 12μm at the furthest time point (72 hours). This rate of Hh distribution is a minimum calculated rate, and is slower than the reported rate of Dpp gradient formation of 6-8 hours (Entchev et al., 2000) and the speed of Activin diffusion of 300μm in a few hours (Gurdon et al., 1994). However, more time points are needed to determine the exact rate of Hh gradient formation for comparison to diffusion or transcytosis rates.

HhNp gradient formation through planar diffusion

Previous studies used a block in endocytosis to try to separate the mechanisms of diffusion, which should not require endocytosis, and transcytosis, which should require

endocytosis. Wild type Shi was expressed in the posterior cells of shi^{ts1} mutant discs and diffusion versus transcytosis of a pulse of newly produced Hh was studied. This enabled a simultaneous production of Hh and a block of endocytosis in the target cells to examine Hh movement. Unexpectedly, HhNp-GFP particles were observed even though endocytosis had been blocked. Upon closer examination, almost all of these particles were associated with the cell surface and not cytoplasmic, indicating these were not intracellular transcytotic vesicles. This suggests that cycles of vesicular endocytosis and exocytosis are unlikely to contribute to movement of HhNp. The absence of HhNp-GFP particles in the lumen when endocytosis was blocked indicates that wild-type Hh has restricted planar movement, as previously demonstrated (Callejo et al., 2006). These observations support the model of HhNp-GFP distribution via planar diffusion.

Cholesterol is required for the steep HhNp gradient

HhN-GFP was observed to be able to travel three times faster than HhNp-GFP (27μm versus 8μm distance of the 90th percentile over the first 8 hours) and to target more distant cells in the anterior compartment (31μm distance of the 90th percentile at the furthest time point of 72 hours), consistent with earlier observations that HhN had a longer range than HhNp (Burke et al., 1999; Callejo et al., 2006; Dawber et al., 2005). HhNp-GFP has a steep gradient with a sharp decline and the cholesterol is required for forming this steep gradient, as demonstrated by the higher percentage of HhNp-GFP particles within the first 8μm from the expressing cells in comparison to HhN-GFP. HhNp activates higher levels of the short range target genes *en* and *ptc* (Callejo et al.,

2006; Dawber et al., 2005), and this suggests that the purpose of the cholesterol modification is to retain HhNp closer to the expressing cells, resulting in a precise region of short range target gene activation.

HhN-GFP without the cholesterol was also able to travel into the anterior compartment in the absence of endocytosis. When endocytosis is blocked, HhN-GFP was found to accumulate at high levels in the extracellular lumenal space between the disc proper and the peripodial layer. This observation is similar to a previous report (Callejo et al., 2006), suggesting that HhN-GFP is free to diffuse three-dimensionally, and again evidence that the cholesterol acts to restrict HhNp movement.

Previous studies have observed that HhN is secreted from the peripodial cells and signals to the columnar epithelial cells (Callejo et al., 2006; Gallet et al., 2006). However, I believe that peripodial HhN-GFP has a minimal contribution on the distribution profile. Since the posterior compartment of the peripodial membrane overlies the section that the measurement data originated from, the contribution from the peripodial membrane was taken into account by subtracting the HhN signal at the end of the distribution profile from the rest of the data set. Subtracting this signal did not significantly alter these results and conclusions.

Ptc independent vesicles

Further examination of the Hh-GFP particles detected four classes of particles including Ptc-independent cytoplasmic vesicles. Interestingly, HhNp-GFP was observed to have a significantly higher percentage of these Ptc-independent vesicles than HhN-

GFP. Previous studies have also observed Ptc-independent structures (Callejo et al., 2006; Gallet and Therond, 2005; Gorfinkiel et al., 2005; Torroja et al., 2004). However, there are distinct differences in my observations from previous studies. Previous results showed that most of HhNp co-localizes with Ptc internally (Callejo et al., 2006; Torroja et al., 2004) while a high proportion of HhN does not co-localize with Ptc (Callejo et al., 2006); however, this study demonstrated that there was an equal fraction of HhNp that did and did not co-localize with Ptc internally while most intracellular HhN co-localized with Ptc. Since these previous studies were done at the HhNp gradient steady state, the Ptc receptor could have been saturated by this point, resulting in higher levels of HhNp and Ptc co-localization (Callejo et al., 2006; Torroja et al., 2004). Additionally, clones looking at HhN and Ptc co-localization appear to be outside of the high Ptc-expressing stripe (Callejo et al., 2006) and since there is less Ptc there, one might conclude that there is less Ptc co-localization.

The Ptc-independent vesicles could represent HhNp-GFP that has somehow dissociated from Ptc after internalization, possibly as a part of a recycling mechanism. *C.elegans* Hh-related peptides are sorted to multivesicular bodies (MVBs), then recycled back to the apical surfaces for secretion (Liegeois et al., 2006). However, a recent study reported that Hh does not go through the Rab11-mediated recycling pathway (Gallet et al., 2006). Another possibility is the presence of another receptor besides Ptc, such as the low density lipoprotein receptor, Megalin, previously demonstrated to interact with vertebrate Shh (McCarthy et al., 2002). The absence of these vesicles when endocytosis

is blocked indicates these vesicles are not essential for transport although further studies of these Ptc-independent vesicles are required to elucidate the nature of these vesicles.

Conclusions

Previous publications have reported that cholesterol modification of Hh is important for its distribution by analyzing target gene expression. However, these studies showed discrepancies in the range of non-cholesterol modified HhN and in the apicobasal localization of the different forms of Hh leading to different models of Hh distribution. A system has been developed to induce a pulse of newly synthesized Hh that can be used to further characterize formation of the Hh gradient. Inducible expression, where a pulse of newly synthesized protein is generated, would enable observations of movement during gradient formation instead of at the gradient steady-state, and at protein concentrations closer to endogenous levels. Since contradictory observations exist about the mechanisms regulating morphogen distribution and gradient formation not only for Hh but also for Dpp and Wg, clarification could come from using an inducible system together with quantitative measurements.

In this study, HhN has been observed to be detected at a longer range than modified HhNp, similar to previous studies. Newly synthesized HhNp-GFP distribution has been quantitatively demonstrated to require cholesterol and can occur without endocytosis in agreement with published results. Additionally, HhNp-GFP is detected in intracellular vesicles that do not co-localize with Ptc but these are not essential for Hh distribution since they are not observed in endocytosis defective cells. Furthermore, in

this inducible system, the modified and unmodified forms of Hh localize at both apical and basolateral regions suggesting there may not be a preferential region for movement. The data from this study supports a model where the cholesterol modification of Hh is required to restrict its planar diffusion, thereby forming a steep gradient.

Materials and Methods

Drosophila stocks and genetic experiments

The following mutants and transgenes have been previously described: hh^{GS1}, an amorphic allele also known as hh^{11} (Mohler, 1988); shi^{ts1} (Grigliatti et al., 1973), UAS-shi^{+} also known as UAS-*dynamin* (Entchev et al., 2000), *tubulin-Gal80ts*^{2} (McGuire et al., 2003), UAS-*dsRed* (Kasuya and Iverson, 2000), UAS-*GFP-dally-like* (Han et al., 2004b), UAS-*ptc-YFP* (Zhu et al., 2003), *Hh-Gal4* (Tanimoto et al., 2000), *Ptc-Gal4* (Speicher et al., 1994), and *71B-Gal4* (Brand and Perrimon, 1993).

UAS-*hhF-GFP* and UAS-*hhN-GFP* transgenic flies were generated. These fusion proteins are similar to those previously described (Gorfinkiel et al., 2005; Torroja et al., 2004). To construct UAS-*hhF-GFP*, *GFP* was inserted in frame into full length *hh* between amino acids 254 (H) and 255 (V). The PCR primers used are as follows:

GAGTC<u>GCGGCCGC</u>ATCATGGATA   and

AT<u>GGATCC</u>GTGGGAACTGATCGACGAATC for the first half of full length *hh* (*hh1*);

AC<u>GGATCC</u>ATGGTGSGCAAGGGCGAG   and

AC<u>GAATTC</u>CTTGGTACAGCTCGTCATGCC   for   *GFP*;

AG<u>GAATTC</u>GTGCACGGCTGCTTCAC   and

TG<u>GGTACC</u>CAGGATTCCATCATCAAT for the second half of full length *hh* (*hh2*). PCR fragments were generated using *hh* cDNA and eGFP-N1 (Clontech) plasmids as templates, and cloned into pBluescript (Stratagene) in the following restriction enzymes

sites (underlined in PCR primer sequence): NotI/BamHI for *hh1*, BamHI/EcoRI for *GFP*, and EcoRI/KpnI for *hh2*. The full *hhF-GFP* (*hh1-GFP-hh2*) sequence was then cloned into pUASp2 (Rorth, 1998) using the NotI/KpnI restriction enzyme sites. To construct UAS-*hhN-GFP* that lacks the cholesterol modification, *hh* was truncated at amino acid 257 (G) and *GFP* was cloned in frame immediately behind truncated *hh*. The PCR primers used were: GA<u>GGTACC</u>GAGAAACAGCAAACAACGAGTCTTAG and AT<u>GGATCC</u>AAGCCGTGGGAACT for *hhN*. The HhN PCR fragment was cloned into pUASp that already contained *GFP* using KpnI/BamHI restriction enzyme sites (underlined in PCR primer sequence). All PCR products were sequenced (Macrogen). Each construct was co-injected with the delta 2-3 transposase helper plasmid into w^{1118} embryos to generate transgenic lines.

For rescue and localization experiments, the following larval genotypes were used:

En-Gal4; UAS-*hhF-GFP hh^{GS1}*

UAS-*dsRed*/+; UAS-*hhF-GFP*/*Hh-Gal4*

UAS-*hhF-GFP*/*71B-Gal4*

UAS-*hhF*/*71B-Gal4*

UAS-*CD8-GFP*/+; *71B-Gal4*/+

UAS-*myrpalm-CFP*; UAS-*hhF-GFP*/*Hh-Gal4*

UAS-*ptc-YFP*/*Ptc-Gal4*

Ptc-Gal4/+; UAS-*GFP-Dlp*

For experiments analyzing Hh temporal distribution, the following larval genotypes were generated:

Hsflp UAS-*dsRed*/+; UAS-*hhF-GFP hh*^{GS1}/*Hh-Gal4 tub-Gal80ts*^{2}

Hsflp UAS-*dsRed*/+; UAS-*hhN-GFP hh*^{GS1}/*Hh-Gal4 tub-Gal80ts*^{2}

To examine Hh distribution in discs with an endocytosis-defect in the anterior compartment, a *shi* mutant allele was used. Shi is the *Drosophila* homologue of mammalian GTPase Dynamin and the *shi*^{ts1} mutant allele is a temperature sensitive allele with the permissive temperature at 18°C and the restrictive temperature at 32°C. These larvae have a *shi* mutant background at the restrictive temperature which coincides with the expression of wild-type Shi under the Gal80-Gal4 system to rescue the mutant phenotype in the posterior compartment. For these experiments, the following larval genotypes were generated:

shi^{ts1} FRT19A; UAS-*shi*$^+$/Hsflp UAS-*dsRed*; UAS-*hhF-GFP hh*^{GS1}/*Hh-Gal4 tub-Gal80ts*^{2}

shi^{ts1} FRT19A: UAS- *shi*$^+$/Hsflp UAS-*dsRed*; UAS-*hhN-GFP hh*^{GS1}/*Hh-Gal4 tub-Gal80ts*^{2}

Western Blot

Using the *71B-Gal4* drivers for expression, salivary glands were dissected from the following larvae: w^{1118} (10 glands), UAS-*CD8:GFP* (5 glands), UAS-*hhN-GFP hh*^{GS1} (10 glands), UAS-*hhF-GFP hh*^{GS1} (10 glands), and UAS-*hhF* (15 glands) and put on ice. Salivary glands were put in 40µL of sample buffer and broken up with a Dounce

Homogenizer. The lysate was spun down and the supernatant was collected and loaded on a 10% polyacrylamide gel for SDS-PAGE. The blot was first labeled for presence of GFP, then stripped and re-probed for a tubulin loading control. Antibodies used were rabbit anti-GFP 1:1500 (Molecular Probes), mouse anti-tubulin 1:3000 (Oncogene), and anti-rabbit and anti-mouse HRP 1:20000 (Jackson Laboratories).

Wing Preparations

Wings were collected from adult flies expressing various transgenes under the control of the *71B-Gal4* driver. Whole flies were put in isopropanol, wings were pulled off fly bodies and mounted in 50% Canada Balsam/isopropanol.

Cuticle Preparations

Embryos were dechorionated and devitellinized, then mounted in Hoyer's medium on slides incubated at 65°C to clear the embryos.

Embryo *in situ* hybridization

Generation of the *rhomboid* (*rho*) probe - a clone containing *rho* cDNA was linearized with the enzyme PvuII and purified using the QIAquick gel extraction kit (Qiagen). DIG-labeled *rho* probe was transcribed using the RiboMAX Large Scale RNA Production Systems (Promega) using T7 and T3 RNA polymerases. Probes were digested for 10 minutes.

Embryos were cleared in ethanol/xylenes for 30 minutes, then fixed in 4% formaldehyde. After a 4 minute 10mg/mL Proteinase K treatment, embryos were fixed again in 4% formaldehyde. Then embryos were hybridized with probe overnight. After hybridization, embryos were washed and equilibrated, then incubated with anti-DIG antibody (1:4000) for 1 hour. Embryos were incubated in the staining solution for up to 1 hour, washed and mounted in 70% glycerol.

Induction of Hh-GFP expression using Gal80ts

Larvae were raised at 18°C. Third instar larvae (day 10-15 at the Gal80 permissive temperature 18°C) were reared at 32°C (the Gal80 restrictive temperature) for 8, 24, or 72 hours. Larvae were dissected at room temperature, and fixed immediately before immunostaining (total time between removal from permissive temperature to fixation was 5-10 minutes).

Imaginal Disc Preparation and Immunostaining

Larvae were removed from 32°C to room temperature, dissected, and fixed immediately (total time of 5-10 minutes). Immunostaining was performed according to Patel (Patel, 1994). For induction studies, the following modifications were used. Briefly, discs were fixed in 4% paraformaldehyde in PBS for 20 minutes, washed in PBS, blocked for 30 minutes in PBS with 0.5% BSA and 5% normal goat serum (NGS), incubated in primary antibody for 1 hour in PBS with 0.1% TritonX-100, 0.5% BSA, and 5% NGS, washed in PBS for 20 minutes, incubated in secondary antibody diluted in the

initial blocking solution for 30 minutes, and washed for 30 minutes. Discs were mounted

in 50% glycerol/PBS. Strips of double-stick tape were added to the slides as spacers to

prevent compression of the discs.

Primary antibodies were used at the following concentrations: rat anti-DCAD

1:50 (Oda et al., 1994); mouse anti-Ptc 1:50 (Capdevila et al., 1994), rabbit anti-dsRed

1:500 (Clontech), rat anti-Ci 1:10 (Motzny and Holmgren, 1995), mouse anti-GFP 1:250

(Molecular Probes). Secondary antibodies used were anti-rabbit and anti-rat Alexa 555

1:1000, anti-mouse Alexa 647 1:1000 (Molecular Probes), and anti-rabbit Cy3 1:600

(Jackson Laboratories).

Protocols for membrane labeling, endosome labeling, and extracellular labeling

have been described previously (Entchev et al., 2000; Greco et al., 2001; Strigini and

Cohen, 2000). Briefly, to label membranes, discs were mounted in 9μM FM4-64

(Molecular Probes) diluted in 1xPBS and incubated for 20 minutes at 25°C before live

imaging. To label endocytic compartments, discs were incubated with 17μM

tetramethylrhodamine-dextran (3000MW, Molecular Probes) diluted in incomplete M3

media for 10 minutes in the dark at 25°C, washed, and mounted in incomplete M3 media,

and incubated for 30 minutes at 25°C before live imaging. For extracellular labeling,

discs were incubated with anti-GFP (1:250 dilution in incomplete M3 media) for 30

minutes on ice before being washed 5x with ice cold 1xPBS and fixed in 4%

paraformaldehyde/PBS for 20 minutes at room temperature. Subsequent processing is

the same as stated above for immunostaining. For Alexa 546 and Alexa 647 Phalloidin (Molecular Probes) labeling, Phalloidin was diluted 1:40 in blocking solution and added during secondary antibody incubation step for 20-30 minutes before washes and mounting.

Microscopy, Image Acquisition, and Analysis

Fluorescence images were collected on a Leica TCSSP2 AOBS confocal microscope, and processed using the Leica Confocal Software 2.5 Build 1347, Adobe Photoshop 7.0, AutoDeBlur & AutoVisualize X 1.4.1 (MediaCybernetics) and Imaris 5.0.1 (Bitplane).

To count Hh-GFP containing vesicles, $79.35um^2$ XY sections were collected using the 63x objective, in the center of the wing pouch every 0.5 μm for the entire depth of the disc (60-100 μm which was approximately 120-200 sections). All discs were imaged under identical microscope settings for laser power, pinhole, and gain. Quantitative analysis was done in the Imaris software program, as described below.

Vesicle identification and distance measurement

For negative controls (the 0 hour time point), surface intensity thresholds were set just below background levels. This resulted in some background to be incorrectly identified as real signal. After this step, surfaces were sorted according to volume and any surface with a volume of less than $0.03um^3$ was discarded, leaving only a few

background surfaces. This strategy was used to maximize true Hh-GFP signal identification and minimize incorrect identification of background signal.

This strategy was applied to Hh-GFP expressing samples. Surface intensity thresholds were set to just below background, then sorted by volume, and surfaces with volumes more than 0.03 μm^3 were counted and measured. Surfaces are objects whose surfaces consist of pixels with the same fluorescent intensity.

After vesicle identification, a "Distance Transformation" tool generated a distance map from the UAS-dsRed signal marking the expressing cells. This map was applied to the surfaces to determine the shortest distance of vesicles from the Hh expressing cells. The distance measurements were then imported into Excel and plotted to generate distribution profiles. For each sample, total particle numbers were normalized by dividing the number of particles at each distance by the total number of particles for that sample. The normalized data was then averaged to generate the overall distribution profile. For each individual sample, the median, 90th percentile distance, and percentage at 8μm were determined, as well as the average value for each genotype and time point. The standard deviation was calculated for the median, 90th percentile distance, and percentage at 8μm values at each genotype and time point.

Statistical Analysis

To determine whether the measurement values of median, 90th percentile distance, and percentage at 8μm were significant between genotypes and/or time points, the measurements were subjected to the analysis of variance (ANOVA). The natural log of

the medians, natural log of the 90th percentile distances and the raw values for percentage at 8μm were analyzed as these met the normality assumptions of the ANOVAs. Specifically, the Tukey's HSD test was used to determine significance. There was no significant interaction between the time factor and the genotype factor. Therefore, the significance of the main effects (time irrespective of genotype or genotype irrespective of time) are described. P-values less than are 0.05 are considered significant.

Quantification of Ptc and Phalloidin co-localization

Particles were identified in the same way as for distance measurement quantification. After particle identification, each particle was analyzed through the z-stack for co-localization with Ptc and Phalloidin, then sorted into the appropriate category.

CHAPTER III

DISCUSSION

The work presented here provides some insight into the mechanism that regulates and shapes the Hh morphogen gradient. Previous studies have presented contradictory observations about how the Hh gradient forms and what the role is of the cholesterol modification. This work sought to clarify the roles of the Hh cholesterol modification and endocytosis in shaping the Hh gradient by using a system developed to look at newly synthesized Hh protein. My results demonstrate that the Hh gradient forms through diffusion, and does not require any transcytosis mechanism. Furthermore, the Hh cholesterol modification is instrumental in properly shaping the gradient by restricting Hh to a planar movement. Thus, the Hh morphogen gradient can form through planar diffusion.

While this study has provided some insight and clarification of previous results, many questions still remain. The main points of interest resulting from our results and implications for Hh and other morphogens will be discussed, including the mechanisms of Hh distribution, the role of cholesterol, and implications for Dpp and Wg.

Models and Mechanisms of Distribution

Hh gradient formation via Planar Diffusion

The results from this study and previous studies rule out free diffusion as a mechanism of Hh distribution. It is clear that Hh requires tighter regulation of the

concentration gradient than free diffusion could provide (Gallet et al., 2006). In addition, HhNp has been shown to be unable to traverse the wing disc lumen, which would be three-dimensional free diffusion (our studies; (Callejo et al., 2006; Gallet et al., 2006)]. Thus, Hh movement occurs via planar movement and not free diffusion. Planar movement could mean either an extracellular planar diffusion or planar transcytosis. My results using the shi^{ts1} mutant demonstrate that Hh is able to travel to target cells in the absence of endocytosis. This implies that a planar diffusion process is sufficient to form the Hh gradient.

Role of transcytosis in shaping the Hh gradient

The study presented here points to planar diffusion as the method of Hh gradient formation; however, it is still unable to conclusively rule out a role for transcytosis. Several questions remain: does any transcytosis of the Hh morphogen occur and what purpose does it serve? Would transcytosis be a mechanism to fine tune the gradient? Or would it be a redundant process that could potentially contribute more to gradient formation in the absence of planar diffusion?

As mentioned above, Ptc-independent vesicles were detected that were internalized by endocytosis. Previous studies have also detected such vesicles but their identity has yet to be determined. These vesicles could potentially represent transcytosing vesicles that were internalized through a receptor other than Ptc. A candidate receptor is Megalin, a member of the low density lipoprotein receptor family, demonstrated to interact with Shh in vertebrate systems (McCarthy et al., 2002).

Interestingly, Megalin has been shown to transcytose an unrelated ligand, thyroglobulin (Marino et al., 2000). Megalin binding to HhNp could potentially result in transcytosis of HhNp. A putative homolog of Megalin has been identified in *Drosophila*, although it has yet to be determined whether this protein is functionally similar to vertebrate Megalin (Fisher and Howie, 2006).

Another possibility is that Ptc-mediated endocytosis could also lead to transcytosis if HhNp-GFP has somehow dissociated from Ptc after internalization and is recycled back outside the cell. A recent study has shown that *C.elegans* Hh-related peptides are sorted to multivesicular bodies (MVBs), and then recycled back to the apical surfaces for secretion (Liegeois et al., 2006). One study has indicated that Hh is not recycled through the conventional Rab11 recycling pathway (Gallet et al., 2006). However, this data was not shown and there remains the possibility that Hh could be resecreted through a non-conventional recycling mechanism.

Finally, it is possible that these Ptc-independent vesicles are argosomes. Argosomes are membranous intracellular vesicles that are able to move from cell to cell (Greco et al., 2001). They have previously been described as carriers of the morphogen Wg and thus represent a potential vehicle for Hh as well (Greco et al., 2001). The nature of these argosomes, though, is not clear and whether endocytosis has a role in argosome movement is yet to be determined. Thus, it cannot be concluded whether the Ptc-independent vesicles are related to these structures.

In order to test for a transcytosis mechanism, evidence for the presence or absence of Hh resecretion is needed. A system has been developed for mammalian tissue culture

cells that has been able detect transcytosis (Marino et al., 2000). In this *in vitro* system, cells are grown on dual layer filter chambers as a polarized cell layer, at 100% confluency. Junctional complexes prevent random leakage of molecules from one side to the other. Once this cell layer has grown, the dual chambers allow exposure to molecules of interest on one side, and analysis of molecule secretion on the other side. Establishment of such a system for *Drosophila* cells could provide evidence for or against an apical-basal transcytosis mechanism, although it would not be able to give evidence of transcytosis if uptake and secretion occur on the same side.

Role of the cholesterol modification in restricting HhNp movement

This study provides evidence that the role of the Hh cholesterol modification is to restrict HhNp movement. The role of the cholesterol moiety has been intensely studied over the years, which has yielded contradictory observations in both *Drosophila* and vertebrate systems.

Studies from the embryo suggested that HhN had a reduced range of distribution, confirmed by later studies in the wing disc from the same laboratory (Gallet et al., 2003; Gallet et al., 2006). This is in direct contrast to wing disc studies by two other groups who found that HhN was able to signal to target cells further away than HhNp and thus had a further range of distribution (Callejo et al., 2006; Dawber et al., 2005). There were technical variations between these studies that might be able to explain these differences (Wendler et al., 2006). The method of detecting HhN differed between the studies as Gallet et al. used an anti-Hh antibody for detection (Gallet et al., 2006), and Callejo et al.

used Hh-GFP fusion proteins (Callejo et al., 2006). If the Hh antibody had reduced detection abilities for HhN, then HhN would not have been detected further away. The use of GFP to locate HhN would have been more accurate for detecting HhN distribution. Although in the wing disc experiments, two different groups used the same method, the clones expressing different forms of Hh from the Gallet et al. study (Gallet et al., 2006) were much smaller than in the Dawber et al. study (Dawber et al., 2005). Smaller clones would have produced less HhN than the larger clones. Less HhN could have been bound by the Hh receptor Ptc surrounding the clone, in effect sequestering all the HhN immediately and reducing any HhN that could have moved further.

This study demonstrates the role of cholesterol in restricting long-range movement; however, the mechanism of this action is unclear. Several hypotheses can be suggested regarded the role of the cholesterol modification. The cholesterol could restrict movement by association with cell membranes or allow association with other factors that sequester HhNp to prevent free diffusion. Interestingly, large multimers of HhNp can be detected biochemically. Therefore, the cholesterol could also promote oligomerization to increase the concentration near the expressing cells, thus promoting activation of high level target genes like *ptc* and concurrently retaining more HhNp at these cells.

While HhN has signaling abilities, it does not activate *ptc* expression as strongly as HhNp does (Callejo et al., 2006; Dawber et al., 2005). Therefore, HhNp expression would result in more *ptc* expression and as a consequence, more HhNp is sequestered closer to the producing cells as there is more Ptc to bind HhNp. Lower HhN activation of

ptc expression would result in less Ptc to bind and sequester HhN, and a further range of distribution. Thus, the restriction of HhNp distribution by the cholesterol modification could be due to both by a membrane-association and stronger binding and sequestration by Ptc. Analysis of the movement of HhNp and HhN over *ptc* mutant clones would be necessary to clarify whether this is indeed the situation.

Hh has also been detected in lipid rafts, microdomains that may function as a platform for signal transduction or intracellular trafficking (Chen et al., 2004; Rietveld et al., 1999). Biochemical studies analyzed fractionated embryos using centrifugation sedimentation assays. Interestingly, HhNp was detected in the lipid raft containing fractions (Rietveld et al., 1999). In addition, ShhNp multimers also co-localized with a lipid raft marker (Chen et al., 2004). Thus, HhNp may be targeted to lipid raft microdomains for distribution or signaling purposes, possibly due to the cholesterol modification (Burke et al., 1999). While the cholesterol requirement for HhNp localization in lipid rafts has not yet been demonstrated, it can be hypothesized that this would be the case considering lipid rafts are rich in cholesterol.

In addition to lipid rafts, HhNp has been detected in lipophorin particles. Recent studies have identified lipophorins as a potential carrier of HhNp (Panakova et al., 2005). Lipophorins are the *Drosophila* version of vertebrate lipoprotein particles that consist of apolipoproteins acting as scaffolding, and a phospholipid monolayer that surrounds a core of esterified cholesterol and triglycerides (Rodenburg and Van der Horst, 2005). Lipid modified proteins like HhNp would be able to attach to lipophorin particles by inserting its lipid moiety into the outer phospholipid monolayer. Panakova et al. showed co-

localization of lipophorin particles with Hh by cell fractionation studies and immunoprecipitation experiments. In addition, *in vivo*, Hh co-localized with exogenous lipophorin in endocytic compartments. Removing lipophorin by RNAi resulted in the accumulation of Hh in the first 5 rows of cells adjacent to the expressing cells and affecting the expression of long range signaling targets. Subsequent addition of purified lipophorin alleviated this effect on signaling. Panakova et al. hypothesized that there is a reversible association of Hh with lipophorin particles, facilitating transfer from the membrane of one cell to the next. When lipophorin levels are lowered, this increases the length of time Hh is at the cell membrane which slows the rate of transfer and increases the probability of Ptc-dependent endocytosis of Hh before Hh can move to the next cell. Short range signaling would still be effective but Hh would be sequestered by Ptc and long range signaling would be affected (Panakova et al., 2005). These studies of Hh and lipid-rich domains have not yet included analysis of the non-cholesterol modified form of Hh. Such studies would be able to elucidate whether cholesterol is the reason for association with these domains, providing more insight to how cholesterol may act to restrict HhNp distribution.

Role of HSPGs in facilitating planar movement

While our study did not involve HSPGs which are a part of the extracellular matrix, future work should still involve HSPGs since they have been shown to be involved in Hh distribution (Bellaiche et al., 1998; Bornemann et al., 2004; Callejo et al., 2006; Gallet et al., 2003; Glise et al., 2005; Gorfinkiel et al., 2005; Han et al., 2004a; Han

et al., 2004b; Lum et al., 2003a; Takei et al., 2004; The et al., 1999). Previous studies have extensively analyzed the effects of losing HSPGs on Hh distribution and signaling in *Ext* and HSPG core protein mutants. Hh is unable to move through *Ext* or HSPG mutant clones and the resulting Hh movement occurs around the clone. From these results, HSPGs have been demonstrated to be necessary for the planar movement of HhNp, while having no effect on HhN (Bellaiche et al., 1998; Callejo et al., 2006; Han et al., 2004b; Takei et al., 2004; The et al., 1999). However, the exact role of HSPGs in Hh signaling and distribution has not been determined. HSPGs could actively facilitate the extracellular movement of HhNp. Alternatively, HSPGs could act as co-receptors, clustering HhNp and enhancing binding to Ptc, promoting high level target gene activation. HSPGs might be required for HhNp endocytosis and transcytosis. HSPGs could also be required for the specific localization of HhNp to lipid-rich domains such as lipid rafts or lipophorins. Interestingly, the lipophorin RNAi phenotype is similar to the HSPG mutant phenotype for Hh distribution where Hh movement is restricted to the mutant cells closest to the expressing cells (Panakova et al., 2005). HSPGs could therefore facilitate Hh association with lipophorins. Furthermore, studies in vertebrate systems have demonstrated that disrupting lipid rafts reduces the association of heparin-binding growth factors to HSPGs (Chu et al., 2004) suggesting a relationship between HSPGs and lipid rafts, and possibly Hh.

The question of whether HSPGs facilitate endocytosis and/or transcytosis can be addressed with double mutant analysis of HSPG and endocytosis mutants, for example analyzing whether any Hh particles can be detected in *ttv/shi* double mutants that are

found in the first one or two rows of a *ttv* mutant clone. Additional experiments include studying any changes in Hh extracellular localization in HSPG mutant clones or changes in HhNp lipid-rich domain association in the absence of HSPGs and/or the cholesterol modification. The answers will indicate whether HSPGs facilitate planar diffusion or planar transcytosis.

A new way to investigate gradient formation and regulation

In this study, a system was developed to specifically investigate the distribution of newly synthesized Hh-GFP. This system enabled this study to avoid limitations of previous studies for several reasons. The Gal80 inducible system generated a pulse of expression of new protein. Thus, the distinction could be made between redistribution of Hh already present and movement of newly synthesized Hh in the endocytosis mutant. Furthermore, by inducing expression for 8 or 24 hours, the overexpression levels of these transgenes that can be seen with the Gal4 system should be reduced. Additionally, previous studies analyzed Hh distribution at the gradient steady state. While this could be informative, studies during gradient formation provide more insight to the mechanisms that are involved with gradient formation. Finally, the generation of Hh-GFP fusion proteins enables direct visualization of Hh and its distribution, instead of relying on antibodies that could be less sensitive.

Tools for studying morphogen movement have been developed in this study that will facilitate future studies of Hh distribution. In addition, recent studies have used other newly developed tools that would be quite useful to incorporate. Integration of these

tools would be necessary to study relationships for example between lipophorins, endocytosis, and the cholesterol modification. In the end, this means that more complex genetics will be required to incorporate these different tools into one system. Further double mutant analyses to study multiple factors involved in Hh gradient formation should provide more information about how each of these factors act to regulate and produce the Hh gradient. In addition to mutants and RNAi transgenic flies, new fluorescent-tagged proteins and markers have also been developed. These fluorescent tags leave the possibility for live imaging open. Ultimately, live imaging of fluorescent proteins in different mutant backgrounds could provide conclusive information about Hh gradient formation and regulation.

Implications for other morphogens

The mechanism of distribution for Dpp and Wg is not clear since contradictory observations have been reported as well. In almost identical experiments, two groups reported conflicting results on whether endocytosis affects Dpp movement (Belenkaya et al., 2004; Entchev et al., 2000). Both studies analyzed shi^{ts1} mutant clones in wing discs. In the first study, the authors took advantage of the temperature sensitivity of Gal4 by rearing the larvae at 16°C where Gal4 is less active. In shifting their larvae up to 25°C, a pulse of Dpp-GFP expression was produced. They found that Dpp-GFP was unable to go through the endocytosis defective clone as demonstrated by an absence of Dpp-GFP behind the clone (Entchev et al., 2000). However, an identical study found that Dpp could be detected behind the clone and extracellular Dpp could be detected within the

clone, suggesting that Dpp was able to move through the mutant tissue (Belenkaya et al., 2004). Two nearly identical experiments with conflicting results suggest that improved tools and techniques are required.

The contradictory observations for Wg do not arise from using the same mutants, but from using different tools to study different mechanisms. The initial studies of Wg distribution found that Wg could move extracellularly and this extracellular movement depends on HSPGs but not endocytosis (Baeg et al., 2001; Han et al., 2005; Strigini and Cohen, 2000). Other studies examined intracellular vesicles that could move from cell to cell and contains Wg, suggesting a transcytosis mechanism (Greco et al., 2001; Panakova et al., 2005). These contradictory Wg results stress the necessity of integrating different tools into the same system.

By using an inducible system and quantification for these morphogens, clarification of these discrepancies can be resolved, and would lead to further explanation of how Dpp and Wg distribution occurs and how their morphogen gradients are regulated.

Conclusions

This work presented in this thesis has demonstrated that the shape of the Hh gradient is regulated by the cholesterol modification. Furthermore, the results demonstrated that the formation of the Hh gradient occurs via a planar diffusion mechanism. In addition, a quantitative system to study the movement of newly synthesized protein during gradient formation has been developed and previously

reported contradictory observations have been resolved. There are still many questions that remain unanswered regarding how the Hh gradient is regulated. Therefore, development of new tools and techniques could provide more insight for future studies to completely elucidate the mechanisms of Hh gradient formation and distribution.

References

Akam, M. (1987). The molecular basis for metameric pattern in the Drosophila embryo. Development *101*, 1-22.

Alberts, B., Bray, D., Lewis, J., Raff, M., Roberts, K., and Watson, J. (1994). Molecular Biology of the Cell, Third edn (New York: Garland Publishing).

Alcedo, J., Ayzenzon, M., Von Ohlen, T., Noll, M., and Hooper, J. E. (1996). The Drosophila smoothened gene encodes a seven-pass membrane protein, a putative receptor for the hedgehog signal. Cell *86*, 221-232.

Alexandre, C., Jacinto, A., and Ingham, P. W. (1996). Transcriptional activation of hedgehog target genes in Drosophila is mediated directly by the cubitus interruptus protein, a member of the GLI family of zinc finger DNA-binding proteins. Genes Dev *10*, 2003-2013.

Amanai, K., and Jiang, J. (2001). Distinct roles of Central missing and Dispatched in sending the Hedgehog signal. Development *128*, 5119-5127.

Aza-Blanc, P., Ramirez-Weber, F. A., Laget, M. P., Schwartz, C., and Kornberg, T. B. (1997). Proteolysis that is inhibited by hedgehog targets Cubitus interruptus protein to the nucleus and converts it to a repressor. Cell *89*, 1043-1053.

Baeg, G. H., Lin, X., Khare, N., Baumgartner, S., and Perrimon, N. (2001). Heparan sulfate proteoglycans are critical for the organization of the extracellular distribution of Wingless. Development *128*, 87-94.

Basler, K., and Struhl, G. (1994). Compartment boundaries and the control of Drosophila limb pattern by hedgehog protein. Nature *368*, 208-214.

Belenkaya, T. Y., Han, C., Yan, D., Opoka, R. J., Khodoun, M., Liu, H., and Lin, X. (2004). Drosophila Dpp morphogen movement is independent of dynamin-mediated endocytosis but regulated by the glypican members of heparan sulfate proteoglycans. Cell *119*, 231-244.

Bellaiche, Y., The, I., and Perrimon, N. (1998). Tout-velu is a Drosophila homologue of the putative tumour suppressor EXT-1 and is needed for Hh diffusion. Nature *394*, 85-88.

Bornemann, D. J., Duncan, J. E., Staatz, W., Selleck, S., and Warrior, R. (2004). Abrogation of heparan sulfate synthesis in Drosophila disrupts the Wingless, Hedgehog and Decapentaplegic signaling pathways. Development *131*, 1927-1938.

Brand, A. H., and Perrimon, N. (1993). Targeted gene expression as a means of altering cell fates and generating dominant phenotypes. Development *118*, 401-415.

Bumcrot, D. A., Takada, R., and McMahon, A. P. (1995). Proteolytic processing yields two secreted forms of sonic hedgehog. Mol Cell Biol *15*, 2294-2303.

Burke, R., Nellen, D., Bellotto, M., Hafen, E., Senti, K. A., Dickson, B. J., and Basler, K. (1999). Dispatched, a novel sterol-sensing domain protein dedicated to the release of cholesterol-modified hedgehog from signaling cells. Cell *99*, 803-815.

Callejo, A., Torroja, C., Quijada, L., and Guerrero, I. (2006). Hedgehog lipid modifications are required for Hedgehog stabilization in the extracellular matrix. Development *133*, 471-483.

Capdevila, J., Pariente, F., Sampedro, J., Alonso, J. L., and Guerrero, I. (1994). Subcellular localization of the segment polarity protein patched suggests an interaction with the wingless reception complex in Drosophila embryos. Development *120*, 987-998.

Chamoun, Z., Mann, R. K., Nellen, D., von Kessler, D. P., Bellotto, M., Beachy, P. A., and Basler, K. (2001). Skinny hedgehog, an acyltransferase required for palmitoylation and activity of the hedgehog signal. Science *293*, 2080-2084.

Chen, M. H., Li, Y. J., Kawakami, T., Xu, S. M., and Chuang, P. T. (2004). Palmitoylation is required for the production of a soluble multimeric Hedgehog protein complex and long-range signaling in vertebrates. Genes Dev *18*, 641-659.

Chen, Y., Gallaher, N., Goodman, R. H., and Smolik, S. M. (1998). Protein kinase A directly regulates the activity and proteolysis of cubitus interruptus. Proc Natl Acad Sci U S A *95*, 2349-2354.

Chen, Y., and Struhl, G. (1996). Dual roles for patched in sequestering and transducing Hedgehog. Cell *87*, 553-563.

Chu, C. L., Buczek-Thomas, J. A., and Nugent, M. A. (2004). Heparan sulphate proteoglycans modulate fibroblast growth factor-2 binding through a lipid raft-mediated mechanism. Biochem J *379*, 331-341.

Crick, F. H., and Lawrence, P. A. (1975). Compartments and polyclones in insect development. Science *189*, 340-347.

Dawber, R. J., Hebbes, S., Herpers, B., Docquier, F., and van den Heuvel, M. (2005). Differential range and activity of various forms of the Hedgehog protein. BMC Dev Biol *5*, 21.

Dellovade, T., Romer, J. T., Curran, T., and Rubin, L. L. (2006). The Hedgehog Pathway And Neurological Disorders. Annu Rev Neurosci 29, 539-563.

Denef, N., Neubuser, D., Perez, L., and Cohen, S. M. (2000). Hedgehog induces opposite changes in turnover and subcellular localization of patched and smoothened. Cell 102, 521-531.

Desbordes, S. C., and Sanson, B. (2003). The glypican Dally-like is required for Hedgehog signalling in the embryonic epidermis of Drosophila. Development 130, 6245-6255.

Entchev, E. V., Schwabedissen, A., and Gonzalez-Gaitan, M. (2000). Gradient formation of the TGF-beta homolog Dpp. Cell 103, 981-991.

Feng, J., White, B., Tyurina, O. V., Guner, B., Larson, T., Lee, H. Y., Karlstrom, R. O., and Kohtz, J. D. (2004). Synergistic and antagonistic roles of the Sonic hedgehog N- and C-terminal lipids. Development 131, 4357-4370.

Fietz, M. J., Jacinto, A., Taylor, A. M., Alexandre, C., and Ingham, P. W. (1995). Secretion of the amino-terminal fragment of the hedgehog protein is necessary and sufficient for hedgehog signalling in Drosophila. Curr Biol 5, 643-650.

Fisher, C. E., and Howie, S. E. (2006). The role of megalin (LRP-2/Gp330) during development. Dev Biol.

Forbes, A. J., Nakano, Y., Taylor, A. M., and Ingham, P. W. (1993). Genetic analysis of hedgehog signalling in the Drosophila embryo. Dev Suppl, 115-124.

Gallet, A., Rodriguez, R., Ruel, L., and Therond, P. P. (2003). Cholesterol modification of hedgehog is required for trafficking and movement, revealing an asymmetric cellular response to hedgehog. Dev Cell 4, 191-204.

Gallet, A., Ruel, L., Staccini-Lavenant, L., and Therond, P. P. (2006). Cholesterol modification is necessary for controlled planar long-range activity of Hedgehog in Drosophila epithelia. Development 133, 407-418.

Gallet, A., and Therond, P. P. (2005). Temporal modulation of the Hedgehog morphogen gradient by a patched-dependent targeting to lysosomal compartment. Dev Biol 277, 51-62.

Gibson, M. C., Lehman, D. A., and Schubiger, G. (2002). Lumenal transmission of decapentaplegic in Drosophila imaginal discs. Dev Cell 3, 451-460.

Gilbert, S. (2000). Developmental Biology, Sixth edn (Sunderland, MA: Sinauer Associates Inc.).

Glise, B., Miller, C. A., Crozatier, M., Halbisen, M. A., Wise, S., Olson, D. J., Vincent, A., and Blair, S. S. (2005). Shifted, the Drosophila ortholog of Wnt Inhibitory Factor-1, controls the distribution and movement of Hedgehog. Dev Cell *8*, 255-266.

Goetz, J. A., Singh, S., Suber, L. M., Kull, F. J., and Robbins, D. J. (2006). A highly conserved amino-terminal region of sonic hedgehog is required for the formation of its freely diffusible multimeric form. J Biol Chem *281*, 4087-4093.

Gofflot, F., Hars, C., Illien, F., Chevy, F., Wolf, C., Picard, J. J., and Roux, C. (2003). Molecular mechanisms underlying limb anomalies associated with cholesterol deficiency during gestation: implications of Hedgehog signaling. Hum Mol Genet *12*, 1187-1198.

Gorfinkiel, N., Sierra, J., Callejo, A., Ibanez, C., and Guerrero, I. (2005). The Drosophila ortholog of the human Wnt inhibitor factor shifted controls the diffusion of lipid-modified hedgehog. Dev Cell *8*, 241-253.

Greco, V., Hannus, M., and Eaton, S. (2001). Argosomes: a potential vehicle for the spread of morphogens through epithelia. Cell *106*, 633-645.

Grigliatti, T. A., Hall, L., Rosenbluth, R., and Suzuki, D. T. (1973). Temperature-sensitive mutations in Drosophila melanogaster. XIV. A selection of immobile adults. Mol Gen Genet *120*, 107-114.

Gurdon, J. B., Harger, P., Mitchell, A., and Lemaire, P. (1994). Activin signalling and response to a morphogen gradient. Nature *371*, 487-492.

Han, C., Belenkaya, T. Y., Khodoun, M., Tauchi, M., Lin, X., and Lin, X. (2004a). Distinct and collaborative roles of Drosophila EXT family proteins in morphogen signalling and gradient formation. Development *131*, 1563-1575.

Han, C., Belenkaya, T. Y., Wang, B., and Lin, X. (2004b). Drosophila glypicans control the cell-to-cell movement of Hedgehog by a dynamin-independent process. Development *131*, 601-611.

Han, C., Yan, D., Belenkaya, T. Y., and Lin, X. (2005). Drosophila glypicans Dally and Dally-like shape the extracellular Wingless morphogen gradient in the wing disc. Development *132*, 667-679.

Heemskerk, J., and DiNardo, S. (1994). Drosophila hedgehog acts as a morphogen in cellular patterning. Cell *76*, 449-460.

Hepker, J., Wang, Q. T., Motzny, C. K., Holmgren, R., and Orenic, T. V. (1997). Drosophila cubitus interruptus forms a negative feedback loop with patched and regulates expression of Hedgehog target genes. Development *124*, 549-558.

Hooper, J. E. (2003). Smoothened translates Hedgehog levels into distinct responses. Development *130*, 3951-3963.

Hooper, J. E., and Scott, M. P. (2005). Communicating with Hedgehogs. Nat Rev Mol Cell Biol *6*, 306-317.

Hsiung, F., Ramirez-Weber, F. A., Iwaki, D. D., and Kornberg, T. B. (2005). Dependence of Drosophila wing imaginal disc cytonemes on Decapentaplegic. Nature *437*, 560-563.

Incardona, J. P., Gruenberg, J., and Roelink, H. (2002). Sonic hedgehog induces the segregation of patched and smoothened in endosomes. Curr Biol *12*, 983-995.

Incardona, J. P., Lee, J. H., Robertson, C. P., Enga, K., Kapur, R. P., and Roelink, H. (2000). Receptor-mediated endocytosis of soluble and membrane-tethered Sonic hedgehog by Patched-1. Proc Natl Acad Sci U S A *97*, 12044-12049.

Ingham, P. W. (1998). Transducing Hedgehog: the story so far. Embo J *17*, 3505-3511.

Ingham, P. W., and Fietz, M. J. (1995). Quantitative effects of hedgehog and decapentaplegic activity on the patterning of the Drosophila wing. Curr Biol *5*, 432-440.

Ingham, P. W., and McMahon, A. P. (2001). Hedgehog signaling in animal development: paradigms and principles. Genes Dev *15*, 3059-3087.

Ingham, P. W., Nystedt, S., Nakano, Y., Brown, W., Stark, D., van den Heuvel, M., and Taylor, A. M. (2000). Patched represses the Hedgehog signalling pathway by promoting modification of the Smoothened protein. Curr Biol *10*, 1315-1318.

Ingham, P. W., Taylor, A. M., and Nakano, Y. (1991). Role of the Drosophila patched gene in positional signalling. Nature *353*, 184-187.

Jia, J., Tong, C., and Jiang, J. (2003). Smoothened transduces Hedgehog signal by physically interacting with Costal2/Fused complex through its C-terminal tail. Genes Dev *17*, 2709-2720.

Jullien, J., and Gurdon, J. (2005). Morphogen gradient interpretation by a regulated trafficking step during ligand-receptor transduction. Genes Dev *19*, 2682-2694.

Kasuya, J., and Iverson, L. (2000). personal communication to FlyBase.

Kinoshita, T., Jullien, J., and Gurdon, J. B. (2006). Two-dimensional morphogen gradient in Xenopus: Boundary formation and real-time transduction response. Dev Dyn.

Kruse, K., Pantazis, P., Bollenbach, T., Julicher, F., and Gonzalez-Gaitan, M. (2004). Dpp gradient formation by dynamin-dependent endocytosis: receptor trafficking and the diffusion model. Development *131*, 4843-4856.

Lander, A. D., Nie, Q., and Wan, F. Y. (2002). Do morphogen gradients arise by diffusion? Dev Cell *2*, 785-796.

Lee, J. D., and Treisman, J. E. (2001). Sightless has homology to transmembrane acyltransferases and is required to generate active Hedgehog protein. Curr Biol *11*, 1147-1152.

Lee, J. J., Ekker, S. C., von Kessler, D. P., Porter, J. A., Sun, B. I., and Beachy, P. A. (1994). Autoproteolysis in hedgehog protein biogenesis. Science *266*, 1528-1537.

Lewis, P. M., Dunn, M. P., McMahon, J. A., Logan, M., Martin, J. F., St-Jacques, B., and McMahon, A. P. (2001). Cholesterol modification of sonic hedgehog is required for long-range signaling activity and effective modulation of signaling by Ptc1. Cell *105*, 599-612.

Li, Y., Zhang, H., Litingtung, Y., and Chiang, C. (2006). Cholesterol modification restricts the spread of Shh gradient in the limb bud. Proc Natl Acad Sci U S A *103*, 6548-6553.

Liegeois, S., Benedetto, A., Garnier, J. M., Schwab, Y., and Labouesse, M. (2006). The V0-ATPase mediates apical secretion of exosomes containing Hedgehog-related proteins in Caenorhabditis elegans. J Cell Biol *173*, 949-961.

Lum, L., Yao, S., Mozer, B., Rovescalli, A., Von Kessler, D., Nirenberg, M., and Beachy, P. A. (2003a). Identification of Hedgehog pathway components by RNAi in Drosophila cultured cells. Science *299*, 2039-2045.

Lum, L., Zhang, C., Oh, S., Mann, R. K., von Kessler, D. P., Taipale, J., Weis-Garcia, F., Gong, R., Wang, B., and Beachy, P. A. (2003b). Hedgehog signal transduction via Smoothened association with a cytoplasmic complex scaffolded by the atypical kinesin, Costal-2. Mol Cell *12*, 1261-1274.

Marino, M., Zheng, G., Chiovato, L., Pinchera, A., Brown, D., Andrews, D., and McCluskey, R. T. (2000). Role of megalin (gp330) in transcytosis of thyroglobulin by thyroid cells. A novel function in the control of thyroid hormone release. J Biol Chem *275*, 7125-7137.

Marois, E., Mahmoud, A., and Eaton, S. (2006). The endocytic pathway and formation of the Wingless morphogen gradient. Development *133*, 307-317.

Martin, V., Carrillo, G., Torroja, C., and Guerrero, I. (2001). The sterol-sensing domain of Patched protein seems to control Smoothened activity through Patched vesicular trafficking. Curr Biol *11*, 601-607.

McCarthy, R. A., Barth, J. L., Chintalapudi, M. R., Knaak, C., and Argraves, W. S. (2002). Megalin functions as an endocytic sonic hedgehog receptor. J Biol Chem *277*, 25660-25667.

McDowell, N., and Gurdon, J. B. (1999). Activin as a morphogen in Xenopus mesoderm induction. Semin Cell Dev Biol *10*, 311-317.

McGuire, S. E., Le, P. T., Osborn, A. J., Matsumoto, K., and Davis, R. L. (2003). Spatiotemporal rescue of memory dysfunction in Drosophila. Science *302*, 1765-1768.

Micchelli, C. A., The, I., Selva, E., Mogila, V., and Perrimon, N. (2002). Rasp, a putative transmembrane acyltransferase, is required for Hedgehog signaling. Development *129*, 843-851.

Mohler, J. (1988). Requirements for hedgehod, a segmental polarity gene, in patterning larval and adult cuticle of Drosophila. Genetics *120*, 1061-1072.

Mohler, J., and Vani, K. (1992). Molecular organization and embryonic expression of the hedgehog gene involved in cell-cell communication in segmental patterning of Drosophila. Development *115*, 957-971.

Monnier, V., Dussillol, F., Alves, G., Lamour-Isnard, C., and Plessis, A. (1998). Suppressor of fused links fused and Cubitus interruptus on the hedgehog signalling pathway. Curr Biol *8*, 583-586.

Motzny, C. K., and Holmgren, R. (1995). The Drosophila cubitus interruptus protein and its role in the wingless and hedgehog signal transduction pathways. Mech Dev *52*, 137-150.

Mullor, J. L., and Guerrero, I. (2000). A gain-of-function mutant of patched dissects different responses to the hedgehog gradient. Dev Biol *228*, 211-224.

Murone, M., Rosenthal, A., and de Sauvage, F. J. (1999). Hedgehog signal transduction: from flies to vertebrates. Exp Cell Res *253*, 25-33.

Nusslein-Volhard, C., and Wieschaus, E. (1980). Mutations affecting segment number and polarity in Drosophila. Nature *287*, 795-801.

Oda, H., Uemura, T., Harada, Y., Iwai, Y., and Takeichi, M. (1994). A Drosophila homolog of cadherin associated with armadillo and essential for embryonic cell-cell adhesion. Dev Biol *165*, 716-726.

Panakova, D., Sprong, H., Marois, E., Thiele, C., and Eaton, S. (2005). Lipoprotein particles are required for Hedgehog and Wingless signalling. Nature *435*, 58-65.

Patel, N. H. (1994). Imaging neuronal subsets and other cell types in whole-mount Drosophila embryos and larvae using antibody probes. Methods Cell Biol *44*, 445-487.

Pepinsky, R. B., Zeng, C., Wen, D., Rayhorn, P., Baker, D. P., Williams, K. P., Bixler, S. A., Ambrose, C. M., Garber, E. A., Miatkowski, K., *et al.* (1998). Identification of a palmitic acid-modified form of human Sonic hedgehog. J Biol Chem *273*, 14037-14045.

Peters, C., Wolf, A., Wagner, M., Kuhlmann, J., and Waldmann, H. (2004). The cholesterol membrane anchor of the Hedgehog protein confers stable membrane association to lipid-modified proteins. Proc Natl Acad Sci U S A *101*, 8531-8536.

Porter, J. A., Ekker, S. C., Park, W. J., von Kessler, D. P., Young, K. E., Chen, C. H., Ma, Y., Woods, A. S., Cotter, R. J., Koonin, E. V., and Beachy, P. A. (1996a). Hedgehog patterning activity: role of a lipophilic modification mediated by the carboxy-terminal autoprocessing domain. Cell *86*, 21-34.

Porter, J. A., Young, K. E., and Beachy, P. A. (1996b). Cholesterol modification of hedgehog signaling proteins in animal development. Science *274*, 255-259.

Ramirez-Weber, F. A., and Kornberg, T. B. (1999). Cytonemes: cellular processes that project to the principal signaling center in Drosophila imaginal discs. Cell *97*, 599-607.

Rietveld, A., Neutz, S., Simons, K., and Eaton, S. (1999). Association of sterol- and glycosylphosphatidylinositol-linked proteins with Drosophila raft lipid microdomains. J Biol Chem *274*, 12049-12054.

Robbins, D. J., Nybakken, K. E., Kobayashi, R., Sisson, J. C., Bishop, J. M., and Therond, P. P. (1997). Hedgehog elicits signal transduction by means of a large complex containing the kinesin-related protein costal2. Cell *90*, 225-234.

Rodenburg, K. W., and Van der Horst, D. J. (2005). Lipoprotein-mediated lipid transport in insects: analogy to the mammalian lipid carrier system and novel concepts for the functioning of LDL receptor family members. Biochim Biophys Acta *1736*, 10-29.

Rorth, P. (1998). Gal4 in the Drosophila female germline. Mech Dev *78*, 113-118.

Ruel, L., Rodriguez, R., Gallet, A., Lavenant-Staccini, L., and Therond, P. P. (2003). Stability and association of Smoothened, Costal2 and Fused with Cubitus interruptus are regulated by Hedgehog. Nat Cell Biol 5, 907-913.

Schuske, K., Hooper, J. E., and Scott, M. P. (1994). patched overexpression causes loss of wingless expression in Drosophila embryos. Dev Biol 164, 300-311.

Sisson, J. C., Ho, K. S., Suyama, K., and Scott, M. P. (1997). Costal2, a novel kinesin-related protein in the Hedgehog signaling pathway. Cell 90, 235-245.

Speicher, S. A., Thomas, U., Hinz, U., and Knust, E. (1994). The Serrate locus of Drosophila and its role in morphogenesis of the wing imaginal discs: control of cell proliferation. Development 120, 535-544.

Strigini, M., and Cohen, S. M. (1997). A Hedgehog activity gradient contributes to AP axial patterning of the Drosophila wing. Development 124, 4697-4705.

Strigini, M., and Cohen, S. M. (2000). Wingless gradient formation in the Drosophila wing. Curr Biol 10, 293-300.

Struhl, G., Barbash, D. A., and Lawrence, P. A. (1997a). Hedgehog acts by distinct gradient and signal relay mechanisms to organise cell type and cell polarity in the Drosophila abdomen. Development 124, 2155-2165.

Struhl, G., Barbash, D. A., and Lawrence, P. A. (1997b). Hedgehog organises the pattern and polarity of epidermal cells in the Drosophila abdomen. Development 124, 2143-2154.

Strutt, H., Thomas, C., Nakano, Y., Stark, D., Neave, B., Taylor, A. M., and Ingham, P. W. (2001). Mutations in the sterol-sensing domain of Patched suggest a role for vesicular trafficking in Smoothened regulation. Curr Biol 11, 608-613.

Tabata, T., Eaton, S., and Kornberg, T. B. (1992). The Drosophila hedgehog gene is expressed specifically in posterior compartment cells and is a target of engrailed regulation. Genes Dev 6, 2635-2645.

Tabata, T., and Takei, Y. (2004). Morphogens, their identification and regulation. Development 131, 703-712.

Takei, Y., Ozawa, Y., Sato, M., Watanabe, A., and Tabata, T. (2004). Three Drosophila EXT genes shape morphogen gradients through synthesis of heparan sulfate proteoglycans. Development 131, 73-82.

Takeo, S., Akiyama, T., Firkus, C., Aigaki, T., and Nakato, H. (2005). Expression of a secreted form of Dally, a Drosophila glypican, induces overgrowth phenotype by affecting action range of Hedgehog. Dev Biol *284*, 204-218.

Tanimoto, H., Itoh, S., ten Dijke, P., and Tabata, T. (2000). Hedgehog creates a gradient of DPP activity in Drosophila wing imaginal discs. Mol Cell *5*, 59-71.

Teleman, A. A., and Cohen, S. M. (2000). Dpp gradient formation in the Drosophila wing imaginal disc. Cell *103*, 971-980.

The, I., Bellaiche, Y., and Perrimon, N. (1999). Hedgehog movement is regulated through tout velu-dependent synthesis of a heparan sulfate proteoglycan. Mol Cell *4*, 633-639.

Torroja, C., Gorfinkiel, N., and Guerrero, I. (2004). Patched controls the Hedgehog gradient by endocytosis in a dynamin-dependent manner, but this internalization does not play a major role in signal transduction. Development *131*, 2395-2408.

Turing, A. M. (1952). The Chemical Basis of Morphogenesis. Philosophical Transactions of the Royal Society of London *237*, 37-72.

van den Heuvel, M., and Ingham, P. W. (1996). smoothened encodes a receptor-like serpentine protein required for hedgehog signalling. Nature *382*, 547-551.

Von Ohlen, T., Lessing, D., Nusse, R., and Hooper, J. E. (1997). Hedgehog signaling regulates transcription through cubitus interruptus, a sequence-specific DNA binding protein. Proc Natl Acad Sci U S A *94*, 2404-2409.

Wang, G., Amanai, K., Wang, B., and Jiang, J. (2000). Interactions with Costal2 and suppressor of fused regulate nuclear translocation and activity of cubitus interruptus. Genes Dev *14*, 2893-2905.

Wang, G., Wang, B., and Jiang, J. (1999). Protein kinase A antagonizes Hedgehog signaling by regulating both the activator and repressor forms of Cubitus interruptus. Genes Dev *13*, 2828-2837.

Wang, Q. T., and Holmgren, R. A. (2000). Nuclear import of cubitus interruptus is regulated by hedgehog via a mechanism distinct from Ci stabilization and Ci activation. Development *127*, 3131-3139.

Wendler, F., Franch-Marro, X., and Vincent, J. P. (2006). How does cholesterol affect the way Hedgehog works? Development *133*, 3055-3061.

Zecca, M., Basler, K., and Struhl, G. (1995). Sequential organizing activities of engrailed, hedgehog and decapentaplegic in the Drosophila wing. Development *121*, 2265-2278.

Zeng, X., Goetz, J. A., Suber, L. M., Scott, W. J., Jr., Schreiner, C. M., and Robbins, D. J. (2001). A freely diffusible form of Sonic hedgehog mediates long-range signalling. Nature *411*, 716-720.

Zhu, A. J., Zheng, L., Suyama, K., and Scott, M. P. (2003). Altered localization of Drosophila Smoothened protein activates Hedgehog signal transduction. Genes Dev *17*, 1240-1252.